01 Nov 1996

Strength of flexural members using structural grade 80 of A653 steel (deck panel tests)

Shaojie Wu

Wei-Wen Yu
Missouri University of Science and Technology, wwy4@mst.edu

Roger A. LaBoube
Missouri University of Science and Technology, laboube@mst.edu

CCFSS LIBRARY
23 1 * 3872
November
1996
Cy2

Shaojie Wu Wei-Wen Yu Roger A. Laboube STRENGTH OF FLEXURAL MEMBERS USING STRUCTURAL GRADE 80 OF A653 STEEL (DECK PANEL TESTS)

DATE	ISSUED TO

Civil Engineering Study 96-4
Cold-Formed Steel Series

Second Progress Report

STRENGTH OF FLEXURAL MEMBERS USING STRUCTURAL GRADE 80 OF A653 STEEL (DECK PANEL TESTS)

by

Shaojie Wu
Research Associate

Wei-Wen Yu
Roger A. LaBoube
Project Directors

A Research Project Sponsored by the American Iron and Steel Institute

November, 1996

Department of Civil Engineering
University of Missouri-Rolla
Rolla, Missouri

ABSTRACT

This second progress report describes the design of deck panel specimens for flexural tests and presents the test results of ninety-three deck panel specimens. The deck panels consisted of single and multiple hat-shaped ribs in their cross sections and were manufactured from 28, 26, and 22 gage steel sheets of Structural Grade 80 of ASTM A653 Steel. Among the ninety-three deck panel specimens, seventy-two panels were tested in simply supported and two-point loading conditions; sixteen panels were tested in simply supported and one-point loading conditions; and five panels with screws penetrating through tension flanges were tested in simply supported and two-point loading conditions. Three yielding conditions were considered in the design of the deck panel specimens, namely first yielding occurring in compression flange only, first yielding occurring in both compression and tension flanges simultaneously, and first yielding occurring in tension flange only. The specimens and the test setup were designed to ensure only a flexural failure mode. The actual average w/t ratio of the specimens ranged from 17.93 to 189.95 and the actual average h/t ratio ranged from 17.67 to 104.43. The actual average angle between planes of the web and bearing surface varied from 59.06 to 62.21 degree. The actual average yield strength of the sheet steels varied from 103.9 to 112.5 ksi.

For the two-point loading condition, the test results indicated that for the panel specimens with small w/t ratios (17.93 to 61.07), the tested yield moments were reached and compared reasonably well with the calculated effective yield moments using actual dimensions, actual yield strength of the steel, and the 1986 AISI Specification. However, for the panel specimens with large w/t ratios (102.86 to 189.95), the tested ultimate moments were lower than the calculated effective yield moments using actual yield strength of the steel, but much larger than the calculated moments using the 75% of the specified minimum yield strength of the steel (that is 60 ksi), and even larger than the calculated moments using 100% of the specified minimum yield strength of the steel (80 ksi). Panel specimens designed for the first yielding in the tension flange developed higher ratios of tested yield moment to calculated effective yield moment. Higher tested

yield moment to weight-per-length ratio of the panel was achieved for specimens designed for the first yielding in both compression and tension flanges simultaneously.

For the one-point loading condition, the test results indicated that for all sixteen panels, the ratios of the tested yield moment to the calculated effective yield moment using actual yield strength of the steel and the ratios of the tested ultimate moment to the calculated effective yield moment followed the similar trend with respect to the w/t ratio as the panels tested in two-point loading condition. In addition, for the one-point loading condition, the panels with small w/t ratios (17.93 to 31.65) developed higher ratios of the tested yield moment to the calculated effective yield moment and higher ratios of the tested ultimate moment to the calculated effective yield moment, but demonstrated less overall ductility in the load-displacement relationship as compared to the panels with the two-point loading condition. The panels with large w/t ratios (118.64 to 189.95) developed only slightly higher ratios of the tested ultimate moment to the calculated effective yield moment as compared to the panels with the two-point loading condition.

For the deck panels with screws penetrating through tension flanges, it was found that the ultimate tested moment and displacement of the panels with screws were nearly equal to those of the panels without screws. Only one 22 gage panel with 27% of reduction in tension flange and designed for first yielding in tension flange experienced tensile fracture and necking near the holes after the panel entered a plateau in its load-displacement curve.

The test results also showed that for almost all the deck panels with either a two-point or a one-point loading condition, the tested central displacements were near or less than the calculated central displacements using effective moment of inertia at service load, actual dimensions, and modulus of elasticity of 29,500 ksi. Fracture in tension was not observed in the tested panels without screws. The flexural strength of the panels was more strongly affected by the w/t ratios of the panels and did not appear to be influenced by the low-ductility and low F_u/F_y ratio of the steel for the panels with small w/t ratios.

It is concluded that the current design practice for designing cold-formed flexural members using 75% of the specified minimum yield strength of the Structural Grade 80 of ASTM A653 steel or 60 ksi (whichever is less) is conservative, especially for the members with small w/t ratios (less than 60). A modified yield strength reduction factor was developed to be used for determining the flexural strength of the panels with yield strength between 80 ksi and 150 ksi (including 80 and 150 ksi) and w/t ratio not exceeding 190. For panels with $(w/t)(F_y/E)$ ratio of 1/15 or less, the actual yield strength of steels can be used for determining the flexural strength of the panels. Reasonable agreements are achieved between tested moments and predicted moments using the modified yield strength reduction factor.

TABLE OF CONTENT

LIST OF TABLES

LIST OF TABLES (CONTINUED)

LIST OF FIGURES

LIST OF FIGURES (CONTINUED)

1. INTRODUCTION

1.1 BACKGROUND

Cold-formed steel decks have been widely used in buildings as load-carrying structural elements, such as floor and roof decks (Yu 1991, SDI 1992, USD 1994). One of the main structural functions for the steel decks is to carry live and dead loads and transfer the loads to beams or girders. As a result, the decks work as flexural members. The steel decks usually consist of several hat-shaped ribs formed together in their cross section. When such decks, either in single-span or multi-span, is subject to uniform or concentrated loads, the overall stability of the decks, such as lateral torsional buckling, often does not control the moment capacity of the members.

In the United States, it is a common practice that steel decks are made of the Structural Grade 80 of ASTM A653 steel (formerly ASTM A446 Grade E steel). The unique property of the Structural Grade 80 steel, as compared to the conventional steels used for cold-formed members, is that it has a high specified yield strength (F_y=80 ksi (551.6 MPa)) and a low tensile-to-yield strength ratio (F_u/F_y=1.03). The ductility of the steel is unspecified (ASTM A446) and was reported to be smaller than the ductility requirements for the conventional steels (Dhalla and Winter 1971).

Due to the lack of ductility and low tensile-to-yield strength ratio of the Structural Grade 80 steel and considering the required ductility for adequate structural performance, Section A3.3.2 of the Specification for the Design of Cold-Formed Steel Structural Members (AISI 1986, AISI 1991) permits the use of the steel for particular configurations provided that (1) the yield strength, F_y, used for the design of members, is taken as 75% of the specified minimum yield point or 60 ksi (413.7 MPa), whichever is less, and (2) the tensile strength, F_u, used for the design of connections and joints, is taken as 75% of the specified minimum tensile strength or 62 ksi (427.5 MPa), whichever is less.

In the past, studies on the strength and performance of structural components made of the Structural Grade 80 steel were limited (Wu, Yu, and LaBoube 1995). The reduction of the specified material properties by 25% for design purposes is based on the fact that the structural performance of cold-formed members and connections made of such a steel has not been fully investigated and understood. Therefore, an in-depth investigation on structural performance of flexural members made of the Structural Grade 80 steel as affected by high yield and tensile strengths, low ductility, and low F_u/F_y ratio of the steel is needed.

1.2 OBJECTIVE AND SCOPE

In September 1994, a research project entitled "Strength of Flexural Members Using Structural Grade 80 of A653 and Grade E of A611 Steels" was initiated at the University of Missouri-Rolla under the sponsorship of American Iron and Steel Institute. The objectives of the overall research is to study the structural performance and strength of the cold-formed steel members and connections made of the Structural Grade 80 of ASTM A653 steel. In addition, appropriate design criteria will be developed for consideration in the AISI Specifications.

The overall research consists of three phases: preliminary study (first phase); experimental investigation (second phase); and development of design recommendations (third phase). The preliminary study has been completed, which included literature review, evaluation of earlier existing test data, and material tests. The results of the first phase of the study were reported in the First Progress Report (Wu, Yu, and LaBoube 1995). The experimental investigation includes several tasks: (1) Design and prepare test specimens for beam tests and connection tests; (2) Conduct beam tests for determining section strength (effective yield moment); (3) Conduct beam tests for determining web crippling strength including end-one-flange loading and interior-one-flange loading; (4) Conduct a preliminary study of screw and welded connections; (5) Evaluate all available test results. This Second Progress Report describes the design of deck panel specimens and test setup, presents the test results on the flexural strength of the deck panels in both two-point and one-point loading conditions, and evaluates the results for all tested deck panels. Web crippling

tests of deck panels are planned for further study. The results of the web crippling tests and the evaluation of the tests will be included in the Third Progress Report. The results of the connection tests and the evaluation of the tests will be reported in the Fourth Progress Report.

2. LITERATURE REVIEW

EFFECT OF YIELD-TO-TENSILE RATIO OF HIGH-STRENGTH STEEL ON STRUCTURAL BEHAVIOR

In a recent reference (Brockenbrough 1995), the effect of yield-to-tensile ratio of high performance steels (high-strength steels) on structural behavior was reviewed based on published literature in the United States, Japan, and the United Kingdom. The review included tests conducted on beams, columns, connections, cold-formed steel members, and pressure vessels by using high performance steels. Particular attention was focused on several recent research projects carried out in Japan to study the effect of the yield-to-tensile ratio of some newly developed high-strength steels on overall ductility of structures under severe seismic actions. Unlike conventional high-strength steels, for which the yield-to-tensile ratio increases with increases in yield strength, the Japanese high-strength steels have low yield-to-tensile ratio with a maximum value of 0.85.

Based on the literature review on beams, it is found that with decreases in the yield-to-tensile ratio of the high-strength steels, the overall ductility of the beam increased significantly and the plastic moment could be reached and exceeded. The beams performed well into the plastic range. Even though a larger ratio of the strain at onset of strain-hardening to the yield strain and a larger ratio of the elastic modulus to the modulus in the strain-hardening range of the stress-strain relationship could increase the overall ductility, a lower yield-to-tensile ratio could overshadow the beneficial effect of the larger strain and modulus ratios and reduce the overall ductility. In column and connection tests, it was also observed that the low yield-to-tensile ratio of the high-strength steels could enlarge deformations and increase stress levels in the members.

The reason for the increase of overall ductility due to a lower yield-to-tensile ratio is the following. When a member is made of a steel having a low yield-to-tensile ratio and is loaded to yield, the moment at the

yielded section can still increase with further increases in strains in the section, since the tensile strength of the steel is larger than the yield strength in the stress-strain relationship of the steel. With the moment further increased, yielding spreads within the first yielded section and to adjacent sections, resulting in a spread of plasticity into a region. This expanding plastic region in the member causes larger increases in overall ductility of the member. An example as reviewed in the reference (Brockenbrough 1995) is that the beam made of A514 steel with a yield-to-tensile ratio ranging from 0.89 to 0.92 and tested in uniform moment and moment gradient conditions can reach plastic moment and develop plastic hinges and desired plastic rotations.

However, it should be noted that the requirement for a lower yield-to-tensile ratio for a better structural performance is particularly true for the members that are required to deform well into the inelastic range, such as under seismic forces, and the members have the ability to perform well by possessing lower flange width-to-thickness or web depth-to-thickness ratios. For other applications other than seismic resistance, the overall ductility level can be relaxed as suggested by Brockenbrough (1995).

3. DESIGN OF DECK PANEL SPECIMENS

Cold-formed steel deck panel specimens for flexural tests were designed by using the Structural Grade 80 of ASTM A653 steel. The design was focused on selecting a wide range of w/t and h/t ratios which are consistent with those used in the current deck panel products. Attention was also paid to designing the panels with different yield conditions in the cross section in order to study any potential effect of low-ductility and partial plastification on flexural strength, and to ensuring only flexural failure mode in the panel tests. Section 3.1 describes different sections of the panel specimens. Section 3.2 discusses the design of different yield conditions in the cross sections. Section 3.3 presents actual dimensions of the panel specimens. Finally, Section 3.4 discusses the design for controlling flexural failure mode, including the determination of total span and shear span.

3.1 SECTIONS AND THICKNESSES OF TEST SPECIMENS

Twenty-four sections with hat-shaped ribs were selected for studying the flexural strength of deck panels tested with a two-point loading condition. Of the twenty-four sections, eight sections were also used for deck panels tested with a one-point loading condition; and five sections were used for panels with screws penetrating through tension flanges and tested with a two-point loading condition. The section parameters include: thickness, flange flat-width-to-thickness ratio (w/t), web flat-depth-to-thickness ratio (h/t), and extreme fiber tension-to-compression stress ratio (f_t/f_c) at first yielding in a cross section.

Three types of steel sheets, namely 22, 26, and 28 gage sheets, were used for the panels in two-point loading condition, while only 22 and 26 gage sheets were used for the panels in one-point loading condition and for the panels with screws. The selected w/t ratios ranged from 17.24 to 189.66 and the h/t ratios ranged from 17.24 to 103.45 for the panels in both two-point and one-point loading conditions and for the panels with screws. The w/t and h/t ratios and the use of four different steel sheets were determined based

on the current cold-formed steel deck products (USD 1994, SDI 1992). Three f_t/f_c ratios, namely 0.8, 1.0, and 1.2, were selected for the panels in two-point loading condition for (1) first yielding in compression flange only, (2) first yielding in both compression and tension flanges simultaneously, and (3) first yielding in tension flange only, respectively, while only two f_t/f_c ratios, 1.0 and 1.2, were selected for the panels in one-point loading condition, and two f_t/f_c ratios, 0.8 and 1.2, were used for the panels with screws. The design inside bend radius, R, was taken as 1/16 inches (1.59 mm) for all three steel sheets, which results in a R/t ratio ranging from 2.16 to 4.17. The design angle between the plane of the web and the plane of the bearing surface, θ, was taken as 60 degree. The number of hat-shaped ribs in the sections varied from one to three ribs to fit the panel specimens to available test apparatus. Table 3.1.1 illustrates the variation of the w/t and h/t ratios used for the twenty-four sections of the panels tested in two-point loading condition, and Figure 3.1.1 shows the shape of the sections. Table 3.1.2 lists the w/t and h/t ratios used for the eight sections of the panels in one-point loading condition. Table 3.1.3 shows the w/t and h/t ratios used for the five sections of the panels with screws. In Table 3.1.1, each combination of w/t and h/t ratios corresponds to three f_t/f_c ratios (0.8, 1.0, and 1.2), while in Table 3.1.2, each combination corresponds to two f_t/f_c ratios (1.0, and 1.2).

The material properties of the Structural Grade 80 steel were determined based on a total of seventy-six tensile coupon tests (Wu, Yu, and LaBoube 1995). The tensile coupons were made of 22, 24, 26, and 28 gage steel sheets and cut from the sheets with the orientation both parallel and perpendicular to the rolling direction of the sheets. The results of the tensile coupon tests are shown in Table 3.1.4. It is noted in the table that with decreases in thickness of the steel sheets, the yield and tensile strengths tend to increase, but the ductility tends to decrease. In the direction perpendicular to the rolling direction, the yield and tensile strengths of the sheets are much higher than those in the rolling direction, while the ductility is much lower than that in the rolling direction.

3.2 DESIGN FOR DIFFERENT YIELD CONDITIONS IN CROSS SECTIONS

For each of the twenty-four sections, with the given compression flange width w, web height h, thickness t, inside bend radius R, angle between plane of web and plane of bearing surface θ, f_t/f_c ratio, and the material properties, the width of the tension flange needs to be determined so that the f_t/f_c ratio reaches exactly the expected values at first yielding in cross section. It is apparent that the width of the tension flange should be different for a section with certain w, h, t, R, θ values and material properties in the three different yield conditions (three different f_t/f_c ratios) in the section. Usually, the determination of the width of the tension flange requires an iterative calculation. To avoid the trial-and-error process, formulas were derived to directly calculate the width of the tension flange and the effective yield moment. The widths of the tension flanges of the twenty-four sections and the effective yield moments of the sections were determined using the formulas and the actual yield strength of the Structural Grade 80 steel, and then checked against the calculated moments using the computer programs CFS (Glauz 1990). It is noticed that the effective yield moments obtained by using the formulas are consistent with the moments calculated using the computer program.

Based on the results of the calculated effective yield moments, it is found that for all the combinations of the w/t and h/t ratios considered, the effective yield moment decreases with the increase in the f_t/f_c ratio at first yielding in the cross section, if the f_t/f_c ratio is the only varying parameter in the section. It indicates that the effective yield moment with first yielding occurring in the compression flange only is always larger than the moment with the first yielding occurring in both compression and tension flanges simultaneously. The latter is even larger than the moment with the first yielding occurring in tension flange only. This result was further verified by taking the derivative of the effective yield moment with respect to the f_t/f_c ratio in the formulas derived.

3.3 ACTUAL DIMENSIONS OF DECK PANEL SECTIONS

For each of the twenty-four sections, the members were manufactured from longer sheets. A segment was cut from the members representing each section. The dimensions of each segment were carefully measured using a calliper with an accuracy of 0.001 inches (0.025 mm). The angle between planes of the web and adjacent flanges was measured twice using an angular ruler, one with respect to the compression flange and the other with respect to the tension flange. The measured dimensions of all elements and the angles of all webs are shown in Tables 3.3.1, 3.3.2 and 3.3.3, and the shape of the sections is shown in Figure 3.3.1. In these tables, each deck panel section is designated as: t**w**h**-*, where "t**" represents gage number (thickness), such as t22 (22 gage); "w**" indicates the flat width of the compression flange, such as w1.5 (w=1.5 inches (38.1 mm)); "h**" represents the flat width of the web, such as h1 (h=1.0 inch (25.4 mm)); "-*" indicates the location of the first yielding, such as -c (occurring in compression flange only); -ct (in compression and tension flanges simultaneously); and -t (in tension flange only). The actual inside bend radius, R, was 1/32 inches (0.79 mm) for all specimens. The actual w/t ratios ranged from 17.18 to 189.95 and the actual h/t ratios ranged from 16.35 to 104.89. The actual angle between the plane of web and the plane of bearing surface varied from 58.00 to 63.25 degree. The actual w/t and h/t ratios are listed in Tables 3.3.4 and 3.3.5, respectively, for the sections.

3.4 DESIGN FOR CONTROL OF FLEXURAL FAILURE MODE

With all the measured dimensions, effective yield moments were re-calculated for all the twenty-four sections using the computer program CFS (Glauz 1990) and the actual yield strength of the steel. The average value of the two measured angles between the web and the two flanges was used in the calculation. The calculated effective yield moments were then used to determine the total length of each panel specimen so that no other failure modes will be possible during a test except the flexural failure mode. This was done by the following calculation.

Firstly, the unfactored shear strength of the webs was computed for each panel specimen using actual dimensions, actual yield strength of the steel, and the AISI Specification (AISI 1986). The shear strength was controlled by one of the shear failure modes of the webs, namely shear yielding. inelastic buckling, and elastic buckling.

Secondly, the unfactored web crippling strength of the webs was calculated for each panel specimen using actual dimensions, actual yield strength of the steel, and the AISI Specification. Both end one-flange loading (EOF) and Interior one-flange loading (IOF) were considered in the calculation. The actual length of bearing was taken as 3 inches (76.2 mm) for IOF loading and 5 inches (127.0 mm) for EOF loading. The web-crippling strength at IOF loading was further reduced by a factor of 0.39 to consider a fully developed effective yield moment at the interior loading. The factor of 0.39 was determined from the web crippling-moment interaction equation in the AISI Specification.

Thirdly, the shear-moment interaction equation in the AISI Specification was used to compute required total length of the specimen. The total length of the specimen is the distance between centers of two roller supports when the specimen is simply supported. The applied shear force was assumed to be 1/4 of the shear strength of the webs or the web-crippling strength of the webs (further reduced by the factor of 0.39), whichever is smaller. According to the shear-moment interaction equation, an applied moment that is more than 95% of the effective yield moment under pure bending can be reached if the applied shear force is 1/4 of the shear strength under pure shear. The applied moment was determined from this applied shear force times a shear span (the distance between center of end load and center of interior load) which was written in terms of a fraction of the total length and can be conceptually regarded as moment-to-shear ratio (a measure for relative magnitude of shear force).

The shear span was taken as equal to or less than the maximum moment-to-shear ratio at the exterior span of a multi-span deck panel under uniform loads (in elastic behavior) and at the interior spans of the multi-span deck panel. The moment-to-shear ratios at the first interior support of 2-span, 3-span, 4-span, and 5-

span deck panels are L/5, L/6, L/5.67, and L/5.77, respectively (with an average of L/5.6), where L is the length of each span, and are L/5, L/6.54, and L/6.33 at the interior support of 3-span, 4-span, and 5-span deck panels, respectively (with an average of L/5.9). If a 2-span deck panel with equal moment strength in both positive and negative bending could develop an overall failure mechanism, the moment-to-shear ratio at the first interior support of the panel can be determined as L/6.9. It is apparent that the effect of shear force becomes larger as additional load increases beyond the first yielding in the panel. As a result, three shear spans (moment-to-shear ratios) were used in the shear-moment interaction equation for the calculation in the two-point loading condition, namely L/6, L/4, and L/3. The shear span for the panels in the one-point loading condition is certain, that is L/2.

Finally, the required minimum total lengths determined from the third step were further modified with consideration of shear lag effect, space needed to locate necessary strain gages between the two interior loads in two-point loading condition, and available test supporting beam. The modification usually leaded to a conservative increase in the total length. The total lengths and the shear spans of the twenty-four deck panel specimens are listed in Table 3.4.1. It is noted in the table that for the panel sections used for both two-point and one-point loading conditions, the moment-to-shear ratios in one-point loading condition are larger than the ratios in two-point loading condition, especially for the sections with small flange width (w=0.5 inches (12.7 mm)). This reveals that the relative magnitude of shear force in the panel specimens in one-point loading condition is smaller than that in the specimens in two-point loading condition; and the effect of the shear force on flexural strength is likely to be smaller in one-point loading condition.

Once the total length of the panel specimens was determined, three specimens were cut from the members representing each section. Thus, in the following discussion, a postfix, "(x)", is added to the section designation, t**w**h**-*, to represent test number such as 1, 2, and 3. A "2p-" is prefixed to the section designation to indicate the panels tested in two-point loading condition, while a "1p-" is prefixed to represent the panels tested in one-point loading condition. A "2ps-" is also prefixed to the section designation to indicate the panels with screws and tested in two-point loading condition.

4. DECK PANEL TESTS

A total of ninety-three deck panel specimens were tested to study the flexural strength of the panels using the Structural Grade 80 steel. Among the ninety-three panel specimens, seventy-two panels were tested for a two-point loading and simply supported condition; sixteen panels were tested for a one-point loading and simply supported condition; and five panels with screws penetrating through tension flanges were also tested with a two-point loading condition. All the tests were conducted through a displacement control program and all the panels were tested to failure. Section 4.1 describes the test setup. Section 4.2 discusses the instrumentation used in the tests. Section 4.3 deals with the test procedure. Section 4.4 presents the test results in two-point loading condition, while Section 4.5 presents the test results in one-point loading condition. Finally, Section 4.6 discusses the test results for the panels with screws.

4.1 TEST SETUP

The MTS 880 Test System located at the Engineering Research Laboratory of the University of Missouri-Rolla, as shown in Fig. 4.1.1, was used to carry out the deck panel tests. It consists of a loading frame with top and bottom platens (on the right of the picture), various control panels (in the middle of the picture), and a data acquisition system (on the left in the picture) with a real time computer monitor (not shown in the picture). The System uses the close-loop control scheme with three main control modes, namely load, strain, and displacement controls which are automatically operated in the System. During a test, the top platen is stationary, while the bottom platen is controlled by the System to move up and down as to apply load.

For the two-point loading condition, the panel specimen was placed on two simple supports (one was a roller condition and the other was a pin condition) which were fastened on a wide flange support beam 84 inches (2134 mm) long. The support beam was firmly connected to the bottom platen of the MTS 880

loading frame. A cross beam was used to establish a two-point loading condition, with one pin and one roller at each end of the beam. Load was applied to the center of the cross beam which was against the unmovable top platen of the loading frame while moving the bottom platen upwards. Bracing was attached to the tension flange of the panel specimen using C-clamps at several locations along the entire length of the panel to prevent the section from changing its shape, with at least two braces at each interior load and one brace at the center of the span as shown in Fig. 4.1.2. For the panels with larger h/t ratios, a piece of segment of the same section was overlapped with the panel at the two interior load locations to further strengthen the webs as shown in Fig. 4.1.3. The test setup in two-point loading condition is illustrated in Figures 4.1.3 and 4.1.4.

For the one-point loading condition, the test setup was similar to that of the two-point loading condition, except that the load was directly applied to a roller at the center of each specimen. No additional overlapping segment was used at the central load location. At least two braces were used on each side of the bearing plate at the central load. The test setup is shown in Fig. 4.1.5.

In the five panels with screws and tested with a two-point loading condition, three pairs of self-driven screws with a nominal diameter of 0.1875" (3/16") were drilled through the tension flanges of the panels as shown in Fig. 4.1.6. Two screws in a pair were separated by the hat-shaped rib. The three pairs of screws were located within the constant moment region, with one pair at the center of the span and two pairs near the two interior loads. Three aluminum angles were used to brace the section at the three screw locations, and the screws were also drilled through the aluminum angles as illustrated in Figures 4.1.6 and 4.1.7. To avoid the damage to the narrow tension flanges while driving the screws through the tension flanges and the aluminum angles by an electrically powered driller, a sharp bit with a diameter less than that of the screws was first used to drill a hole through the tension flanges and the aluminum angles. Then the screws were driven through the holes by a hand socket wrench to create a snug contact with the tension flanges. The setup for the panels with screws was similar to that for the panels without screws in two-point loading condition.

4.2 INSTRUMENTATION

The instrumentation installed for the tests was designed to measure strains and displacements of the panel specimens and to detect initiation of local flange buckling. For the two-point loading condition, two LVDTs were used to record the displacements at the center of the span, with each LVDT on each side of the panel. Two additional LVDTs were located at two interior load locations as shown in Figure 4.1.3 and 4.1.4. Twelve to eighteen strain gages were used throughout the constant moment region to record top and bottom extreme fiber strains and local flange buckling. For the one-point loading condition, only two LVDTs were located at the center of the span, with each LVDT on each side of the panel as shown in Fig. 4.1.5. Ten or twelve strain gages were used near each edge of the central bearing plate. For the panels with screws, the LVDT setup was similar to that for the panels without screws in two-point loading condition. Six strain gages were used in the constant moment region. The layout of the strain gages are shown in Figures 4.2.1, 4.2.2, and 4.2.3. All of the LVDT and strain gage data were simultaneously and automatically recorded through a CAMAC data acquisition system with a sampling rate of three samples per second during testing.

4.3 TEST PROCEDURE

Prior to testing, the panel specimen was cut from the longer members to a predetermined total length and then was cleaned with commercial products of Acerton and Paint Thinner. Lines were marked on the panel to indicate the locations of strain gages, loads, and supports. Sand paper was used to remove the coating of the panel at the strain gage locations. The surface of the strain gage locations was further cleaned according to a standard requirement by Micro Measurement Inc.. Strain gages were then placed on the panel at the indicated locations. Wires were connected to the strain gages and the resistivity of the strain gages was measured with a voltage meter to check any defect due to mishandling the strain gages. The panel was put on the support beam on the MTS loading frame and the strain gages were further connected to a strain gage conditioner box through the wires. The strain gage conditioners were turned to a balanced

condition and the load conditioner in the MTS system was zeroed.

Before the panel specimen was loaded, the initial readings of the LVDTs and the strain gages were recorded. The cross beam and its accessories (for two-point loading condition) or the central roller (for one-point loading condition) were placed on the top of the panel and the readings of the LVDTs and the strain gages were recorded again. The displacement control mode of the MTS system was then started immediately after continuous data recording was initiated. The bottom platen of the MTS loading frame moved upwards to push the cross beam against the top platen, resulting in an applied load at the center of the cross beam (two-point loading condition) or at the central roller (one-point loading condition). The displacement mode continued throughout testing with a displacement rate of 0.000125 inches (0.0032 mm) per second. After the specimen had failed, the displacement control mode was terminated while the data recording continued until the cross beam was automatically and gradually released away from the top platen in order to obtain the descending branch in the load-displacement relationship.

4.4 TEST RESULTS FOR PANELS WITH TWO-POINT LOADING CONDITION

Seventy-two deck panel specimens were tested with the two-point loading condition, which involved twenty-four different sections as shown in Tables 3.3.1, 3.3.2, and 3.3.3. For each section, three panels were tested. The summary of the test results and behavior of the panels are presented as follows. In the following discussion, the sections designed for first yielding in compression flange only, in both compression and tension flanges, and in tension flange only are referred to as c-section, ct-section, and t-section, respectively for convenience. The average yield strain obtained from the coupon tests was 5282, 5739, and 5722 microstrains for the 22, 26, and 28 gage sheets, respectively. The compressive strain is indicated by a negative sign "-".

(1) Panel specimens 2p-t28w1.5h1-c(1,2,3), 2p-t28w1.5h1-ct(1,2,3), and 2p-t28w1.5h1-t(1,2,3) (actual w/t=101.55 to 105.05 and h/t=65.17 to 70.07): All the panels had two hat-shaped ribs in the cross section.

Eighteen strain gages for each panel were used in the constant moment region. Predicted yield loads using actual yield strength of the steel were 718, 630, and 573 lbs. for the c-section, ct-section, and t-section, respectively. Flange local buckling occurred at about 130 to 170 lbs. for all the panels. The maximum central deflections at service load were L/123 for the c-section, L/137 for the ct-section, and L/129 for the t-section where L is the length of the span. Six panels indicated yielding in cross section, with the yield load of 587 lbs. for the c-section, 560, 587, 552 lbs. for the ct-section, and 539, 524 lbs. for the t-section. All the panels failed suddenly due to the formation of a local failure mechanism in the constant moment region shortly after the ultimate load was reached, resulting in a large drop of load. The ultimate loads were 603, 601, 592 lbs. for the c-section, 581, 588, 579 lbs. for the ct-section, and 550, 548, 532 lbs. for the t-section. Local buckles of the flanges and webs gradually increased the local deformation and largely developed at ultimate load in all the panels. The maximum ratio of central deflection to span at ultimate load was L/29 for the c-section, L/25 for the ct-section, and L/22 for the t-section. The maximum edge strains or strains in the tension flange at ultimate load were -4387, -4828, -6050 microstrains for the c-section, -13420, -5760, -8935 microstrains for the ct-section, and -7805, -5673, -7383 microstrains for the t-section.

(2) Panel specimens 2p-t26w0.5h0.5-c(1,2,3), 2p-t26w0.5h0.5-ct(1,2,3), and 2p-t26w0.5h0.5-t(1,2,3) (actual w/t=30.19 to 33.52 and h/t=26.24 to 31.77): All the panels had three hat-shaped ribs in the cross section. Eighteen strain gages for each panel were used in the constant moment region. Predicted yield loads were 736, 688, and 596 lb for the c-section, ct-section, and t-section, respectively. Flange local buckling occurred shortly prior to yielding at about 550 to 650 lbs. The maximum central deflections at service load were L/63 for the c-section, L/73 for the ct-section, and L/64 for the t-section. All of the panels experienced yielding in cross section, with the yield load of 710, 689, 701 lbs for the c-section, 687, 786, 709 lbs for the ct-section, and 650, 718, 660 lbs. for the t-section. A plateau in the load vs. central deflection curve was developed for all the panels prior to a sudden failure due to the formation of a local failure mechanism in the constant moment region, resulting in a large drop of load. The ultimate loads were reached at 714, 731, 740 lbs. for the c-section, 720, 788, 710 lbs. for the ct-section, and 656, 722, 665 lbs.

for the t-section. Local buckles of the flanges and webs gradually increased local deformation and largely developed prior to failure. The maximum ratio of central deflection to span prior to failure was L/15 for the c-section, L/14 for the ct-section, and L/12 for the t-section. The maximum edge strains or strains in the tension flange prior to failure were -6049, -8686, -8703 microstrains for the c-section, -8789, -5853, 5740 microstrains for the ct-section, and 6496, -6778, -6914 microstrains for the t-section.

(3) Panel specimens 2p-t26w1h0.75-c(1,2,3), 2p-t26w1h0.75-ct(1,2,3), and 2p-t26w1h0.75-t(1,2,3) (actual w/t=59.19 to 62.57 and h/t=43.85 to 46.30): All the panels had two hat-shaped ribs in the cross section. Sixteen strain gages for each panel were used in the constant moment region. Predicted yield loads were 916, 824, and 688 lbs. for the c-section, ct-section, and t-section, respectively. Flange local buckling occurred at about 400 to 450 lbs. for all the panels. The maximum central deflections at service load were L/104 for the c-section, L/113 for the ct-section, and L/112 for the t-section. Five panels yielded in cross section, with the yield load of 865 lbs. for the c-section, 923, 891 lbs. for the ct-section, and 808, 782, 813 lbs. for the t-section. A plateau in the load vs. central deflection curve was developed especially for the panels with the t-section. All the panels failed suddenly due to the formation of a local failure mechanism in the constant moment region, resulting in a large drop of load. The ultimate loads prior to failure were 927, 930, 938 lbs. for the c-section, 930, 893, 900 lbs. for the ct-section, and 851, 862, 847 lbs. for the t-section. Local buckles of the flanges and webs gradually increased deformation and largely developed prior to failure. The maximum ratio of central deflection to span prior to failure was L/22 for the c-section, L/18 for the ct-section, and L/15 for the t-section. The maximum edge strains or strains in the tension flange prior to failure were -9576, -4877, 3501 microstrains for the c-section, 5739, -5651, 5271 microstrains for the ct-section, and -8336, -10226, -9774 microstrains for the t-section.

(4) Panel specimens 2p-t26w2h1.5-c(1,2,3), 2p-t26w2h1.5-ct(1,2,3), and 2p-t26w2h1.5-t(1,2,3) (actual w/t=118.36 to 122.23 and h/t=86.11 to 91.26): All the panels had two hat-shaped ribs in the cross section. Eighteen strain gages for each panel were used in the constant moment region. Predicted yield loads were 689 lbs. for the c-section, 660 lbs. for the ct-section, and 603 lbs. for the t-section. Flange local buckling

occurred at about 110 to 140 lbs for all the panels. The maximum central deflections at service load were L/138, L/141, and L/148 for the c-section, ct-section, and t-section, respectively. Four panels yielded in cross section, with the yield load of 543 lbs. for the c-section, 532, 553 lbs. for the ct-section, and 551 lbs. for the t-section. All the panels failed suddenly due to the formation of a local failure mechanism in the constant moment region, resulting in a large drop of load. The ultimate loads prior to failure were 563, 568, 574 lbs. for the c-section, 557, 551, 563 lbs. for the ct-section, and 544, 550, 556 lbs. for the t-section. Local buckles of the flanges and webs gradually increased local deformation and largely developed prior to failure. The maximum ratio of central deflection to span prior to failure was L/38, L/33, and L/31 for the c-section, ct-section, and t-section, respectively. The maximum edge strains or strains in the tension flange prior to failure were -4633, -8614, -4583 microstrains for the c-section, -7850, -5693, -7270 microstrains for the ct-section, and -4813, -4943, -6984 microstrains for the t-section.

(5) Panelspecimens2p-t22w0.5h0.5-c(1,2,3), 2p-t22w0.5h0.5-ct(1,2,3), and2p-t22w0.5h0.5-t(1,2,3) (actual w/t=17.18 to 19.44 and h/t=16.35 to 18.53): All the panels had three hat-shaped ribs in the cross section. Fourteen strain gages for each panel were used in the constant moment region. Predicted yield loads were 1304, 1180, and 1052 lbs. for the c-section, ct-section, and t-section, respectively. The maximum central deflections at service loads were L/74, L/70, and L/67 for the c-section, ct-section, and t-section, respectively. All the panels yielded in the section and continued to carry additional load beyond first yielding until an ultimate load was reached. The yield loads were 1375, 1316 lbs. (not available for one panel) for the c-section, 1236, 1229 lbs. (not available for one panel) for the ct-section, and 1145, 1117, 1141 lbs. for the t-section. Both strain reading and visual observation indicated that no local buckling occurred at yielding. Shortly prior to reaching an ultimate load, sections within one of the braced segments in the constant moment region tended to open up (change shape), resulting in a reduction in effective depth of the section. The locations of the section that changed shape appeared to be random within the constant moment region. The ultimate loads were reached at 1458, 1539, 1467 lbs. for the c-section, 1366, 1314, 1432 lbs. for the ct-section, and 1196, 1158, 1207 lbs. for the t-section. After the ultimate load was reached, the decrease in applied load was small and gradual with further increase in displacement. Tests

were terminated because of excessively large displacement. A large plateau in the load vs. central deflection curve was developed for the panels with the ct-section and t-section where both compressive and tensile strains were far beyond the yield strain. Sudden formation of a local failure mechanism did not occur before test was terminated. The panels showed sufficient ductility. The maximum ratio of central deflection to span prior to terminating test was L/11, L/11, and L/9 for the c-section, ct-section, and t-section, respectively. The maximum edge strains or strains in the tension flange prior to terminating test were -8233, -8253, -10210 microstrains for the c-section, -8299, -8786, -8002 microstrains for the ct-section, and 8455, 9304, 11463 microstrains for the t-section.

(6) Panel specimens 2p-t22w1h0.75-c(1,2,3), 2p-t22w1h0.75-ct(1,2,3), and 2p-t22w1h0.75-t(1,2,3) (actual w/t=34.94 to 35.86 and h/t=25.41 to 27.48): All the panels had two hat-shaped ribs in the cross section. Sixteen strain gages for each panel were used in the constant moment region. Predicted yield loads were 1852, 1130, and 895 lbs. for the c-section, ct-section, and t-section, respectively. Flanges buckled locally shortly before yielding in all the panels. The maximum central deflections at service load were L/88, L/86, and L/89 for the c-section, ct-section, and t-section, respectively. Six panels yielded in cross section and continued to carry additional load beyond first yielding. The yield loads were 1111, 1073, 1135 lbs. for the ct-section and 915, 930 lbs. (not available for one panel) for the t-section. A plateau in the load vs. central deflection curve was developed in all the panels before a local failure mechanism formed gradually within the constant moment region. The local failure mechanism formed less gradually in the panels with the c-section. With the formation of the local failure mechanism, the panels failed with quick decrease in load. The ultimate loads prior to failure were 1942, 1194, 1195 lbs. for the c-section, 1111, 1086, 1137 lbs. for the ct-section, and 933, 986, 979 lbs. for the t-section. Local buckles developed slightly prior to failure only in the flanges. The maximum ratio of central deflection to span prior to failure was L/17, L/19, and L/16 for the c-section, ct-section, and t-section, respectively. The maximum edge strains or strains in the tension flange prior to failure were -4344, -5005, -3648 microstrains for the c-section, 6659, 5382, -6461 microstrains for the ct-section, and 6834, -10378, 8058 microstrains for the t-section.

(7) Panel specimens 2p-t22w3h2-c(1,2,3), 2p-t22w3h2-ct(1,2,3), and 2p-t22w3h2-t(1,2,3) (actual w/t=103.00 to 103.33 and h/t=69.10 to 70.10): All the panels had one hat-shaped rib in the cross section. Eighteen strain gages for each panel were used in the constant moment regions. Predicted yield loads were 1052, 982, and 807 lbs. for the c-section, ct-section, and t-section, respectively. Flanges buckled locally at about 220 to 270 lbs. for all the panels. The maximum central deflections at service load were L/169, L/168, and L/191 for the c-section, ct-section, and t-section, respectively. Seven panels yielded in cross section, with the yield load of 907 lbs. for the c-section, 807, 828, 834 lbs. for the ct-section, and 793, 786, 794 lbs. for the t-section. A plateau in the load vs. central deflection curve was developed in most of the panels before a local failure mechanism suddenly formed in the constant moment region in all the panels, resulting in a large drop of load. Local buckles gradually increased local deformation and largely developed in the flanges and webs prior to failure. The ultimate loads before failure were 893, 917, 927 lbs. for the c-section, 820, 830, 838 lbs. for the ct-section, and 793, 786, 794 lbs. for the t-section. The maximum ratio of central deflection to span prior to failure was L/42, L/39, and L/36 for the c-section, ct-section, and t-section, respectively. The maximum edge strains or strains in the tension flange prior to failure were -4643, -6088, -4026 microstrains for the c-section, -7966, -5424, -6689 microstrains for the ct-section, and 5453, 5341, 5447 microstrains for the t-section.

(8) Panel specimens 2p-t22w5.5h3-c(1,2,3), 2p-t22w5.5h3-ct(1,2,3), and 2p-t22w5.5h3-t(1,2,3) (actual w/t=188.98 to 189.95 and h/t=102.12 to 104.89): All the panels had one hat-shaped rib in the cross section. Eighteen strain gages for each panel were used in the constant moment region. Predicted yield loads were 1245, 1263, and 1113 lbs. for the c-section, ct-section, and t-section, respectively. Flanges buckled at about 90 to 120 lbs. for all the panels. At service load, the maximum central deflections were L/167 for the c-section, L/172 for the ct-section, and L/171 for the t-section. Only two panels indicated yielding in cross section, with the yield load of 1074 lbs. for the c-section and 1011 lbs. for the ct-section. All of the panels failed suddenly due to the formation of a local failure mechanism in the constant moment region, resulting in a large drop of load. The ultimate loads were reached at 1074, 1082, 1103 lbs. for the c-section, 1026, 1036, 1011 lbs. for the ct-section, and 1010, 1006, 995 lbs. for the t-section. The maximum ratio of central

deflection to span prior to failure was L/58, L/50, L/47 for the c-section, ct-section, and t-section, respectively. The maximum edge strains or strains in the tension flange prior to failure were -5426, -4214, -4358 microstrains for the c-section, -5236, -4029, -6373 microstrains for the ct-section, and -4254, -4212, -4597 microstrains for the t-section.

Examining the test results for all the tested panel specimens, the following observations were made:

A. Yield and Ultimate Loads

For each w/t ratio considered in this study, the panels designed for first yielding in compression flange tended to develop the largest ultimate loads and the panels designed for first yielding in tension flange tended to develop the smallest ultimate loads, with the panels designed for first yielding in both compression and tension flanges in between. By converting the ultimate loads to ultimate moments, this trend is clearly shown in Fig. 4.4.1. It is noted in the figure that this trend is apparent for the panels made from the thicker sheet (22 gage), but not significant for the panels made from the thinner sheets (26 and 28 gages). The yield loads indicated the similar trend as the ultimate loads. This was consistent with what was found when the sections were designed as discussed in Section 3.2. In Section 5, the yield and ultimate moments will be compared to the weight-per-length of the panels to show some economical benefit due to the use of different yielding conditions in cross section.

B. Yielding and Maximum Strains Prior to Failure

Forty-two out of fifty-four panels with the w/t ratios of 105.05 or less experienced yielding in cross section and continued to yield after first yielding, while with further increases in the w/t ratios (larger than 105.05), only six out of eighteen panels underwent yielding in cross section. For the panels that did not indicate yielding in the cross section prior to failure, the maximum strains in twenty-two out of twenty-four panels exceeded 4000 microstrains, with two panels having the maximum strain of more than 3500 but less than

4000 microstrains. This 4000 microstrains level corresponded to at least 95 ksi stress (655.0 MPa) of the three different steels based on the material tests. The possible reason for the two lower strains (more than 3500 but less than 4000 microstrains) may be the following. As observed during the tests, local buckles in the flange formed in valleys and ridges, and the strain gages near the corners between flange and webs could be either near or on top of the local buckled ridges. The flange was bent upward locally at the buckled ridges, resulting in a local tensile strain in the extreme compressive fiber. This additional tensile strain in the extreme compressive fiber offsets the continuously developed compressive strain due to overall bending of the panel. With further increase in load, the extreme compressive strain increased slowly.

Figures 4.4.2 and 4.4.3 show the yield strains and the maximum strains prior to failure against the w/t ratio, respectively. In Fig. 4.4.2, the yield strains and the largest strains in the opposite flange in the same section at onset of yielding are plotted together. Yielding in the panels does not appear to depend on the thickness of the panels, but more strongly on the w/t ratio since more panels with smaller w/t ratios yielded in cross section. Figure 4.4.2 also indicates that with the w/t ratios larger than 40, the first yielding tended to occur in the compression flanges even though some sections were designed with first yielding in tension flanges only or in both compression and tension flanges. This reveals a possible movement of the neutral axis location throughout a test. The change of relative magnitude between extreme compressive and tensile fiber stresses was also observed during tests. The maximum compressive and tensile strains in the same section at yielding are listed in Table 4.4.1.

In Fig. 4.4.3, the maximum strains in the panels prior to failure are also plotted together with the largest strains in the opposite flange in the same section prior to failure. The maximum strains also tended to form in the compression flanges as shown in Fig. 4.4.3. With increases in the w/t ratios, the magnitude of the maximum strains decreased. All of the recorded maximum strains prior to failure were less than 1.4% in./in. and no tensile fracture was observed in the tested panels. The maximum compressive and tensile strains in the same section prior to failure are listed in Table 4.4.2.

C. Maximum Central Deflection at Service Load and Prior to Failure

For all the panel specimens, the maximum central deflection prior to failure tended to be the largest for the sections designed with first yielding in tension flange only and the smallest for the sections designed with first yielding in compression flange only. However, under the service loads, this trend did not appear to exist in all the panels. The reason for this may be explained as follows. As noticed in most of the panels discussed above, the failure of the panels were usually initiated from a formation of a local failure mechanism except for the 22 gage sections with smaller w/t ratio. This local failure mechanism was characterized by crushing the corners between the flange and webs in compression. For the panels designed with first yielding in tension flange only, the stress in the extreme tensile fiber was higher than the stress in the extreme compressive fiber after load was applied. With further increase in load, the compressive stress tended to increase faster than the tensile stress, possibly due to the fact that the stress-strain relationship in the tension flange became nonlinear at higher stress level while the relationship in the compression flange was still linear. Thus, with similar strain increment in both compression and tension flanges, the stress increment in the compression flange would be higher. Eventually at a later state, the compressive stress became higher than the tensile stress in cross section and finally crushed the corners between the flange and the webs. This process of changing relative magnitude of stresses in compression and tension flanges tended to delay an early crushing of the corners as observed in the tests, resulting in an increase in central deflection. However, at service loads, the stresses in both compression and tension flanges were low. The delay process did not come into effect. Three typical load vs. central deflection curves are shown in Figures 4.4.4, 4.4.5, and 4.4.6. The central deflections at service load, at yielding, and prior to failure are listed in Table 4.4.3.

D. Failure Mode

Except for the 22 gage panels with the smallest w/t ratio of 11.18 to 19.44 (six specimens), the rest of the seventy-two panels failed due to a formation of a local failure mechanism in the constant moment region.

The local failure mechanism usually formed suddenly especially for the panels with larger w/t ratios no matter what design yielding conditions were. Only six 22 gage panels having the w/t ratios around 35 formed the mechanism relatively gradually. The formation of the local mechanism was accompanied by crushing the corners between the flange and webs in compression. Even though the webs were largely deformed prior to failure, it was mainly the largely deformed local buckles in the flange that caused webs to deform out of plane in compatible with buckled waves of the flange. It was noticed from tests that the out-of-plane deformation in the webs recovered after load was released, while the deformations in the flange remained permanent in many panels. This indicated that the web out-of-plane deformation was in elastic nature. The tests showed that the failure of the panels all occurred within the constant moment region if a local failure mechanism formed in the region. The failure mode was apparently a flexural failure mode. Figures 4.4.7, 4.4.8, 4.4.9, 4.4.10, 4.4.11, and 4.4.12 illustrate some typical failures of the panels. A typical case of largely deformed web prior to failure is shown in Fig. 4.4.13.

Based on the above observations, two issues are addressed regarding the effect of the low-ductility and high-strength of the Structural Grade 80 steel on structural performance of flexural members:

Firstly, the effective yield moment of a section is calculated based on the first yielding that occurs in the effective section. An actual section that starts to yield should carry a moment that is equivalent to the predicted effective yield moment. At the first yielding, the strain at the yielding location is the largest in the section. The strain corresponding to the yield strength of the steel is usually much less than the tensile strain (tensile fracture strain) of the steel. Thus, the low ductility of the steel may not have strong effect on the effective yield moment since the steel will not fracture at the first yielding. Low ductility does not mean no ductility. However, the ductility of the steel is important to the strength reserve of a flexural member after the effective yield moment is reached and if a local failure mechanism does not form immediately at the yield moment. This strength reserve is necessary to the increase in overall ductility of the member (raising warning to a failure) and is essential to the moment redistribution in multi-span deck panels (increasing load-carrying capacity).

On the other hand, there is a possibility that the effective yield moment can not be reached because of an early formation of local failure mechanism in a member. This may be due to the high yield strength of the steel. For members made from thinner sheet and with larger w/t ratio, sections may be distorted more severely due to the formation of local buckles at higher compressive stress. The effective area at the corner between compression flange and web may be further reduced to carry much higher stress. The corner can be crushed at a stress that is lower than the high yield strength of the steel. Imperfection may occur in a wide element with larger w/t ratio rather than at the corners between flat elements. Thus, it may cause formation of local buckles at relatively lower stress and reduce effective area at the corners at the lower stress, leading to an early crushing of the corners. Also, the buckled waves of a largely deformed flange along the corner direction may tend to deform the straight corners at a buckled valley, contributing to early crushing of the corners. In addition, at the buckled valley, the compressive stress of the extreme fiber in the already compressed flange under overall bending of a panel is further increased due to the local bending of the flange induced from local buckling. This increase in stress was observed during tests in which the strains at or near a buckled valley were usually higher than the strains at or near a buckled ridge. Thus, it is possible that the larger the w/t ratio, the lower the stress level at which a local failure mechanism forms. The higher the yield strength of a sheet steel, the lower the percentage of the yield strength at which the corners crush since the crushing strain or stress of the corners may not depend on the yield strength of the steel. Calculation of effective yield moment using reduced yield strength of high-strength sheet steels has been addressed elsewhere (Pan 1987).

Secondly, the stress distribution in flexural members and connections is different. In flexural members such as floor decks, highly localized stress concentration does not usually exist unless there are openings in some critical locations of the members or sections change geometry at the regions with large internal forces. However, in connections, highly localized stress concentration usually exist along with out-of-plane deformation of connected elements. Thus, the ductility of a steel, both local and uniform elongations, may be more essential to wipe out the stress concentration in connections rather than in flexural members. In other word, it is the ultimate strength of a structural component, rather than yield strength, that more likely

depends on the ductility of the steel.

4.5 TEST RESULTS FOR PANELS WITH ONE-POINT LOADING CONDITION

Sixteen deck panel specimens were tested with a one-point loading condition, which involved eight different sections, namely the 26 and 22 gage sections with the smallest and the largest w/t ratios as listed in Tables 3.3.2 and 3.3.3 and designed with first yielding in both compression and tension flanges and in tension flange. The only geometrical difference between the panels with one-point and two-point loading conditions was the total length. For each section, two panels were tested. The summary of the test results and behavior of the panels is presented in this section. In the following discussion, the sections designed for first yielding in both compression and tension flanges and in tension flange only are referred to as ct-section and t-section, respectively, for convenience. Since the strain gages could only be located near the edges of the central bearing plate and were a distance away from the center of span, the strain values were converted to the values at the central load using a linear proportion. The reported strain values herein are the converted values.

(1) Panel specimens 1p-t26w0.5h0.5-ct(1,2) and 1p-t26w0.5h0.5-t(1,2): Twelve strain gages for each panel were used near the two edges of the central bearing plate. Predicted yield loads were 574 lbs. for the ct-section and 497 lbs. for the t-section. Local buckling in compression flanges became apparent at a load of about 320 to 420 lbs. The maximum central deflections at service load were L/240 for the ct-section and L/264 for the t-section, where L is the length of span. All the panels indicated yielding using converted strains at central load, with the yield load of 706, 671 lbs. for the ct-section and 563, 559 lbs. for the t-section. After a ultimate load was reached, all the panels failed gradually due to a formation of a local failure mechanism near one edge of the central bearing plate. The ultimate loads were 719, 754 lbs. for the ct-section and 691, 682 lbs. for the t-section. Local buckles gradually increased the local deformation but were limited near the two edges of the central bearing plate. The maximum ratio of central deflection to span at ultimate load was L/42 for the ct-section and L/41 for the t-section. The maximum converted

edge strains or strains in the tension flange at ultimate load were -6365, 9714 microstrains for the ct-section and 13166, 14342 microstrains for the t-section.

(2) Panel specimens 1p-t26w2h1.5-ct(1,2) and 1p-t26w2h1.5-t(1,2): Ten strain gages for each panel were used near the two edges of the central bearing plate. Predicted yield loads were 528 lbs. for the ct-section and 482 lbs. for the t-section. Local buckling in compression flanges became apparent at a load of about 90 to 120 lbs. The maximum central deflections at service load were L/241 for the ct-section and L/270 for the t-section. All the panels indicated yielding using converted strains at central load, with the yield load of 431 lbs. for the ct-section (not available for one panel) and 409, 431 lbs. for the t-section. After a ultimate load was reached, all the panels failed gradually and then quickly due to a formation of a local failure mechanism near one edge of the central bearing plate. The ultimate loads were 454, 442 lbs. for the ct-section and 427, 461 lbs. for the t-section. Local buckles gradually increased the local deformation and largely developed near the two edges of the central bearing plate at ultimate load. The maximum ratio of central deflection to span at ultimate load was L/62 for the ct-section and L/57 for the t-section. The maximum converted edge strains or strains in the tension flange at ultimate load were -7103, -6751 microstrains for the ct-section and 5739, -16288 microstrains for the t-section.

(3) Panel specimens 1p-t22w0.5h0.5-ct(1,2) and 1p-t22w0.5h0.5-t(1,2): Twelve strain gages for each panel were used near the two edges of the central bearing plate. Predicted yield loads were 983 lbs. for the ct-section and 877 lbs. for the t-section. Local buckling in compression flanges did not occur even after ultimate load was reached. The maximum central deflections at service load were L/185 for the ct-section and L/279 for the t-section. All the panels indicated yielding using converted strains at central load, with the yield load of 1279, 1330 lbs. for the ct-section and 1031 lbs. for the t-section (not available for one panel). After a ultimate load was reached, all the panels experienced a very slow decrease in load. Tests were terminated without forming a complete local failure mechanism. Only flanges near one edge of the central bearing plate indicated visible permanent deformation, while web permanent deformation was very small near the flanges. The ultimate loads were 1499, 1529 lbs. for the ct-section and 1335, 1376 lbs. for

the t-section. The maximum ratio of central deflection to span at ultimate load was L/33 for the ct-section and L/32 for the t-section. The maximum converted edge strains or strains in the tension flange at ultimate load were 14973, 14202 microstrains for the ct-section and 23162, 22624 microstrains for the t-section.

(4) Panel specimens 1p-t22w5.5h3-ct(1,2) and 1p-t22w5.5h3-t(1,2): Twelve strain gages for each panel were used near the two edges of the central bearing plate. Predicted yield loads were 758 lbs. for the ct-section and 668 lbs. for the t-section. Local buckling in compression flanges became apparent at a load of about 120 lbs. The maximum central deflections at service load were L/227 for the ct-section and L/235 for the t-section. Three panels indicated yielding using converted strains at central load, with the yield load of 657, 630 lbs. for the ct-section and 631 lbs. for the t-section. After a ultimate load was reached, all the panels failed gradually and soon quickly due to a formation of a local failure mechanism near one edge of the central bearing plate. The ultimate loads were 661, 638 lbs. for the ct-section and 644, 653 lbs. for the t-section. Local buckles gradually increased the local deformation and largely developed near the two edges of the central bearing plate at ultimate load. The maximum ratio of central deflection to span at ultimate load was L/69 for the ct-section and L/62 for the t-section. The maximum converted edge strains or strains in the tension flange at ultimate load were -6039, -7481 microstrains for the ct-section and -12040, -4209 microstrains for the t-section.

Examining the test results for all the tested panels in one-point loading condition, the following observations are made:

A. Yield and Ultimate Loads

Similar to the test results for the two-point loading condition, the panels designed for first yielding in both compression and tension flanges tended to develop the largest yield and ultimate loads and the panels designed for first yielding in tension flange tended to develop the smallest yield and ultimate loads, however this trend is apparent especially for the 26 and 22 gage panels with the smaller w/t ratios. For the panels

with the larger w/t ratios, this trend does not appear to exist.

B. Yield and Maximum Strains Prior to Failure

Fifteen out of sixteen panels indicated yielding in cross section using the converted strains at the central load. Comparing the test results for the two-point loading condition, the converted ultimate strains at the central load for all the panels with one-point loading condition tended to be larger than the ultimate strains measured in the constant moment region for the two-point loading condition. Only one of the 22 gage panels with the largest w/t ratio did not indicate yielding in cross section, but the converted strain at the central load was larger than 4000 microstrains which corresponded to a stress level of at least 95 ksi for this sheet. Also for this panel, it was observed that the local failure mechanism formed out side of the strain gage where the maximum strain reading was recorded. Even though all the panels indicated yielding with a one-point loading condition, the panels with smaller w/t ratios tended to develop higher ultimate strains than the panels with larger w/t ratios. The maximum compressive and tensile strains in the same section at yielding and prior to failure are listed in Table 4.5.1 and 4.5.2.

C. Maximum Central Deflection at Service Load and Prior to Failure

Similar to the test results with the two-point loading condition, for all the panels with a one-point loading condition, the maximum central deflection prior to failure was largest for the sections designed with first yielding in tension flange only and the smallest for the sections designed with first yielding in compression flange only. However, under the service loads, this trend did not exist in all the panels. Figures 4.5.1 and 4.5.2 illustrate two typical load vs. central deflection curves. The central deflections at service load, at yielding, and prior to failure are listed in Table 4.5.3.

D. Failure Mode

Except for the 22 gage panels with the smallest w/t ratio, all the panels failed gradually due to a formation of a local failure mechanism near one edge of the central bearing plate after the ultimate load was reached. The local failure mechanism in the 26 gage panels with smaller w/t ratio was initiated gradually and further developed slowly until tests were terminated due to relatively large drop of load. For the panels with larger w/t ratios, the local failure mechanism was initiated gradually, but soon quickly developed along with a large drop of load. Similar to the test results in two-point loading condition, the local failure mechanism was characterized by crushing the corners between flange and webs in compression at a flange buckled valley. The failure mode for all the panels was apparently flexural failure even though all the failures occurred in the region where both moment and shear forces co-existed. For the 22 gage panels with smaller w/t ratio, slight permanent deformation near one edge of the central bearing plate was observed only in flange after test. Webs had very small permanent out-of-plane deformation near the compression flange. Some failed panels are shown in Figures 4.5.3 and 4.5.4.

4.6 TEST RESULTS FOR PANELS WITH SCREWS

Five deck panel specimens with self-driven screws penetrating through tension flanges were tested with a two-point loading condition. The use of the screws was to study the effect of stress concentration near the holes created by the screws on the strength and ductility of the panels. The five panels involved with five different sections which are listed in Table 3.1.3. Of the five sections, four were designed for first yielding in compression flange, and one for first yielding in tension flange. The dimensions and the test setup of the panels with screws were the same as those of the panels without screws for the two-point loading condition, except that three pairs of self-driven screws were drilled through the tension flange in the constant moment region. The test results of the panels with screws are summarized as follows.

(1) Panel specimen 2ps-t26w0.5h0.5-c: This panel had a 17% of reduction in tension flange at the screw

locations. The distances between two pairs of the screws in the span direction was 7" and 3-3/4". The test showed that the behavior of the panel was similar to that of 2p-t26w0.5h0.5-c. The predicted yield load was 720 lb, while the tested yield load was 753 lb. The panel experienced a sudden failure due to the crushing of the compression flanges within the constant moment region. The failure was similar to that observed in 2p-26w0.5h0.5-c. No tension fracture near the holes at all screw locations was observed after the test. The tested ultimate load was 785 lb. The maximum central deflection at failure was L/15, where L is the span length. At failure the measured compressive edge strain ranged from -6891 to -10077 microstrains, and the measured strain in the tension flanges ranged from 3686 to 3848 microstrains.

(2) Panel specimen 2ps-t26w2.0h1.5-c: This panel had a 20% of reduction in tension flange at the screw locations. The distances between two pairs of the screws in the span direction was 7" and 3-1/8". The test showed that the behavior of the panel was similar to that of 2p-t26w2.0h1.5-c. The predicted yield load was 675 lb. The strain gage reading did not indicate yielding in the section. The panel experienced a sudden failure due to the crushing of the compression flanges within the constant moment region. The failure was similar to that observed in 2p-26w2.0h1.5-c. No tension fracture near the holes at all screw locations was observed after the test. The tested ultimate load was 547 lb. The maximum central deflection at failure was L/39, where L is the span length. At failure the measured compressive edge strain ranged from -1898 to -3425 microstrains, and the measured strain in the tension flanges ranged from 2540 to 2796 microstrains.

(3) Panel specimen 2ps-t22w0.5h0.5-c: This panel had a 13% of reduction in tension flange at the screw locations. The distances between two pairs of the screws in the span direction was 6-3/4" and 3-9/16". The test showed that the behavior of the panel was similar to that of 2p-t22w0.5h0.5-c. The predicted yield load was 1288 lb, while the tested yield load was 1457 lb. Similar to what was observed in 2p-26w0.5h0.5-c, the crushing of the compression flanges did not occur before the test was terminated. The tested ultimate load was reached at 1618 lb. After the ultimate load, sections within one of the braced segments in the constant moment region tended to open up, resulting in a gradual decrease in applied load. The test was

terminated because of excessively large displacement. No tension fracture near the holes at all screw locations was observed after the test. The maximum central deflection at failure was L/11, where L is the span length. At the termination of the test, the measured compressive edge strain ranged from -8912 to -10497 microstrains, and the measured strain in the tension flanges ranged from 4297 to 4622 microstrains.

(4) Panel specimen 2ps-t22w0.5h0.5-t: This panel had a 27% of reduction in tension flange at the screw locations and was the only panel designed for first yielding in tension flange in this five panel group. The distances between two pairs of the screws in the span direction was 6-3/4" and 3-5/16". The test indicated that the behavior of the panel was different from that of 2p-t26w0.5h0.5-c only after a plateau portion of the load-deflection curve of the panel was reached and further extended. The predicted yield load was 1040 lb, while the tested yield load was 1183 lb. After the panel entered the plateau portion of its load-deflection curve, sections in the largest unbraced segment of the panel within the constant moment region tended to open up. The tested ultimate load was reached at 1237 lb. Shortly after the ultimate load, the panel experienced a sudden drop of applied load due to a formation of tensile fracture near the holes at two screws and necking in tension flanges at all screw locations. At this moment, no failure in compression flanges and webs was observed in the panel. The test was soon terminated. The maximum central deflection at failure was L/10, where L is the span length. At failure the measured compressive edge strain ranged from -6364 to -7301 microstrains, and the measured strain in the tension flanges ranged from 6694 to 7838 microstrains.

(5) Panel specimen 2ps-t22w5.5h3.0-c: This panel had a 25% of reduction in tension flange at the screw locations. The distances between two pairs of the screws in the span direction was 11-5/8" and 7-1/2". The test showed that the behavior of the panel was similar to that of 2p-t22w5.5h3.0-c. The predicted yield load was 1238 lb, while the tested yield load was 1111 lb. The tested ultimate load was reached at 1115 lb. The panel experienced a sudden failure due to the crushing of the compression flanges within the constant moment region. The failure was similar to that observed in 2p-22w5.5h3.0-c. No tension fracture near the holes at all screw locations was observed after the test. The maximum central deflection at failure was

L/57, where L is the span length. At failure the measured compressive edge strain ranged from -2877 to -6477 microstrains, and the measured strain in the tension flanges ranged from 2194 to 2727 microstrains.

Examining the test results for all the panels with screws, the following observations are made:

A Yield Loads, Ultimate Loads, and Central Deflection at Failure

Even though the tension flanges of the five panels with screws were reduced by as much as 27% at three screw locations within the constant moment region, the yield and ultimate loads of the panels were similar to those of the counterpart panels without screws. The behavior of the panels with screws were also similar to that of the panels without screws, except for the panel 2ps-t22w0.5h0.5-t which demonstrated a sudden drop of the applied load after a plateau in the load-displacement curve was reached. The drop of the load was due to a formation of tensile fracture and necking near the holes at the screw locations. This panel 2ps-t22w0.5h0.5-t had the largest reduction in tension flanges (27%) and was designed to result in the largest tensile stress in the tension flanges. The central deflection of the panel at failure happened to be close to that of the panel 2p-t22w0.5h0.5-t without screws.

B Failure Mode

The failure mode of the panels with screws was also similar to that of the counterpart panels without screws as shown in Figures 4.6.1 and 4.6.2, except for one 22 gage panel with a 27% of reduction in tension flanges and designed for first yielding in compression flanges. This panel failed due to a formation of tensile fracture and necking near the holes at screw locations as illustrated in Figures 4.6.3 and 4.6.4, while its counterpart panel without screws did not fracture at the termination of applied load.

5. EVALUATION OF TEST RESULTS

The test results of the seventy-two deck panel specimens with a two-point loading condition, the sixteen panels with a one-point loading condition, and the five panels with screws for the two-point loading condition were evaluated using the AISI Specification (AISI 1986), actual and specified material properties, and the measured dimensions. This section presents the results of the evaluation. In the following discussion, Section 5.1 evaluates the test results for the two-point loading condition. Section 5.2 deals with the test results for the one-point loading condition. A comparison of the test results between the panels with two-point and one-point loading conditions is presented in Section 5.3. Finally, Section 5.4 evaluates the test results for the panels with screws.

5.1 EVALUATION OF TEST RESULTS IN TWO-POINT LOADING CONDITION

For the two-point loading condition, the deck panels had one constant moment region where shear forces did not exist. As discussed in Section 4, the failure of the panels all occurred within this constant moment region when a local failure mechanism formed in the region. Thus, the tested moments can be compared with the effective moments calculated without shear and web-crippling interaction. Tested moments were determined from the tested loads for all the panels.

The tested flexural strengths of the seventy-two panels with a two-point loading condition were compared to the predicted strengths using the AISI Specification (AISI 1986) and the measured dimensions. The effective moments were predicted using the actual yield strength, 75% of the actual yield strength, the specified 60 ksi (413.7 MPa), and a yield strength reduction factor developed by Pan (1987). In addition, the tested central deflections at service loads were compared with predicted deflections using the effective section properties. Moment-to-weight ratios were calculated to check the effectiveness of the panels. The modulus of elasticity was taken as 29,500 ksi (203 GPa) for all the strength calculations. The results of the

evaluation are summarized as follows.

A. Effective Moments

As the current practice of designing cold-formed flexural members made of the Structural Grade 80 steel requires the use of 75% of the specified minimum yield strength, the effective moments of the panels were predicted using the specified 60 ksi (equal to 75% of the specified minimum yield strength (80 ksi (551.6 MPa)) of the steel) as listed in Table 5.1.1 and compared to the tested ultimate moments for all the panels as shown in Fig. 5.1.1 and Table 5.1.2. Figure 5.1.1 indicates that for all the panels, the ratio of the tested ultimate moment to the calculated effective moment using the 60 ksi is larger than 1.2. The moment ratio ranges from 1.60 to 2.23 for the panels with the average w/t ratio varying from 17.93 to 61.07, and ranges from 1.22 to 1.72 for the panels with the average w/t ratio varying from 102.86 to 189.95. This demonstrates that the predicted flexural strength of cold-formed steel decks made of the Structural Grade 80 steel by using the specified 60 ksi stress is conservative. As shown in Fig. 5.1.1, the moment ratios tend to decrease with increases in the w/t ratios.

Figure 5.1.2 and Table 5.1.3 also show the ratios of the tested ultimate moment to the calculated effective moment by using 75% of the actual yield strength of the steel against the w/t ratios. The stress levels corresponding to the 75% of the actual yield strength are 83.3, 84.4, and 77.9 ksi for the 28, 26, and 22 gage steel sheets, respectively. These stress levels are close to the specified minimum yield strength of the Structural Grade 80 steel (80 ksi (551.6 MPa)). It is clear in the figure that the moment ratios all tend to be larger than 1.0. The moment ratio ranges from 1.27 to 1.58 for the panels having the average w/t ratio varying from 17.93 to 61.07, and ranges from 0.99 to 1.29 for the panels having the average w/t ratio varying from 102.86 to 189.95. As a result, the predicted flexural strength of the panels using 75% of the actual yield strength is also conservative, especially for the low w/t ratios.

The tested ultimate moments are compared with the effective yield moments calculated by using the actual

yield strength of the steel as shown in Table 5.1.4 and Fig. 5.1.3 for all the tested panels. The figur indicates that the ratio of the tested ultimate moment to the calculated effective yield moment using th actual yield strength decreases from 1.25 to about 0.80 with increases in the w/t ratios. The moment ratio are usually larger than 1.0 for the w/t ratios of 61.07 or less, and less than 1.0 for the w/t ratios of 102.8(or larger, with a tendency to converge to 0.85 at larger w/t ratios (120 to 190). The moment ratio range: from 0.97 to 1.24 for the panels having w/t ratios varying from 17.93 to 61.07, with only three values les: than 1.00 (0.97, 0.99, and 0.99), and the ratio ranges from 0.81 to 1.00 for the panels having w/t ratios varying from 102.86 to 189.95. It is also noted from Figure 5.1.3 that the highest moment ratios tend to be achieved for the sections designed with first yielding in tension flange as compared to the sections designed with first yielding in compression flange and in both compression and tension flanges.

A comparison between the tested yield moments and the calculated effective yield moments using the actual yield strength of the steel is shown in Table 5.1.5 and Fig. 5.1.4. Similar to what is observed in Fig. 5.1.3, the ratio of the tested yield moment to the calculated effective yield moment by using the actual yield strength of the steel decreases with increases in the w/t ratios, with a tendency of converging to 0.80 at the larger w/t ratios (120 to 190). The lower moment ratios correspond to the panels with the larger w/t ratios, in which the chance of yielding in a section is small. The moment ratio ranges from 0.96 to 1.23 for the panels having w/t ratios varying from 17.93 to 61.07, and ranges from 0.80 to 1.00 for the panels having w/t ratios varying from 102.86 to 189.95. Figure 5.1.4 and Table 5.1.5 illustrate that the tested yield moments are predicted reasonably well by the calculated effective yield moments for the w/t ratios of 61.07 or less. Figure 5.1.4 also indicates that larger moment ratios tend to be achieved with the panel sections designed for the first yielding in tension flange only.

B. Effective Moment Using Yield Strength Reduction Factor Developed by Pan (1987)

Because the ultimate strains in deck panels made of high-strength steel and having larger w/t ratios are often lower than the yield strain, the equation, developed by Pan (1987) to account for a yield strength reduction

when predicting the effective moment, was used to predict the effective moments of the panel sections designed for the first yielding in compression flange and in both compression and tension flanges. The yield strength reduction factor was derived to reduce the design yield stress in the effective width formulas stated in Section B2.1 and B3.1 of the Specification (AISI 1986). The reduction factor is only applicable for the stiffened elements with a w/t ratio ranging from 17.7 to 136.7, a yield strength ranging from 84.3 to 153.3 ksi, and a value of $(\sqrt{w/t})(\sqrt{F_y/E})$ ranging from 0.286 to 0.843 (Pan 1987). The percent elongation in a 2-inch gage length of the steels ranged from 4.3 to 20.4%. The factor for stiffened elements is written as:

$$\varphi_s = 1.0 - 0.2 \sqrt{\left(\frac{w}{t}\right)} \sqrt{\left(\frac{F_y}{E}\right)} \qquad (5\text{-}1)$$

Where w= full width of stiffened element.

t= thickness of sheet steel.

F_y= yield stress of steel.

E= modulus of elasticity, 29,500 ksi.

For the panels tested in this study, the average w/t ratio ranged from 17.93 to 189.95, the yield strength from 103.9 to 112.5 ksi, and the $(\sqrt{w/t})(\sqrt{F_y/E})$ value from 0.251 to 0.818. It is noted that except for some w/t ratios, the equation is basically applicable for the panels in this study.

The effective moments for the panels designed with first yielding in compression flange only and in both compression and tension flanges were then calculated using the yield strength reduction factor, and compared with the tested yield moments of the panels as shown in Table 5.1.6. Figure 5.1.5 shows the ratios of the tested yield moment to the effective moment calculated using the reduction factor plotted against the w/t ratios. As indicated in Table 5.1.6, the moment ratio ranges from 1.03 to 1.24 for the panels with w/t ratios varying from 17.93 to 61.07, and ranges from 0.88 to 1.05 for the panels with w/t ratios varying from 102.86 to 189.95. It is noted that a slight improvement in predicting the yield moment is achieved with the use of the reduction factor for the panels with the w/t ratios of 102.86 or larger.

However, the prediction using the reduction factor is conservative for the panels with the w/t ratios of 61.07 or less when compared to the moment ratios determined without the reduction factor shown in Fig. 5.1.4 and Table 5.1.5.

C. Central Deflection

In many applications in building construction, cold-formed steel deck panels are often manufactured with thin steel sheets and shallow depth. Deflection of the deck panels can be a controlling factor in design of the panels rather than the strength of the panels. As a result, appropriate prediction of the maximum deflection of the deck panels under service loads or at effective yield moment is necessary in design practice. In this regard, the central deflections of the deck panel specimens at service loads were predicted using the actual dimensions and the section properties under service moment, and compared with the tested central deflections of the panels. The service loads were determined from the service moments which are the effective yield moments calculated using the specified stress of 60 ksi, divided by the safety factor of 1.67. The section properties under the service moment was then calculated through an iterative process. The tested deflections were obtained from the recorded central deflections at a tested load that is equivalent to the calculated service load.

The ratios of the tested central deflection to the calculated central deflection at service load are listed in Table 5.1.7 and the ratios are also shown in Fig. 5.1.6 against the w/t ratios of the panels. The modulus of elasticity of 29,500 ksi was used in predicting the central deflections. It is noted in the table and the figure that the deflection ratios are usually smaller than one except for three values (1.00, 1.02, and 1.05 for the panels with smaller w/t ratios) and tend to decrease with increases in the w/t ratios. This indicates that the central deflections of the panel specimens were overpredicted using the calculated service moments, resulting in a conservative solution.

Since the calculated central deflections are usually larger than the tested deflections, the central deflections

of the panel specimens were also predicted using the actual tested modulus of elasticity which was usually larger than 29,500 ksi. The average tested modulli of elasticity were 30,342, 30,526, and 31,755 ksi for the 28, 26, and 22 gage steel sheets, respectively. The ratios of the tested central deflection to the calculated central deflection using the actual modulus of elasticity are listed in Table. 5.1.8 and the ratios are shown in Fig. 5.1.7 against the w/t ratios. As compared with Fig. 5.1.6, some improvement on predicting the central deflection was made, but not significant. The tested central deflections are usually smaller than the calculated ones especially for the panels with larger w/t ratios.

The central deflections of the panel specimens were also predicted at the effective yield moment calculated using the actual yield strength of the steel. The modulus of elasticity of 29,500 ksi was used in the calculation. The ratios of the tested central deflection to the calculated deflection at the effective yield moment are listed in Table 5.1.9 and Fig. 5.1.8 shows the ratios against the w/t ratios of the panels. It is noted that the deflection ratios are all larger than one except for three values (0.93, 0.96, and 0.99). This indicates that the calculated central deflections underestimate the actual deflections at the yield moments. Since the proportional limit of the Structural Grade 80 steel is lower than the yield strength of the steel, the deck panels can behavior nonlinearly prior to yielding. And this nonlinearity in material property can lead to an increase in deformation, resulting in a larger deflection. Therefore, predicting the deflection of the deck panels beyond the proportional limit should be carried out using an appropriate method as suggested by Fertis (1994) to consider geometric and material nonlinearity.

E. Moment-to-Weight Ratio

As far as economical design is concerned, the ratio of the tested yield moment to weight per feet of section was computed for all the panel specimens designed with different f_t/f_c ratios and plotted against the w/t ratios as shown in Fig. 5.1.9. It is apparent that the panels designed for first yielding in both compression and tension tend to result in higher moment-to-weight ratios as compared to the panels designed for first yielding in either compression or tension flange only. Even though with larger w/t ratios, the panels with

larger h/t ratios and thicker steel sheet result in larger moment-to-weight ratios, that is, more economical design.

The ratio of the tested ultimate moment-to-weight per feet of section was computed for all the panels and is plotted against the w/t ratios as shown in Fig. 5.1.10. The panels designed for first yielding in both compression and tension flanges and in tension flange only tend to result in larger moment-to-weight ratio than those designed for first yielding in compression flange. However, this trend does not seem to be significant for the thicker 22 gage section. Again, the panels with larger h/t ratios and thicker steel sheet result in larger moment to weight ratios.

5.2 EVALUATION OF TEST RESULTS IN ONE-POINT LOADING CONDITION

For the one-point loading condition, tested moments of the sixteen panels were also determined from the tested loads, and compared to the predicted effective moments using the AISI Specification (AISI 1986) and the measured dimensions. The effective moments were predicted using the actual yield strength, 75% of the actual yield strength, the specified 60 ksi (413.7 MPa), and yield strength reduction factor developed by Pan (1987). In addition, the tested central deflections at service load were compared with predicted deflections using the effective section modulus. Moment-to-weight ratios were calculated to check the effectiveness of the panels. The modulus of elasticity was taken as 29,500 ksi (203 GPa) for all the strength calculations. The results of the evaluation are summarized as follows.

A. Effective Moments

The effective moments of the sixteen panels predicted using the specified stress of 60 ksi are listed in Table 5.1.1 and compared to the tested ultimate moments of the panels as shown in Fig. 5.2.1 and Table 5.2.1. Figure 5.2.1 indicates that for all panels, the ratio of the tested ultimate moment to the calculated effective moment using the 60 ksi is larger than 1.4. The moment ratio ranges from 1.42 to 2.71 for all the panels

with the w/t ratio varying from 17.93 to 189.95. The predicted effective moments using the specified 60 ksi stress is apparently conservative. As shown in Fig. 5.2.1, the moment ratios decrease with increases in the w/t ratios.

The ratios of the tested ultimate moment to the effective moment calculated using the 75% of the actual yield strength of the steel are also listed in Table 5.2.1 and shown in Figure 5.2.1 against the w/t ratios. Figure 5.2.1 indicates that the moment ratios are all larger than 1.0, ranging from 1.11 to 2.09, and decrease with increases in the w/t ratios. As a result, the effective moment predicted using the 75% of the actual yield strength is also conservative.

The tested ultimate moments are compared with the effective yield moments calculated by using the actual yield strength of the steel as shown in Table 5.2.2 and Fig. 5.2.2 for all the sixteen panels. The figure indicates that the ratio of the tested ultimate moment to the calculated effective yield moment using the actual yield strength decreases from 1.59 to 0.85 with increases in the w/t ratios. The moment ratios are larger than 1.0 for the w/t ratios of 31.65 or less and less than 1.0 for the w/t ratios of 118.64 or larger, with a tendency to converge to 0.85 at larger w/t ratios (120 to 190). It is also shown in Figure 5.2.2 that the larger moment ratios tend to be developed for the sections designed with first yielding in tension flange as compared to the sections designed with first yielding in both compression and tension flanges.

A comparison between the tested yield moments and the effective yield moments calculated using the actual yield strength of the steel is made as shown in Table 5.2.3 and Fig. 5.2.3. Figure 5.2.3 indicates that the ratio of the tested yield moment to the effective yield moment calculated using the actual yield strength decreases from 1.37 to 0.83 with increases in the w/t ratios, with a tendency of converging to 0.80 at the larger w/t ratios (120 to 190). For the panels with the smaller w/t ratios, the calculated effective yield moment conservatively predicts the tested yield moment, and the larger moment ratios were developed for the panels designed with first yielding in both compression and tension flanges. However, for the panels with the larger w/t ratios, the effective yield moment overestimates the tested yield moment, and the larger

moment ratios tend to be achieved with the panels designed with first yielding in tension flange only.

B. Effective Moment Using Yield Strength Reduction Factor Developed by Pan (1987)

The effective moments of the panels designed with first yielding in both compression and tension flanges were calculated using the yield strength reduction factor developed by Pan (1987), and compared with the tested yield moments of the panels as listed in Table 5.2.4. The ratios of the tested yield moment to the effective moment calculated using the reduction factor are shown in Figure 5.2.4 against the w/t ratios, with the moment ratio ranging from 0.92 to 1.44 for all the panels. The calculated effective moment using the reduction factor predicts reasonably well the tested yield moment for the panels with the larger w/t ratios. However, the prediction using the reduction factor is conservative for the panels with the smaller w/t ratios.

C. Central Deflection

The central deflections of the panel specimens at service loads were predicted using the same method as used for the panels with the two-point loading condition, and compared with the tested central deflections of the panels. The ratios of the tested central deflection to the calculated central deflection at service load are listed in Table 5.2.5 and are shown in Fig. 5.2.5 against the w/t ratios. The modulus of elasticity of 29,500 ksi was used in predicting the central deflections. Figure 5.2.5 illustrates that the deflection ratios are usually smaller than 1.0 except for two values (1.25 and 1.27 for the panels with the smallest w/t ratios). This indicates that the central deflections of the panels were usually overestimated using the calculated service moments.

The central deflections of the panels were also predicted at the effective yield moment calculated using the actual yield strength of the steel. The modulus of elasticity of 29,500 ksi was used in the calculation. The ratios of the tested central deflection to the calculated deflection at the effective yield moment are listed in Table 5.2.6 and Fig. 5.2.6 shows the ratios against the w/t ratios. It is noted that the deflection ratios are

basically larger than 1.0 for the panels with the smaller w/t ratios and less than but close to 1.0 for the panels with the larger w/t ratios, ranging from 0.92 to 1.20 for all the panels. The relative smaller ratios for the panels with the larger w/t ratios may be attributed to smaller tested central deflections obtained based on converted yield strains at the central load location.

E. Moment-to-Weight Ratio

The ratio of the tested yield moment-to-weight per feet of section and the ratio of the tested ultimate moment-to-weight per feet of section were computed for all the sixteen panels and plotted against the w/t ratios as shown in Figures 5.2.7 and 5.2.8. It is noted that the difference in the moment-to-weight ratio is not significant between the panels designed with first yielding in both compression and tension flanges and the panels designed for first yielding in tension flange only. The panels with larger h/t ratios and thicker steel sheet resulted in larger moment to weight ratios.

5.3 COMPARISON OF TEST RESULTS BETWEEN THE TWO LOADING CONDITIONS

The test results of the sixteen panels having two-point loading condition and the sixteen panels having one-point loading condition were compared since they had the same section dimensions and calculated effective moments of the sections, except loading condition and length of span. As stated in Sections 5.1 and 5.2, all the panels with the two-point loading condition failed in the constant moment region while all the panels with the one-point loading condition failed in the region where both moment and shear forces existed at the same time. Thus, it is necessary to compare the flexural strength and behavior of the panels in both loading conditions to examine any effect on flexural strength due to shear force. The comparison was focused on tested yield moment, tested ultimate moment, measured maximum strain prior to failure, and failure mode. The results of the comparison are presented in the following subsections.

Tested Yield and Ultimate Moments

Average tested yield moments of the panels with two-point loading condition were compared with average tested yield moments of the panels with one-point loading condition as listed in Table 5.3.1. The ratio of the average tested yield moment in one-point loading condition to the average tested yield moment in two-point loading condition is plotted against the w/t ratios as shown in Fig. 5.3.1. The tested yield moments for the one-point loading condition were obtained based on the converted yield strains at the center of the span. Figure 5.3.1 shows that the moment ratio tends to be larger than 1.0 with the ratio ranging from 0.95 to 1.27 (only two ratios less than 1.0 (0.95 and 0.99)). This indicates that the tested yield moments for the one-point loading condition tended to be larger than the tested yield moment for the two-point loading condition, especially for the panels with the smaller w/t ratios. The higher ratio associated with the smaller w/t ratios may be attributed to a less accurate estimation of the converted yield strains at the central load for the panels in one-point loading condition, where a relatively larger ratio of the length of bearing plate to the length of span exited.

The ratios of the average tested ultimate moment for the one-point loading condition to the average tested ultimate moment for the two-point loading condition were also calculated as listed in Table 5.3.1 and plotted against the w/t ratios as shown in Fig. 5.3.1. As indicated by the figure, the moment ratios are all larger than 1.0 with the ratio varying from 1.00 to 1.37 for the w/t ratio ranging from 17.93 to 189.95 and tend to decrease with increases in the w/t ratios. The larger moment ratios are achieved for the panels with the smaller w/t ratios. The moment gradient appeared to increase the ultimate moment of the panels with a one-point loading condition. It suggests that the shear force in the panels in one-point loading condition does not, in this case, have significant effect on the tested ultimate moments of the panels due to smaller shear effect on bending moment. The maximum tested shear forces that occurred in the panels in both two-point and one-point loading conditions are compared with the shear capacities of the panels as listed in Table 5.3.2. The ratios of the maximum tested shear force to the shear capacity are shown in Fig. 5.3.2. For the one-point loading condition, the shear ratio varies from 0.12 to 0.17, while in two-point loading condition

the shear ratio varies from 0.12 to 0.26. Apparently the shear effect on bending moment is small.

Ultimate Strain Prior to Failure

The ultimate strains of the panels in both two-point and one-point loading conditions are listed in Tables 4.4.2 and 4.5.2 and plotted against the w/t ratios as shown in Fig. 5.3.3. The ultimate strains in one-point loading condition were the converted strains at the central load, obtained from the measured strains at the edges of the central bearing plate of the panels. It is noted that the ultimate strains of the panels in one-point loading condition tend to be larger than the ultimate strains of the panels in two-point loading condition for all the w/t ratios considered. This may lead to the higher ratio of the tested ultimate moment in one-point loading to the tested ultimate moment in two-point loading as discussed above. All the ultimate strains are less than the elongation in 2-inch gage length of the steel (2.4% for the 26 gage steel sheet and 3.67% for the 22 gage steel sheet), which is consistent with the observation that tensile fracture did not occur in all the panels. As shown in Fig. 5.3.3, the ultimate strains tend to decrease with increases in the w/t ratios in both loading conditions.

Failure Mode

As discussed in Section 4, the failure of the panels having a two-point loading condition was characterized by a formation of a local failure mechanism in the constant moment region where shear force did not exist. The local failure mechanism was initiated by crushing the corners between flange and webs in compression. For the 22 gage panels with the smallest w/t ratio, the failure did not occur before tests were terminated. Similar to the panels with a two-point loading condition, all the panels with a one-point loading condition failed due to a formation of a local failure mechanism near one edge of the central bearing plate. The local failure mechanism was also initiated by crushing the corners between flange and webs in compression. It was noticed during tests that the process of forming a complete local failure mechanism was more gradual in the panels with a one-point loading condition than in the panels with a two-point loading condition.

However, prior to forming the local failure mechanism, the panels with smaller w/t ratios for the two-point loading condition demonstrated a plateau in the load vs. central deflection curve, while this plateau usually was not developed in the panels with the one-point loading condition.

Based on all test results of the eighty-eight deck panels, it is found that the low ductility of the Structural Grade 80 of ASTM A653 steel does not appear to have an adverse effect on the flexural strength of the tested panels having either two-point or one-point loading condition. This is due to the fact that the recorded ultimate strains prior to failure of the panels were less than the percent elongation in a 2-inch (50.8 mm) gage length of the steel. The corners between the flange and webs tended to crush in compression at a certain strain level, resulting in a formation of a local failure mechanism and a failure of the panels prior to reaching a much higher strain level. The level of strain at which the corners crushed appeared to depend on the w/t ratio of the flange, possibly the h/t and R/t ratios of the webs and the corners respectively, and moment gradient if the presence of shear forces has low magnitude along with moment, but could not reach the ultimate strain of the steel in the panels studied.

In addition, the F_u/F_y ratio of the steel, ranging from 1.03 to 1.06 for the 28, 26, and 22 gage sheets, does not appear to have significant effect on yield moment of the panels. This is justified by the fact that with the same low tensile-to-yield ratio for all the panels, the yield moments were usually reached for the panels with smaller w/t ratios, while were rarely reached for the panels with larger w/t ratios. As indicated in the First Progress Report (Wu, Yu, and LaBoube 1995), the 2% offset yield strength of the steel was reached before entering the plateau in the stress-strain curves of the steel sheets. The low F_u/F_y ratio does not come into effect to strongly affect the behavior of the flexural members prior to yielding. However, how the low F_u/F_y ratio of the steel can affect the ultimate moment and overall ductility of the panels with smaller w/t ratios deserves further study since the strain in the panels with smaller w/t ratios can be far beyond the yield strain of the steel. The point here is that if the strain that causes crushing of the corners between the flange and webs is a limited value and smaller than the tensile strain of the steel, the low F_u/F_y ratio of the steel may not continuously increase the ultimate moment of the panels after the plateau in the stress-strain curve

is reached, but may reduce overall ductility of the panels due to a possibly fast spread of plasticity in the cross section that yields first and without large spread of plasticity along the length of high moment regions.

5.4 EVALUATION OF TEST RESULTS FOR PANELS WITH SCREWS

The concern for the performance of the panels with screws penetrating through tension flanges is about whether the reduction in tension flanges due to the use of screws in the low-ductility steel sheets may affect the structural performance of the panels, specifically the strength and deformation capacity of the panels. As discussed earlier, the reduction in tension flanges of the tested panels with screws ranged from 13% to 27% of gross area of the tension flanges. This amount of reduction in tension flanges may be considered to be excessive, but it may be possible in the construction. Also it was intended to amplify the effect of the holes in this study. In the following discussion, the tested moments and displacements of the panels with screws are compared with those of the panels without screws to evaluate the effect of the holes on structural performance of the panels. The dimensions of the panels with screws were the same as those of the panels without screws except that the holes in tension flanges were caused by screws.

A. Tested Yield and Ultimate Moments

The tested yield and ultimate moments of the panels with screws are compared with those of the panels without screws as shown in Table 5.4.1 and Fig. 5.4.1. It is clear that the tested yield and ultimate moments of the panels with screws are close to and tend to be slightly larger than those of the panels without screws. Apparently in this test program, the holes in the tension flanges created by the screws did not appear to have a significant effect on the structural performance of the panels, including ultimate strength and failure mode as shown in Figures 4.6.1 and 4.6.2. This may be because, for the panels that failed due to a formation of a local failure mechanism and were designed for first yielding in compression flanges, the recorded tensile strains in the tension flanges were lower than their yield strains at the time of failure. This was especially true for the panels with larger w/t ratios, since at failure, the yield strength of the steel could not usually

be reached in these panels designed for first yielding in either the compression or tension flange. Even for the panels with smaller w/t ratios and designed for first yielding in compression flange, the recorded tensile strains were still lower than their yield strains after a ultimate load was reached and sections in the largest unbraced segment tended to open up. As a result, the stress concentration near the holes at the screw locations could not be raised to a level that could cause tensile fracture in the tension flanges before compression flanges were crushed to form a local failure mechanism.

A different situation exists for the panel 2ps-t22w0.5h0.5-t. This panel had the largest reduction of area in tension flanges (27%) and was designed for first yielding in tension flanges (to result in a larger stress in tension flanges). Even though the panel achieved a ultimate load that was slightly higher than that of its counterpart without screws, it eventually failed due to the tensile fracture formed near the holes at the screw locations as shown in Figures 4.6.3 and 4.6.4. In contrast, this failure mode did not occur in its counterpart panel without screws. In the test of this counterpart panel, the sections in the largest unbraced segment tended to open up, resulting in a slight decrease in applied load after a ultimate load was reached. The test was terminated because of excessive large deformation of the panel. Based on this observation, it is possible that the effect of the holes on structural performance of the panels can be significant. For this situation to occur, the panel has to be designed with a substantially higher ratio of extreme fiber tensile stress to extreme fiber compressive stress in the section, and the tension flanges have to be largely reduced by the use of screws. In addition, the w/t ratio of the compression flanges has to be small.

B. Maximum Central Displacement Prior to Failure

The ratios of the maximum central displacements of the panels with screws to those of the panels without screws at failure are shown in Table 5.4.2 and Fig. 5.4.2. Apparently the maximum displacements of the panels with screws at failure are similar to those of the panels without screws. This also indicates that the holes considered in this test program did not have significant effect on structural performance of the panels. For the panel that failed in tensile fracture near the holes, the fairly good comparison of the displacement

of this panel with that of the panel without screws may be attributed to the particular amount of reduction in tension flanges. If the tension flanges were reduced by more than 27%, the situation could be different.

C. Failure Mode

The failure mode of the panels with screws was similar to that of the panels without screws. Only one 22 gage panel with the smallest w/t ratio and designed for first yielding in tension flange experienced tensile fracture and necking near the holes. The tensile fracture caused a sudden reduction of applied load after the panel entered a plateau in its load-displacement curve, while this did not occur for the counterpart panel without screws. Figures 4.6.3 and 4.6.4 illustrate the fracture failure of the panel.

6. DEVELOPMENT OF MODIFIED YIELD STRENGTH REDUCTION FACTOR FOR DESIGN OF DECK PANELS USING HIGH-STRENGTH STEELS

The test results discussed in Sections 4 and 5 reveal that it is conservative to predict the flexural strength of the deck panels made of the Structural Grade 80 of ASTM A653 steel by using the 75% of the specified minimum yield strength of the steel or 60 ksi (whichever is less) and the AISI Specifications (AISI 1991, 1986). The test results also indicate that the flexural strength of the panels with smaller w/t ratios can be predicted reasonably well by using the actual yield strength of the steel. However, for the panels with larger w/t ratios, the flexural strength predicted by using the actual yield strength of the steel is larger than the tested flexural strength of the panels, resulting in a nonconservative solution. To reflect these observations, a modified yield strength reduction factor was developed to be used along with the AISI effective width equation for designing the flexural members made of the Structural Grade 80 steel. In the following discussion, Section 6.1 reviews the background for the AISI design approach and the development of the yield strength reduction factor. Section 6.2 discusses the development of a modified yield strength reduction factor. Finally, Section 6.3 compares tested flexural strength of the panels with predicted flexural strength by using the modified yield strength reduction factor.

6.1 BACKGROUND

According to the AISI Specifications (AISI 1986, 1991), the nominal section strength of flexural members that are made of the Structural Grade 80 of ASTM A653 steel (former ASTM A446 Grade E steel) and uncoupled from axial load, shear, and local concentrated forces or reactions should be determined by the Procedure I in Section C3.1.1 of the Specifications, that is, the nominal section strength equals to a design stress, F_y, times the elastic section modulus of the effective section, S_e, calculated with the extreme

compression or tension fiber at the design stress. For most of the conventional cold-formed sheet steels listed in Sections A3.1 and A3.2 of the Specifications, this design stress is usually taken as the specified minimum yield strength of the steels, indicating that the section strength of a flexural member is reached when yielding is initiated in the section.

However, since the ductility of the Structural Grade 80 of ASTM A653 steel does not meet the provisions of Section 3.1.1 of the AISI Specifications for ductility requirement in the cold-formed structural members, the Specifications require that the design stress, F_y, be taken as 75% of the specified minimum yield strength of the steel or 60 ksi, whichever is less, for determining the section strength of structural members made of this grade of steel.

In the calculation of the elastic section modulus of the effective section, S_e, the effective width equations as specified in Section B of the Specifications should be used for the elements subjected to compressive stress. The effective width formulas were developed based on the sheet steels whose yield strength did not usually exceed 60 ksi.

In 1987, a research project entitled "Effective Design Widths of High Strength Cold-Formed Steel Members" was completed at the Department of Civil Engineering at the University of Missouri-Rolla (Pan 1987). The research dealt with experimental and analytical investigations of the effective design widths of stiffened and unstiffened compression elements using high-strength sheet steels with yield strength ranging from 84.3 to 153.3 ksi. The objective was to determine whether the strength of the cold-formed steel structural members fabricated from high-strength steel sheets could be predicted by using the current AISI effective width equation which was primarily developed based on the tests using yield strength not higher than 60 ksi.

Among a total of twenty-three beams and forty-eight stub columns tested, twelve beams and seventeen stub columns had stiffened compression flanges and were tested to failure for determining the ultimate strength

of the members. The w/t ratios of the stiffened compression flanges varied from 17.7 to 136.7. The thickness of the members ranged from 0.046" to 0.088". The percent elongation of the steels in a 2-inch gage length ranged from 4.30% to 20.40%.

The test results indicated that the strength of the members fabricated from high-strength steel sheets with yield strength exceeding 84.3 ksi could be overestimated by using the effective width formula stated in the current AISI Specifications (AISI 1991, 1986) and actual yield strength of the steels. This difference between the tested and predicted strengths of the members was found to be attributed to the fact that the ultimate edge stress of the compression elements could not reach the yield strength of the steels at the failure of the members. It was also found that the ratio of the tested ultimate edge stress to the yield strength of the steels was a function of w/t ratio, yield strength of steel, and configuration of cross section.

As a result of this investigation, it was suggested that a reduced yield stress should be used in the current AISI effective width formula to design the strength of structural members with stiffened compression flanges fabricated from high-strength steel sheets. The reduced yield stress can be obtained by multiplying the actual yield strength of the steels by a yield strength reduction factor. Two yield strength reduction factors were developed based on the test results and regression analyses. One was for designing stiffened compression elements, and the other was for designing unstiffened compression elements. The equation for the yield strength reduction factor used for stiffened compression elements is expressed as follow:

$$\varphi_s = 1.0 - 0.2\sqrt{\left(\frac{w}{t}\right)}\sqrt{\left(\frac{F_y}{E}\right)} \qquad (6\text{-}1)$$

where w= full width of stiffened element.

t= thickness of sheet steel.

F_y= yield stress of steel, ksi.

E= modulus of elasticity, 29,500 ksi.

The yield strength reduction factor is only applicable for the stiffened elements with a w/t ratio ranging from 17.7 to 136.7, a yield strength ranging from 84.3 to 153.3 ksi, and a value of $(\sqrt{w/t})(\sqrt{F_y/E})$ ranging from 0.286 to 0.843 (Pan 1987).

By using the yield strength reduction factor, Pan re-evaluated the strengths of the members with stiffened elements and compared them with the test results. He found that reasonable agreements were reached between the predicted and the tested strengths.

6.2 DEVELOPMENT OF MODIFIED YIELD STRENGTH REDUCTION FACTOR

The use of the yield strength reduction factor for designing structural members made of high-strength steels as discussed in the previous section has three advantages. First, it addresses the fact that the ultimate edge compressive stress in the compression flanges at failure usually can not reach the higher yield strength of the steels for the members with large w/t ratios. Second, it accounts for two important parameters that can affect the strength of the members. One is w/t ratio, and the other is the actual yield strength of the steel, F_y. Third, it is convenient to design structural members made of high-strength steels by simply substituting a reduced stress, $\varphi_s * F_y$, for the design yield stress, F_y, in the AISI effective width formula. As a result, it does not require a change in the effective width equation for high-strength steels.

On the other hand, as shown in Section 5.1, the flexural strength of the panels with smaller w/t ratios studied in this research was predicted reasonably well by using Equation 6-1, but for the panels with large w/t ratios, the flexural strength was still slightly overestimated by the equation. In addition, Equation 6-1 indicates that if its application is extended for members with small w/t ratios, the strength reduction factor has to be used for designing the members. This includes the situation where either w/t or F_y/E can approach to zero. For members with small w/t ratios, it may be possible that the members can reach higher yield strength of steel in compression flanges, therefore it is not necessary to use the yield strength reduction

factor. As a result, Equation 6-1 needs to be modified to reflect additional test data. A limit for the w/t ratio and yield strength may also need to be included in the yield strength reduction factor, below which sections can be designed with full yield strength of steel.

In order to modify Equation 6-1 to better fit all test data, the following procedure was used. (1) Develop individual theoretical stress-strain relationship for the three different steel sheets used in this study, namely 22, 26, and 28 gage steel sheets; and compare the theoretical stress-strain curves with all coupon test data. (2) For each panel specimen tested in two-point loading condition in this study, obtain the average compressive edge strains and the average tensile strains recorded at the failure of each panel. Then obtain the corresponding tested ultimate stresses, f_{max}, based on the average compressive and tensile strains at the failure and the theoretical stress-strain relationships; and calculate the ratio of the tested ultimate stress to the yield strength of the steel, f_{max}/F_y, for each panel. (3) Examine the effect of w/t and F_y/E ratios on the f_{max}/F_y ratio, based on the plots of the f_{max}/F_y ratio vs. w/t ratio and the f_{max}/F_y ratio vs. F_y/E ratio for the panels tested in this study and those members with stiffened flanges tested by Pan (1987). (4) Construct the relationship between f_{max}/F_y ratio and the parameter $(w/t)(F_y/E)$, based on the plot of the f_{max}/F_y ratio vs. $(w/t)(F_y/E)$ for all the specimens used in (3). The modified yield strength reduction factor, φ, is equal to f_{max}/F_y. Each step of this procedure is discussed as follows.

(1) Develop individual theoretical stress-strain relationship.

As shown in the First Progress Report (Wu, Yu, and LaBoube 1995), the stress-strain curve of the Structural Grade 80 steel is of gradual-yielding type for the 22, 26, and 28 gage steel sheets. The average material properties of the steels are listed in Table 3.1.4. Thus, it is assumed that the theoretical stress-strain relationship for the three gage steel sheets can be represented by the following equation:

$$\sigma = A\,\varepsilon^n + B \qquad (6\text{-}2)$$

Where A, B, and n are constants to be determined; σ is the stress; and ε is the strain. The shape of the stress-strain curve is shown in Fig. 6.2.1. Equation 6-2 has to satisfy several conditions. The equation starts from the proportional limit of the steel, σ_{pr} and ε_{pr}, which is considered as 80% of the yield strength of the steel, $0.8F_y$. Prior to the proportional limit, a linear stress-strain relationship is assumed. The initial stiffness of the linear stress-strain relationship is taken as E equal to 29,500 ksi. Equation 6-2 has to pass through the proportional limit and to have the same initial slope (E) at the proportional limit. In addition, the equation has to pass through the point of average yield strength and yield strain for each gage steel, F_y and ε_y.

Based on the above conditions, prior to the proportional limit, the stress-strain relationship is $\sigma = E\varepsilon$ for all three steels. Starting from the proportional limit, the stress-strain relationship is derived as:

$$\sigma = \frac{\sigma_{pr}}{n}\left(\frac{\sigma_{pr}}{E}\right)^{-n}\varepsilon^{n} + \sigma_{pr}\left(1-\frac{1}{n}\right) \qquad (6\text{-}3)$$

Where $\sigma_{pr}=0.8F_y$; E=29,500 ksi; n=-3.60 for 28 gage steel, -3.58 for 26 and 22 gage steels; and F_y is the actual yield strength of the steel. The theoretical stress-strain relationship for each individual sheet steel was compared with all the coupon test data made from that individual steel as shown in Figures 6.2.2, 6.2.3, and 6.2.4 for the 22, 26, and 28 gage sheet steels, respectively. It is indicated in the figures that reasonable agreements are reached between the theoretical stress-strain curves and the test data.

(2) Calculate the ratio of the tested ultimate stress to the yield strength of the steel, f_{max}/F_y, for each panel.

Based on the theoretical stress-strain relationships, the ultimate tested compressive and tensile stresses at failure of the panels in two-point loading condition can be determined from the average compressive and tensile strains recorded at the failure. The ratio of the tested ultimate stress to the yield strength, f_{max}/F_y,

can be calculated for each panel. The f_{max}/F_y ratios for all the panels tested in two-point loading condition are listed in Tables 6.2.1 and 6.2.2. Table 6.2.1 is for the ratio of the tested ultimate compressive stress to the yield strength; and Table 6.2.2 is for the ratio of the tested ultimate tensile stress to the yield strength. The reason of using the ratios for the tested ultimate tensile stress is that in some panels designed for first yielding in tension flanges, the average tested ultimate tensile stress at failure was larger than the average tested ultimate compressive stress, but still less than the yield strength. The magnitude of the average ultimate tensile stress also depends on the w/t ratio of the compression flange. For the panels with large w/t ratios, the compression flanges can crush before yielding is reached at both tension and compression flanges.

(3) Examine the effect of the w/t and F_y/E ratios on the f_{max}/F_y ratio.

For the panels with stiffened flanges, the ratio of the tested ultimate stress to the yield strength, f_{max}/F_y, can be affected by the flat-width-to-thickness ratio of the flanges (w/t ratio) and the yield-strength-to-stiffness ratio (F_y/E). This issue was addressed by Pan (1987) in his experimental studies. Similar discussion can be found in Yu (1991) for design of cylindrical tubular members. Some additional comments are discussed as follows.

As presented in Section 4.4, the failure of the panels in the two-point loading condition was characterized by crushing the corners between the compression flange and webs, resulting in a formation of local failure mechanism. The corner region between the compression flange and web usually has a shape of partial cylindrical tube and is subject to a higher membrane compressive stress. The classical elastic buckling theory for flat plates and short cylindrical tubes indicates that the elastic buckling stress mainly depends on the slenderness ratios of the plates (w/t ratio) and tubes (R/t ratio) and initial stiffness E. The yield strength of the material does not come into the picture. It means that no matter how high the yield strength of the material may be, the plate or tube with large slenderness ratio will buckle under a certain elastic buckling

stress. Similarly, in the situation of inelastic buckling, beside the slenderness ratio and the initial stiffness, the buckling stress is also affected by an additional parameter, that is, the tangent modulus of material, but again is not related to the yield strength of the material. For the plates and tubes made of gradual-yielding type of steels with relative low proportional limits, buckling can occur far before the yield strength of the material is reached. Particularly in the case of tubular members, the buckling form itself is usually unstable and the members can fail at the time of inelastic buckling. For the gradual-yielding type of the Structural Grade 80 steel, it becomes known that the F_u/F_y ratio is close to 1. This indicates that the steel has a large reduction in stiffness at the yield strength, which makes the corners between the compression flange and webs more vulnerable to crushing under inelastic buckling stress before reaching yielding. Therefore, it is possible that the use of higher yield strength steels may not contribute to a significant increase in the overall strength of members. The higher the yield strength of the steels is, the less the contribution of the high-strength steels to the overall strength of members may be (that is, the smaller the f_{max}/F_y ratio is at failure of the members). As a result, the yield strength, F_y, can affect the f_{max}/F_y ratio.

The effect of the w/t ratio on the f_{max}/F_y ratio is addressed in Section 4.4 and is more apparent for the panels with large w/t ratios. When panels consist of stiffened compression flanges with large w/t ratios, the post-buckling deformation of the top flanges increases considerably under flange membrane compressive stress. The post-buckling behavior of the top flanges becomes a large deformation issue. The largely deformed top flanges further reduce the effective area at the corners between the compression flange and webs and cause the increase of stress at the corners. This increased stress can crush the corners before reaching higher yield strength of the steel and developing large overall deformation of members, which is the similar issue discussed earlier.

To illustrate the variation of the f_{max}/F_y ratio with the w/t and F_y/E ratios for the members made of high-strength steels, the f_{max}/F_y ratio is plotted against the w/t ratio as shown in Fig. 6.2.5, and the f_{max}/F_y ratio is plotted against the F_y/E ratio as shown in Fig. 6.2.6. It is clear that the f_{max}/F_y ratio tends to decrease with

the increases in the w/t and F_y/E ratios. Dashed lines are used in Figures 6.2.5 and 6.2.6 to demonstrate approximate trend of the data. In Fig. 6.2.5, the dashed line starts from a limit value of w/t for yield strength of 80 ksi; and in Fig. 6.2.6, the dashed line starts from a yield strength of 80 ksi. The dashed lines indicate that the rate of reduction in the f_{max}/F_y ratio tends to decrease with further increase in the w/t and F_y/E ratios. This implies that the relationship between either the f_{max}/F_y and w/t ratios or the f_{max}/F_y and F_y/E ratios is not linear.

(4) Determine the modified yield strength reduction factor.

Based on the observations made in (3), a non-dimensional parameter, $(w/t)(F_y/E)$, is constructed to account for an overall effect of the w/t and F_y/E ratios on the f_{max}/F_y ratio. This parameter was also recognized by Pan (1987). By relating the f_{max}/F_y ratio with the parameter $(w/t)(F_y/E)$ along with the test data, a modified yield strength reduction factor, φ, can be determined.

Figure 6.2.7 illustrates the relationship between the f_{max}/F_y ratio and the parameter $(w/t)(F_y/E)$. The test data shown in the figure consist of those members with stiffened compression flanges tested in Pan's study and those panels tested in the two-point loading condition in this study. The f_{max}/F_y ratios for the panels tested in this study include the ratios of tested ultimate compressive stress to yield strength and the ratios of the tested ultimate tensile stress to yield strength. As stated earlier, the use of the average tested ultimate tensile stress is due to the fact that for some panels, the ultimate tensile stress in the tension flanges of these panels was larger than the stress in the compression flange, but still less than the yield strength of the steel at the failure of the panels. Thus, the yield strength reduction factor may be derived to be used in the design of members for first yielding in both compression and tension flanges.

In Fig. 6.2.7, two equations relating the f_{max}/F_y ratio (that is, the yield strength reduction factor) with the parameter $(w/t)(F_y/E)$ are shown. Equation 6-1 is the yield strength reduction factor developed by Pan

(1987). Based on the additional test data from this study, the modified yield strength reduction factor is shown in Fig. 6.2.7 and is written as follows:

$$\varphi = \frac{f_{max}}{F_y} = 1 - 0.26\left(\frac{w}{t}\frac{F_y}{E} - C\right)^{0.4} \leq 1.0 \qquad (6\text{-}4)$$

Where w/t is the flat-width-to-thickness ratio of compression flange; F_y is the actual yield strength of steel; E is the modulus of elasticity and equal to 29,500 ksi; and C represents the limit value for the steels with yield strength of 80 ksi, and is equal to:

$$C = \left(\frac{219.76}{\sqrt{F_y}} \times \frac{F_y}{E}\right)_{F_y = 80\ ksi} = \frac{219.76}{\sqrt{80}} \times \frac{80}{29500} = \frac{1}{15} \qquad (6\text{-}5)$$

When $(w/t)(F_y/E)$ is equal to C, φ=1.0, meaning that no reduction in yield strength of steel is needed in the design of flexural strength of members. It is noticed in the figure that Equation 6-4 tends to be a lower bound for the ratios of tested ultimate compressive stress to yield strength.

Equation 6-4 was developed based on the test results of the specimens with the yield strength of steels ranging from 84.3 to 153.3 ksi and the w/t ratio ranging from 17.7 to 189.95. Corresponding to this range of yield strength and w/t ratio, the reduction factor ranges from 0.75 to near 1.00. It is apparent that using the yield strength reduction factor is beneficial as compared to using one value of 0.75 as specified in the AISI Specification for determining the flexural strength of the panels made of the Structural Grade 80 steel.

6.3 COMPARISON OF TESTED MOMENTS WITH PREDICTED MOMENTS USING THE MODIFIED YIELD STRENGTH REDUCTION FACTOR

The tested yield moments for the panels in two-point loading condition studied in this research and for those members with stiffened compression flanges tested by Pan are compared with the moments predicted using

the modified yield strength reduction factor Equation 6-4. The ratios of tested yield moment to predicted moment are listed in Tables 6.3.1 and 6.3.2 and plotted in Fig. 6.3.1. against the w/t ratios. The figure indicates that better improvement is achieved in predicting the flexural strength of the panels made of the Structural Grade 80 steel, especially for the panels with large w/t ratios. Reasonable agreements are reached between the tested yield moments and the predicted moments for both the members tested by Pan and the panels tested in this study. The ratios tend to be larger than 1.0, resulting in a conservative solution. The average ratio of tested yield moment to predicted moment is 1.080 with a standard deviation of 0.099.

The tested ultimate moments are also compared with the predicted moments using the modified yield strength reduction factor Equation 6-4. The ratios of tested ultimate moment to predicted moment are listed in Tables 6.3.1 and 6.3.2 and plotted in Fig. 6.3.2 against the w/t ratios. The ratios are much larger than 1.0, especially for the members with small w/t ratios. This indicates that an inelastic strength reserve exists in the members as observed in the tests. The prediction of the flexural strength of the members tends to be on the conservative side.

7. SUMMARY

A total of ninety-three deck panel specimens were tested to study the flexural strength of the panels. Among the ninety-three panels, seventy-two panels and another five panels with screws were tested in simply supported and two-point loading conditions; and sixteen panels were tested in simply supported and one-point loading condition. The tested panels involved twenty-four different hat-shaped sections. All the panels were fabricated using the Structural Grade 80 of ASTM A653 steel and 28, 26, and 22 gage sheet steels. The preliminary research findings and the evaluation of the results are summarized in the following discussions:

Panels Tested In Two-Point Loading Condition

(1) For the two-point loading condition, yield strains were recorded in forty-eight panels with the w/t ratios ranging from 17.93 to 189.95, however, only six panels with the w/t ratio of 118.64 or larger experienced yielding, while yielding occurred in forty-two panels with the w/t ratio of 103.52 or less. The number of panels that underwent yielding tends to decrease with increases in the w/t ratios. Ultimate strains prior to failure of the panels were much larger than the yield strains in the majority of the panels with the w/t ratio of 103.52 or less, but less than the percent elongation in a 2-inch gage length of the steel. The magnitude of the ultimate strains decreases with increases in the w/t ratios. The specimens without flange local buckling showed sufficient ductility. Fracture in tension was not observed in the tested panel specimens.

(2) For the panels with the w/t ratio of 61.07 or less, the tested yield moments compared reasonably well with the calculated effective yield moments by using the actual panel dimensions, actual yield strength of the steel, and the 1986 AISI Specification, with the ratio of the yield moment to the calculated effective yield moment ranging from 0.96 to 1.23. However, for the panels with the w/t ratio of 102.86 or larger, the tested ultimate moments were lower than the calculated effective yield moments using the actual yield

strength, with the ratio of the tested ultimate moment to the calculated effective yield moment ranging from 0.81 to 1.00, but the tested ultimate moments were much larger than the calculated moments using the 60 ksi stress or 75% of the actual yield strength for all the panels. As a result, it is conservative to predict the effective moment using the specified 60 ksi stress for the cold-formed steel panels made of the Structural Grade 80 of ASTM A653 steel. This is justified by the fact that the ultimate strains in almost all the panels were larger than 4000 micro strain which corresponded to at least 95 ksi (655.0 MPa) in the three types of steel sheets.

(3) The tested ultimate moments are larger than the calculated effective yield moments for most of the panels having the w/t ratio of 61.07 or less and equal to or larger than the tested yield moments of all the panels, indicating a potential inelastic reserve capacity as justified by the recorded higher ultimate strains.

(4) Panel specimens which were designed for first yielding in the tension flange developed a higher ratio of the tested ultimate moment, or yield moment, to the calculated effective yield moment as compared to the panels designed for first yielding in both compression and tension flanges and in the compression flange only.

(5) The equation developed by Pan (1987) to account for a yield strength reduction factor in predicting the effective moment of flexural members made of high-strength steel, slightly improves the prediction of effective moment for the panels with the w/t ratio of 102.86 or larger, but was found to be conservative for the panels with the w/t ratio of 61.07 or less.

(6) Tested central deflections at service loads were less than the calculated central deflections using effective section properties and modulus of elasticity of 29,500 ksi for most of the panels. The ratio of the tested central deflection to calculated central deflection ranges from 0.78 to 1.05 for all the panels and tends to decrease with increases in the w/t ratios. Slight improvement on the ratio of the tested central deflection to the calculated central deflection was made by using the actual modulus of elasticity of the steel.

However, for the majority of the panels, the tested central deflections at yield moment were larger than the calculated central deflection using effective section properties at yield moment and the modulus of elasticity of 29500 ksi. This indicates that the material nonlinearity beyond the proportional limit of the steel has to be considered when determining deflections at yield moment. The load vs. central deflection curves of the panels with smaller w/t ratios showed a plateau.

(7) Higher ratio of the tested yield moment or tested ultimate moment to weight-per-feet of section tended to be achieved for the panels designed with first yielding in both compression and tension flanges and in tension flange only as compared to the panels designed with first yielding in compression flange only.

(8) For all the panels except the 22 gage panels with the smallest w/t ratios, a local failure mechanism was formed in the constant moment region by crushing the corners between flange and webs in compression.

Panels Tested In One-Point Loading Condition

(1) Fifteen panels with the w/t ratios ranging from 17.93 to 189.95 indicated yielding in cross section based on the converted yield strains at the central load location. One 22 gage panel with the w/t ratio of 189.95 did not indicate yielding prior to failure. The magnitude of the converted ultimate strains at the central load tended to decrease with increases in the w/t ratios and were much larger than the yield strains of the steel prior to failure for all the panels except two panels with large w/t ratios. The converted ultimate strains of all the panels exceeded 4,000 microstrains. The maximum converted ultimate strain was 23,162 microstrains but still less than the percent elongation in 2-inch gage length of the steel. The panels tended to develop higher ultimate strains as compared to the ultimate strains of the panels in two-point loading condition. Fracture in tension was also not observed in the panels.

(2) For all the panels, the tested ultimate moments tended to be larger than the tested ultimate moments of the panels in two-point loading condition. The ratio of the tested ultimate moment in one-point loading

condition to the tested ultimate moment in two-point loading condition tends to decrease with increases in the w/t ratios and ranges from 1.37 to 1.00 with the w/t ratio ranging from 17.93 to 189.95. The moment gradient appeared to increase the ultimate moment of the panels in one-point loading condition. This results in a higher ratio of the tested ultimate moment to the calculated effective yield moment using actual yield strength of the steel, with the ratio ranging from 1.28 to 1.59 for the w/t ratios of less than 40 and ranging from 0.85 to 0.98 for the w/t ratios of larger than 118. The tested ultimate moments were also much larger than the calculated moments using the 60 ksi stress or 75% of the actual yield strength for all the panels. The panels designed for first yielding in the tension flange tended to develop a higher ratio of the tested ultimate moment to the calculated effective yield moment as compared to the panels designed for first yielding in both compression and tension flanges and in compression flange only. The tested shear forces prior to failure were much less than the calculated shear capacities using actual yield strength of the steel and actual dimensions, with the ratio of the tested shear force to the calculated shear capacity ranging from 0.12 to 0.17 for all the panels. The calculated moment-to-shear ratio (equal to L/2, where L is the length of span) is larger than the ratio of the panels in two-point loading condition (ranging from L/3.11 to L/6). All the panels failed at one edge of the central bearing plate due to a formation of a local failure mechanism in which the corners between flange and webs were crushed in compression.

(3) Tested central deflections at service load were less than the calculated central deflections using effective section properties and modulus of elasticity of 29,500 ksi for all the panels except for two specimens. The load vs. central deflection curves of all the panels did not show any plateau.

Panels with Screws and Tested in Two-Point Loading Condition

The flexural strength and central deflection of the panels with screws are similar to those of the panels without screws, based on the reduction of area in the tension flange ranging from 13% to 27%. One 22 gage panel with the smallest w/t ratio and designed for first yielding in tension flanges developed tensile fracture and necking near the holes at all screw locations and caused failure of the panel. This panel failed

after it entered a plateau on its load-deflection curve. Smaller tensile stress in the tension flanges of these panels was usually less than the yield strength of steel at the time of formation of a local failure mechanism in the compression flanges, and is not considered to have significant effect on the increase of stress near the holes.

Finally, it is concluded that for the deck panels made of the Structural Grade 80 of ASTM A653 steel, the current design practice for determining flexural strength of the panels is conservative by using 75% of the specified minimum yield strength of the steel, especially for the panels with small w/t ratios (less than 60). A modified yield strength reduction factor was developed to be used for the design of flexural strength of the panels with yield strength between 80 ksi and 150 ksi (including 80 and 150 ksi) and w/t ratio not exceeding 190. For panels with $(w/t)(F_y/E)$ ratio of 1/15 or less, actual yield strength of the steel can be used in determining flexural strength of the panels. Reasonable agreements are reached between tested moments and predicted moments using the modified yield strength reduction factor.

8. FUTURE RESEARCH WORK

The research work reported herein is a part of the second phase of an overall research project on Strength of Flexural Members Using Structural Grade 80 of A653 and Grade E of A611 Steels, sponsored by the American Iron and Steel Institute. The first phase of the project has been completed and the results were reported by Wu, Yu, and LaBoube (1995). The future research work of the project is described as follows.

An experimental program for testing web-crippling strength of the deck panels using the Structural Grade 80 steel is under development. Deck specimens for the web-crippling tests have been designed and manufactured. Two types of steel sheets, 22 and 26 gage, were used to fabricate the panel specimens. The depth of the webs was taken as 0.75, 1.5, 2, 3, 4.5, and 6 inches, with h/t ratio ranging from 25.86 to 206.90. Two inside bend radii, 1/8" and 1/16", were used for the design of the panels, with R/t ratio ranging from 2.16 to 7.35. Two bearing lengths, 1 and 1.5 inches, were considered for the tests, with N/t ratio ranging from 34.48 to 88.24. A total of 128 web-crippling tests, which will involve sixteen different sections of the deck panels, will be conducted at the Department of Civil Engineering of the University of Missouri-Rolla to determine web crippling strength of the panels including end-one-flange loading, end-two-flange loading, interior-one-flange loading, and interior-two-flange loading conditions. In addition, a preliminary investigation on screwed and welded connection made of the Structural Grade 80 steel will be carried out following the web crippling tests. Test results for the web crippling tests will be evaluated and the Third Progress Report will be prepared. The results for the connection tests will be included in the Fourth Progress Report.

ACKNOWLEDGEMENTS

The research work reported herein was conducted at the Department of Civil Engineering at the University of Missouri-Rolla under the sponsorship of the American Iron and Steel Institute. Drs. Wei-Wen Yu and R.A. LaBoube are the directors of the project.

The financial assistance granted by the Institute and the technical guidance provided by members of the Subcommittee 24 - Flexural Members of the AISI Committee on the Specification for the Design of Cold-Formed Steel Structural Members and the AISI Staff (R.B. Haws, H. Chen, K.C. Slaughter, and S.P. Bridgewater) are gratefully acknowledged. The Subcommittee members are: J.N. Nunnery (Chairman), R.E. Albrecht, R.L. Brockenbrough, R.E. Brown, C.R. Clauer, D.S. Ellifritt, S.J. Errera, J.M. Fisher, T.V. Galambos, M. Golovin, G.J. Hancock, A.J. Harrold, R.B. Haws, R.B. Heagler, D.L. Johnson, W.E. Kile, R.A. LaBoube, M.R. Loseke, R. Madsen, T.H. Miller, T.M. Murray, T.B. Pekoz, D.C. Perry, R.M. Schuster, P.A. Seaburg, W.L. Shoemaker, T. Sputo, T.W. Trestain, and W.W. Yu.

All of the steel sheet materials used for the coupon tests and beam specimens were kindly donated by the Wheeling Corrugating Company, Wheeling, West Virginia. Mr. F. C. Rosenberger from the Wheeling-Pittsburgh Steel Corporation Steubenville Plant and Mr. R.E. Brown from the Wheeling Corrugating Company are acknowledged for their technical advice.

Thanks are also due to J.J. Bradshaw, J.M. McCracken, and S.D. Gabel, staff of the Department of Civil Engineering, for their technical support and to Mr. Dennis Cox and Ms. Debora Black for their assistance in the preparation of the deck panel specimens.

REFERENCES

American Iron and Steel Institute. (1991). "Load and Resistance Factor Design Specification for Cold-Formed Steel Structural Members," March 16, 1991 Edition.

American Iron and Steel Institute. (1986). "Specification for the Design of Cold-Formed Steel structural Members," August 19, 1986 Edition with December 11, 1989 Addendum.

ASTM A446. "Standard Specification for Steel Sheet, Zinc-Coated (Galvanized) by the Hot-Dip Process, Physical (Structural Quality)." Annual Book of ASTM Standards.

Brockenbrough, R.L. (1995). "Effect of Yield-Tensile Ratio on Structural Behavior-High Performance Steels for Bridge Construction," Draft Final Report to ONR-AISI, March 6, 1995.

Dhalla, A.K., and Winter, G. (1971). "Influence of Ductility on the Structural Behavior of Cold-formed Steel Members." Report No. 336, Cornell University, June.

Fertis, D.G. (1993). "Nonlinear Mechanics," CRC Press.

Glauz, R.S. (1990). "Cold-Formed Steel Design Program, User's manual,"

Pan, L.C. (1987). "Effective Design Widths of High Strength Cold-Formed Steel Members." Ph.D. Dissertation, Department of Civil Engineering, University of Missouri-Rolla, Rolla, MO.

Steel Deck Institute (SDI). (1992). "Steel Deck Institute Design Manual for Composite Decks, Form Decks, Roof Decks, and Cellular Metal Floor Deck with Electrical Distribution." Steel Deck Institute, Publication No. 28.

United Steel Deck (USD). (1994). "Steel Decks for Floors and Roofs, Design Manual and Catalog of Products." Nicholas J. Bouras, Inc.

Wu, S., Yu, W.W., and LaBoube, R.A. (1995). "Strength of Flexural Members Using Structural Grade 80 of A653 and Grade E of A611 Steels." First Progress Report, Civil Engineering Study 95-5, Department of Civil Engineering, University of Missouri-Rolla, Rolla, MO.

Yu, Wei-Wen. (1991). "Cold-Formed Steel Design," Second Edition, John Wiley & Sons. Inc..

APPENDIX

NOTATIONS

The following symbols are used in this report:

d_u = maximum central deflection at failure
E = modulus of elasticity, 29,500 ksi.
f_{max}= ultimate compressive or tensile stress
f_t/f_c = ratio of the tensile to the compressive stress.
F_y = specified yield strength of sheet steel.
F_u = specified tensile strength of sheet steel.
h = flat width of web.
L = span length, measured between centers of two supports of the panel.
R = inside bend radius.
t = thickness of panel sheet.
w = flat width of compression flange.
θ = angle between planes of the web and bearing surface.
φ = yield strength reduction factor.
σ = stress
ε = strain

Table 3.1.1 w/t and h/t Ratios Used for the *Design* of Panel Specimens with Two-Point Loading Condition 70

t (gage#) (inches)	w (inches)					
	0.5	1.0	1.5	2.0	3.0	5.5
0.015 (28)	--	--	100.00	--	--	--
0.017 (26)	29.41	58.82	--	117.65	--	--
0.029 (22)	17.24	34.48	--	--	103.45	189.66
t (gage #) (inches)	h (inches)					
	0.5	0.75	1.0	1.5	2.0	3.0
0.015 (28)	--	--	66.67	--	--	--
0.017 (26)	29.41	44.12	--	88.24	--	--
0.029 (22)	17.24	25.86	--	--	68.97	103.45
f_t/f_c	0.8,1.0,1.2	0.8,1.0,1.2	0.8,1.0,1.2	0.8,1.0,1.2	0.8,1.0,1.2	0.8,1.0,1.2

Note: See Figure 3.1.1 for the measurement of the flat width of flange "w" and the flat depth of web "h".
1 inch = 25.4 mm.

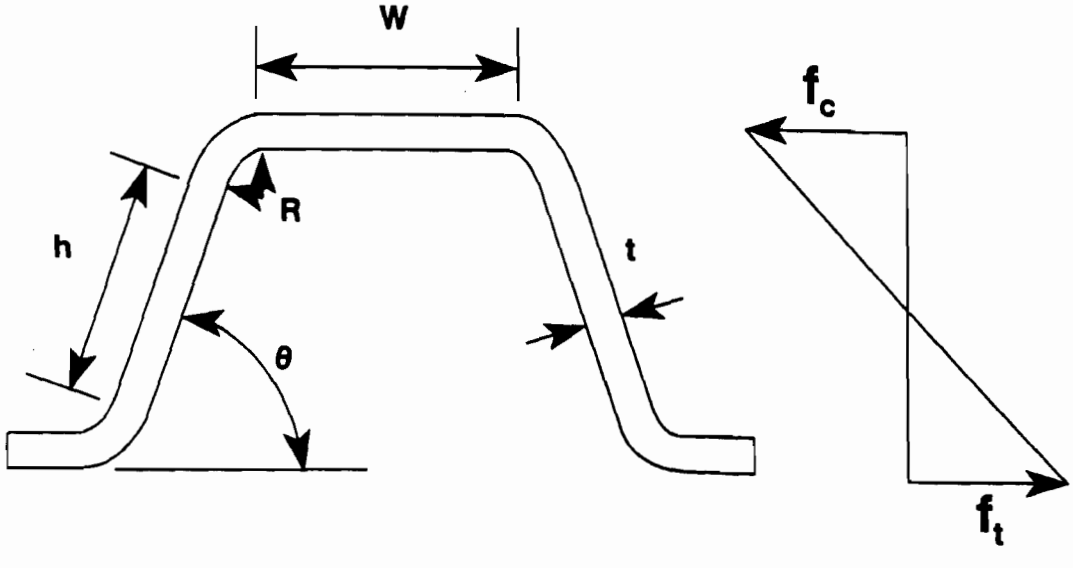

Figure 3.1.1 Cross Section Used for the *Design* of Panel Specimens

Table 3.1.2 w/t and h/t Ratios Used for the *Design* of Panel Specimens with One-Point Loading Condition 71

t (gage#) (inches)	w (inches)					
	0.5	--	--	2.0	--	5.5
0.017 (26)	29.41	--	--	117.65	--	--
0.029 (22)	17.24	--	--	--	--	189.66
t (gage #) (inches)	h (inches)					
	0.5	--	--	1.5	--	3.0
0.017 (26)	29.41	--	--	88.24	--	--
0.029 (22)	17.24	--	--	--	--	103.45
f_t/f_c	1.0,1.2	--	--	1.0,1.2	--	1.0,1.2

Note: See Figure 3.1.1 for the measurement of the flat width of flange "w" and the flat depth of web "h".
1 inch = 25.4 mm.

Table 3.1.3 w/t and h/t Ratios Used for the Panels with Screws and Tested in Two-Point Loading Condition

t (gage#) (inches)	w (inches)						
	0.5	0.5	--	2.0	--	--	5.5
0.017 (26)	29.41	--	--	117.65	--	--	--
0.029 (22)	17.24	17.24	--	--	--	--	189.66
t (gage #) (inches)	h (inches)						
	0.5	0.5	--	1.5	--	--	3.0
0.017 (26)	29.41	--	--	88.24	--	--	--
0.029 (22)	17.24	17.24	--	--	--	--	102.45
f_t/f_c	0.8	1.2	--	0.8	--	--	0.8

Note: See Figure 3.1.1 for the measurement of the flat width of flange "w" and the flat depth of web "h".
1 inch = 25.4 mm.

Table 3.1.4 Material Properties of 22, 24, 26, and 28 Gage Sheet Steels

Direction	Gage	Thickness (in.)	0.2% Offset Yield Strength F_y (ksi)	Tensile Strength F_u (ksi)	Tensile-to-Yield Ratio F_u/F_y	Local Elongation in 1/2-in. Gage Length (%)	Uniform Elongation Outside Fracture (%)	Elongation in 2-in. Gage Length (%)
Parallel to Rolling Direction	22	0.029	103.9	107.7	1.04	11.98	1.29	3.67
	24	0.024	110.1	116.4	1.06	9.33	1.23	2.69
	26	0.017	112.5	115.9	1.03	9.13	0.77	2.40
	28	0.015	111.0	116.1	1.05	7.89	1.04	2.77
Perpendicular to Rolling Direction	22	0.029	119.6	121.2	1.02	7.29	0.41	1.99
	24	0.024	126.0	128.5	1.02	6.40	0.35	1.78
	26	0.017	129.7	132.6	1.02	3.78	0.43	1.32
	28	0.015	127.3	130.1	1.02	3.78	0.43	1.38

Note: All steel sheets were made of the Structural Grade 80 of ASTM A653 Steel. 1 inch = 25.4 mm. 1 ksi = 6.895 MPa.

Table 3.3.1 Measured Dimensions of Panel Specimens Made of 28 Gage Sheet Steel

Section Type of Specimen (#)	$L_{1,2}$ (in.)	$L_{2,3}$ (in.) ($\theta_{2,3}$ in degree)	$L_{3,4}$ (in.)	$L_{4,5}$ (in.) ($\theta_{4,5}$ in degree)	$L_{5,6}$ (in.)	$L_{6,7}$ (in.) ($\theta_{6,7}$ in degree)	$L_{7,8}$ (in.)	$L_{8,9}$ (in.) ($\theta_{8,9}$ in degree)	$L_{9,10}$ (in.)	$L_{10,11}$ (in.) ($\theta_{10,11}$ in degree)	$L_{11,12}$ (in.)	$L_{12,13}$ (in.) ($\theta_{12,13}$ in degree)	$L_{13,14}$ (in.)
t28w1.5h1-c (1)	0.469	1.094 (60,60)	1.594	1.085 (63,58)	0.865	1.091 (58,62)	1.607	1.053 (59,61)	0.465	--	--	--	--
t28w1.5h1-ct (2)	0.271	1.085 (62,62)	1.585	1.083 (63.5,59)	0.472	1.105 (59,62)	1.630	1.036 (61,61)	0.268	--	--	--	--
t28w1.5h1-t (3)	0.222	1.062 (64,59)	1.578	1.085 (62,60)	0.348	1.098 (62.5,63.5)	1.619	1.034 (64.5,61)	0.218	--	--	--	--

Note: see Figure 3.3.1 for the measurement of the dimensions. 1 inch = 25.4 mm.

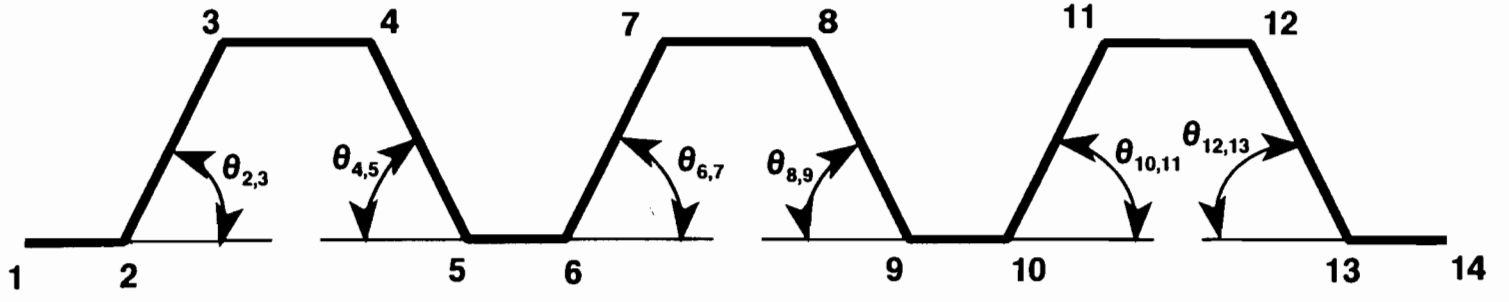

Figure 3.3.1 Cross Section of Panel Specimen

Table 3.3.2 Measured Dimensions of Panel Specimens Made of 26 Gage Sheet Steel (see Figure 3.3.1 for Dimensions)

Type of Specimen (#)	$L_{1,2}$ (in.)	$L_{2,3}$ (in.) ($\theta_{2,3}$ in degree)	$L_{3,4}$ (in.)	$L_{4,5}$ (in.) ($\theta_{4,5}$ in degree)	$L_{5,6}$ (in.)	$L_{6,7}$ (in.) ($\theta_{6,7}$ in degree)	$L_{7,8}$ (in.)	$L_{8,9}$ (in.) ($\theta_{8,9}$ in degree)	$L_{9,10}$ (in.)	$L_{10,11}$ (in.) ($\theta_{10,11}$ in degree)	$L_{11,12}$ (in.)	$L_{12,13}$ (in.) ($\theta_{12,13}$ in degree)	$L_{13,14}$ (in.)
t26w05h0.5-c (4)	0.365	0.589 (61, 60)	0.584	0.566 (60.5,60)	0.748	0.585 (60,60.5)	0.574	0.581 (60,61)	0.748	0.591 (60,61)	0.614	0.562 (62,61.5)	0.375
t26w0.5h0.5-ct (5)	0.242	0.596 (61,59.5)	0.588	0.560 (61.5,60)	0.499	0.585 (60.5,61.5)	0.570	0.575 (61,60.5)	0.494	0.593 (58,61)	0.598	0.572 (61,62)	0.254
t26w0.5h0.5-t (6)	0.218	0.564 (61.5,60.5)	0.585	0.549 (62,63)	0.391	0.597 (60.5,61.5)	0.574	0.575 (60,62)	0.377	0.591 (60,61.5)	0.630	0.510 (70,64)	0.220
t26w1h0.75-c (7)	0.434	0.843 (62,62)	1.071	0.828 (63.5,62)	0.854	0.844 (61,61)	1.121	0.813 (60.5,63)	0.452	--	--	--	--
t26w1h0.75-ct (8)	0.283	0.821 (58.5,57.5)	1.072	0.834 (61,61.5)	0.577	0.834 (58,58.5)	1.090	0.841 (56.5,61)	0.273	--	--	--	--
t26w1h0.75-t (9)	0.209	0.804 (61,64)	1.077	0.824 (62,62)	0.344	0.830 (60,60.5)	1.063	0.813 (60,63)	0.212	--	--	--	--
t26w2h1.5-c (10)	0.483	1.594 (63.5,59)	2.072	1.578 (60,59)	0.889	1.596 (62,64)	2.136	1.521 (63,59.5)	0.489	--	--	--	--
t26w2h1.5-ct (11)	0.289	1.590 (62.5,57)	2.067	1.580 (59.5,58)	0.529	1.610 (62,63)	2.079	1.568 (62.5,58.5)	0.298	--	--	--	--
t26w2h1.5-t (12)	0.214	1.562 (61.5,62.5)	2.073	1.578 (64,62.5)	0.340	1.602 (59,60.5)	2.084	1.538 (60.5,65)	0.221	--	--	--	--

Table 3.3.3 Measured Dimensions of Panel Specimens Made of 22 Gage Sheet Steel (see Figure 3.3.1 for Dimensions)

Section Type of Specimen (#)	$L_{1,2}$ (in.)	$L_{2,3}$ (in.) ($\theta_{2,3}$ in degree)	$L_{3,4}$ (in.)	$L_{4,5}$ (in.) ($\theta_{4,5}$ in degree)	$L_{5,6}$ (in.)	$L_{6,7}$ (in.) ($\theta_{6,7}$ in degree)	$L_{7,8}$ (in.)	$L_{8,9}$ (in.) ($\theta_{8,9}$ in degree)	$L_{9,10}$ (in.)	$L_{10,11}$ (in.) ($\theta_{10,11}$ in degree)	$L_{11,12}$ (in.)	$L_{12,13}$ (in.) ($\theta_{12,13}$ in degree)	$L_{13,14}$ (in.)
t22w05h0.5-c (13)	0.472	0.598 (60,62.5)	0.596	0.554 (62,63.5)	0.979	0.602 (60.5,61)	0.568	0.587 (59,60)	0.946	0.599 (62,60.5)	0.628	0.564 (63,63)	0.469
t22w0.5h0.5-ct (14)	0.319	0.601 (59,60)	0.587	0.563 (61,61)	0.664	0.602 (58,59)	0.583	0.577 (57.5,58.5)	0.644	0.607 (61,59)	0.634	0.545 (61,61)	0.316
t22w0.5h0.5-t (15)	0.233	0.581 (61,61.5)	0.583	0.565 (62,61)	0.457	0.600 (60.5,60.5)	0.571	0.594 (60,61.5)	0.445	0.607 (62,60)	0.619	0.559 (61,62.5)	0.233
t22w1h0.75-c (16)	0.612	0.842 (59,60)	1.086	0.841 (60.5,59)	1.205	0.864 (58.5,58)	1.084	0.833 (58,60.5)	0.625	--	--	--	--
t22w1h0.75-ct (17)	0.414	0.845 (59,61)	1.084	0.838 (61.5,61.5)	0.867	0.854 (59.5,58.5)	1.111	0.811 (65,61.5)	0.411	--	--	--	--
t22w1h0.75-t (18)	0.270	0.841 (59.5,60)	1.084	0.847 (61,62)	0.534	0.846 (60,59)	1.088	0.843 (58,62.5)	0.286	--	--	--	--
t22w3h2-c (19)	0.860	2.095 (59.5,59.5)	3.066	2.085 (60,61)	0.864	--	--	--	--	--	--	--	--
t22w3h2-ct (20)	0.474	2.104 (60.5,62)	3.059	2.081 (59.5,64.5)	0.496	--	--	--	--	--	--	--	--
t22w3h2-t (21)	0.292	2.106 (61,64)	3.068	2.075 (62,60)	0.313	--	--	--	--	--	--	--	--
t22w5.5h3-c (22)	0.738	3.097 (62.5,60.5)	5.552	3.103 (61,62)	0.739	--	--	--	--	--	--	--	--
t22w5.5h3-ct (23)	0.445	3.112 (60.5,60.5)	5.573	3.078 (60.5,61.5)	0.460	--	--	--	--	--	--	--	--
t22w5.5h3-t (24)	0.296	3.112 (61,60)	5.579	3.032 (59.5,62)	0.313	--	--	--	--	--	--	--	--

Table 3.3.4 Actual w/t Ratios of the Tested Panels

Sections	Thickness (in.)	Flange 3-4 w/t	Flange 7-8 w/t	Flange 11-12 w/t	Average w/t
t28w1.5h1-c	0.015	102.69	103.57	--	103.13
t28w1.5h1-ct	0.015	101.99	105.05	--	103.52
t28w1.5h1-t	0.015	101.55	104.16	--	102.86
t26w0.5h0.5-c	0.017	31.05	30.46	32.77	31.43
t26w0.5h0.5-ct	0.017	31.28	30.19	31.87	31.11
t26w0.5h0.5-t	0.017	31.02	30.42	33.52	31.65
t26w1h0.75-c	0.017	59.56	62.57	--	61.07
t26w1h0.75-ct	0.017	59.81	60.94	--	60.38
t26w1h0.75-t	0.017	59.93	59.19	--	59.56
t26w2h1.5-c	0.017	118.58	122.23	--	120.41
t26w2h1.5-ct	0.017	118.36	118.92	--	118.64
t26w2h1.5-t	0.017	118.49	119.23	--	118.86
t22w0.5h0.5-c	0.029	18.05	17.18	19.15	18.13
t22w0.5h0.5-ct	0.029	17.83	17.79	19.44	18.35
t22w0.5h0.5-t	0.029	17.64	17.26	18.88	17.93
t22w1h0.75-c	0.029	35.07	35.04	--	35.06
t22w1h0.75-ct	0.029	34.94	35.86	--	35.40
t22w1h0.75-t	0.029	34.95	35.12	--	35.04
t22w3h2-c	0.029	103.33	--	--	103.33
t22w3h2-ct	0.029	103.00	--	--	103.00
t22w3h2-t	0.029	103.31	--	--	103.31
t22w5.5h3-c	0.029	188.98	--	--	188.98
t22w5.5h3-ct	0.029	189.74	--	--	189.74
t22w5.5h3-t	0.029	189.95	--	--	189.95

Note: 1 inch = 25.4 mm. See Fig. 3.3.1 for flange numbering.

Table 3.3.5 Actual h/t Ratios of the Tested Panels

Specimens	Thickness (in.)	Web 2-3 h/t	Web 4-5 h/t	Web 7-6 h/t	Web 8-9 h/t	Web 10-11 h/t	Web 12-13 h/t	Average h/t
t28w1.5h1-c	0.015	69.37	68.74	69.17	66.64	--	--	68.48
t28w1.5h1-ct	0.015	68.63	68.55	70.07	65.43	--	--	68.17
t28w1.5h1-t	0.015	67.13	68.70	69.42	65.17	--	--	67.61
t26w0.5h0.5-c	0.017	31.34	30.00	31.12	30.87	31.45	29.66	30.74
t26w0.5h0.5-ct	0.017	31.76	29.61	31.07	30.50	31.64	30.27	30.81
t26w0.5h0.5-t	0.017	29.83	28.85	31.77	30.48	31.44	26.24	29.77
t26w1h0.75-c	0.017	46.18	45.24	46.30	44.43	--	--	45.54
t26w1h0.75-ct	0.017	45.15	45.70	45.90	46.28	--	--	45.76
t26w1h0.75-t	0.017	43.85	45.06	45.53	44.45	--	--	44.72
t26w2h1.5-c	0.017	90.40	89.58	90.40	86.11	--	--	89.12
t26w2h1.5-ct	0.017	90.27	89.75	91.26	88.92	--	--	90.05
t26w2h1.5-t	0.017	88.47	89.33	90.97	87.01	--	--	88.95
t22w0.5h0.5-c	0.029	18.16	16.57	18.32	17.87	18.20	16.90	17.67
t22w0.5h0.5-ct	0.029	18.35	16.97	18.43	17.59	18.53	16.35	17.70
t22w0.5h0.5-t	0.029	17.57	17.01	18.27	18.05	18.48	16.79	17.70
t22w1h0.75-c	0.029	26.66	26.61	27.48	26.36	--	--	26.78
t22w1h0.75-ct	0.029	26.74	26.42	27.10	25.41	--	--	26.42
t22w1h0.75-t	0.029	26.61	26.73	26.80	26.66	--	--	26.70
t22w3h2-c	0.029	69.87	69.47	--	--	--	--	69.67
t22w3h2-ct	0.029	70.09	69.26	--	--	--	--	69.68
t22w3h2-t	0.029	70.10	69.10	--	--	--	--	69.60
t22w5.5h3-c	0.029	104.32	104.53	--	--	--	--	104.43
t22w5.5h3-ct	0.029	104.89	103.69	--	--	--	--	104.29
t22w5.5h3-t	0.029	104.89	102.12	--	--	--	--	103.51

Note: 1 inch = 25.4 mm. See Fig. 3.3.1 for web numbering.

Table 3.4.1 Span Length and Shear Span

Sections	Thickness (in.)	Average w/t	Panels with Two-Point Loading Condition		Panels with One-Point Loading Condition	
			Span Length (in.)	Shear Span (in.)	Span Length (in.)	Shear Span (in.)
t28w1.5h1-c	0.015	103.13	36	8	--	--
t28w1.5h1-ct	0.015	103.52	36	8	--	--
t28w1.5h1-t	0.015	102.86	36	8	--	--
t26w0.5h0.5-c	0.017	31.43	30	5	--	--
t26w0.5h0.5-ct	0.017	31.33	30	5	12	6
t26w0.5h0.5-t	0.017	31.65	30	5	12	6
t26w1h0.75-c	0.017	61.07	30	5	--	--
t26w1h0.75-ct	0.017	60.38	30	5	--	--
t26w1h0.75-t	0.017	59.56	30	5	--	--
t26w2h1.5-c	0.017	120.41	52	16	--	--
t26w2h1.5-ct	0.017	118.64	52	16	40	20
t26w2h1.5-t	0.017	118.86	52	16	40	20
t22w0.5h0.5-c	0.029	18.13	30	5	--	--
t22w0.5h0.5-ct	0.029	18.35	30	5	12	6
t22w0.5h0.5-t	0.029	17.93	30	5	12	6
t22w1h0.75-c	0.029	35.06	36	8	--	--
t22w1h0.75-ct	0.029	35.40	36	8	--	--
t22w1h0.75-t	0.029	35.04	36	8	--	--
t22w3h2-c	0.029	103.33	56	18	--	--
t22w3h2-ct	0.029	103.00	56	18	--	--
t22w3h2-t	0.029	103.31	56	18	--	--
t22w5.5h3-c	0.029	188.98	80	24	--	--
t22w5.5h3-ct	0.029	189.74	80	24	80	40
t22w5.5h3-t	0.029	189.95	80	24	80	40

Note: 1 inch = 25.4 mm. 1 kip = 4.448 kN.

Table 4.4.1 Maximum Compressive and Tensile Strains in the Same Section at Yielding in Two-Point Loading Condition

Specimens	Thickness (in.)	Average w/t	Compressive Strain (Test 1)	Tensile Strain (Test 1)	Compressive Strain (Test 2)	Tensile Strain (Test 2)	Compressive Strain (Test 3)	Tensile Strain (Test 3)
2p-t28w1.5h1-c(1,2,3)	0.015	103.13	--	--	--	--	5722	2883
2p-t28w1.5h1-ct(1,2,3)	0.015	103.52	n/a	n/a	5722	4409	5722	3698
2p-t28w1.5h1-t(1,2,3)	0.015	102.86	5722	4601	--	--	5722	4538
2p-t26w0.5h0.5-c(1,2,3)	0.017	31.43	5739	3520	5739	3240	5739	3202
2p-t26w0.5h0.5-ct(1,2,3)	0.017	31.33	5739	4568	5739	5323	4039	5739
2p-t26w0.5h0.5-t(1,2,3)	0.017	31.65	4847	5739	5739	5703	5739	5724
2p-t26w1h0.75-c(1,2,3)	0.017	61.07	5739	2892	--	--	--	--
2p-t26w1h0.75-ct(1,2,3)	0.017	60.38	5314	5739	5739	5337	--	--
2p-t26w1h0.75-t(1,2,3)	0.017	59.56	5739	5029	5739	4619	5739	5382
2p-t26w2h1.5-c(1,2,3)	0.017	120.41	--	--	5739	2352	--	--
2p-t26w2h1.5-ct(1,2,3)	0.017	118.64	5739	3185	--	--	5739	3350
2p-t26w2h1.5-t(1,2,3)	0.017	118.86	--	--	--	--	5739	3995
2p-t22w0.5h0.5-c(1,2,3)	0.029	18.13	5282	3092	n/a	n/a	5282	3223
2p-t22w0.5h0.5-ct(1,2,3)	0.029	18.35	5282	4529	5282	4534	n/a	n/a
2p-t22w0.5h0.5-t(1,2,3)	0.029	17.93	4836	5282	4833	5282	4644	5282
2p-t22w1h0.75-c(1,2,3)	0.029	35.06	--	--	--	--	--	--
2p-t22w1h0.75-ct(1,2,3)	0.029	35.40	4591	5282	4929	5282	5282	4943
2p-t22w1h0.75-t(1,2,3)	0.029	35.04	3332	5282	n/a	n/a	3390	5282
2p-t22w3h2-c(1,2,3)	0.029	103.33	--	--	5282	2852	--	--
2p-t22w3h2-ct(1,2,3)	0.029	103.00	5282	3940	5282	3961	5282	4150
2p-t22w3h2-t(1,2,3)	0.029	103.31	5142	5282	4409	5281	5210	5282
2p-t22w5.5h3-c(1,2,3)	0.029	188.98	5282	2500	--	--	--	--
2p-t22w5.5h3-ct(1,2,3)	0.029	189.74	--	--	--	--	5282	3012
2p-t22w5.5h3-t(1,2,3)	0.029	189.95	--	--	--	--	--	--

Note: 1 inch = 25.4 mm. The yield strains for the 28, 26, and 22 gage sheet steels are 5722, 5739, and 5282 microstrain, respectively. "--" indicates no yielding in the cross section. "n/a" indicates that data is not available.

Table 4.4.2 Maximum Compressive and Tensile Strains in the Same Section at Failure of the Panels in Two-Point Loading Condition

Specimens	Thickness (in.)	Average w/t	Compressive Strain (Test 1)	Tensile Strain (Test 1)	Compressive Strain (Test 2)	Tensile Strain (Test 2)	Compressive Strain (Test 3)	Tensile Strain (Test 3)
2p-t28w1.5h1-c(1,2,3)	0.015	103.13	4387	2953	4828	2840	6150	2997
2p-t28w1.5h1-ct(1,2,3)	0.015	103.52	13420	4550	5760	4429	8935	4308
2p-t28w1.5h1-t(1,2,3)	0.015	102.86	7805	5463	5673	4969	7383	4808
2p-t26w0.5h0.5-c(1,2,3)	0.017	31.43	6049	3603	8686	3819	8703	3835
2p-t26w0.5h0.5-ct(1,2,3)	0.017	31.33	8789	5656	5852	5431	4039	5715
2p-t26w0.5h0.5-t(1,2,3)	0.017	31.65	5409	6496	6778	6297	6914	6661
2p-t26w1h0.75-c(1,2,3)	0.017	61.07	9576	3601	4877	3384	2738	3501
2p-t26w1h0.75-ct(1,2,3)	0.017	60.38	5038	5663	5651	5298	5254	5271
2p-t26w1h0.75-t(1,2,3)	0.017	59.56	8336	7137	10226	7090	9774	8213
2p-t26w2h1.5-c(1,2,3)	0.017	120.41	4633	2641	8614	2618	4583	2647
2p-t26w2h1.5-ct(1,2,3)	0.017	118.64	7850	3552	5693	3571	7270	3561
2p-t26w2h1.5-t(1,2,3)	0.017	118.86	4813	4231	4943	4247	6984	4122
2p-t22w0.5h0.5-c(1,2,3)	0.029	18.13	8233	4039	8253	4620	10210	4912
2p-t22w0.5h0.5-ct(1,2,3)	0.029	18.35	8299	7075	8786	7473	8002	6941
2p-t22w0.5h0.5-t(1,2,3)	0.029	17.93	8384	8455	7809	9304	9266	11463
2p-t22w1h0.75-c(1,2,3)	0.029	35.06	4344	3666	5005	4129	3648	3529
2p-t22w1h0.75-ct(1,2,3)	0.029	35.40	5062	6659	4992	5382	6461	6121
2p-t22w1h0.75-t(1,2,3)	0.029	35.04	3423	6834	10378	8830	4053	8058
2p-t22w3h2-c(1,2,3)	0.029	103.33	4643	2746	6088	2906	4026	2810
2p-t22w3h2-ct(1,2,3)	0.029	103.00	7966	4368	5424	4035	6689	4324
2p-t22w3h2-t(1,2,3)	0.029	103.31	5224	5453	4422	5341	5322	5447
2p-t22w5.5h3-c(1,2,3)	0.029	188.98	5426	2529	4214	2427	4358	2505
2p-t22w5.5h3-ct(1,2,3)	0.029	189.74	5236	3020	4029	3086	6073	3067
2p-t22w5.5h3-t(1,2,3)	0.029	189.95	4254	3599	4212	3391	4597	3785

Note: 1 inch = 25.4 mm. The yield strains for the 28, 26, and 22 gage sheet steels are 5722, 5739, and 5282 microstrains, respectively.

Table 4.4.3 Central Deflections at Service Load, at Yielding, and at Failure of the Panels in Two-Point Loading Condition

Specimens	Deflection at Service Load (in.)			Deflection at Yielding (in.)			Deflection at Failure (in.)		
	Test 1	Test 2	Test 3	Test 1	Test 2	Test 3	Test 1	Test 2	Test 3
2p-t28w1.5h1-c(1,2,3)	0.289	0.272	0.292	--	--	1.181	1.192	1.232	1.246
2p-t28w1.5h1-ct(1,2,3)	0.259	0.263	0.259	n/a	1.451	1.141	1.397	1.467	1.429
2p-t28w1.5h1-t(1,2,3)	0.269	n/a	0.280	1.290	--	1.345	1.643	1.564	1.488
2p-t26w0.5h0.5-c(1,2,3)	0.473	0.453	0.444	1.825	1.517	1.571	1.890	1.849	2.026
2p-t26w0.5h0.5-ct(1,2,3)	0.409	0.384	0.397	1.715	2.063	2.207	2.110	2.105	2.200
2p-t26w0.5h0.5-t(1,2,3)	0.469	0.413	0.454	1.990	1.997	2.083	2.192	2.280	2.430
2p-t26w1h0.75-c(1,2,3)	0.289	0.276	0.278	0.981	--	--	1.299	1.235	1.334
2p-t26w1h0.75-ct(1,2,3)	0.261	0.266	0.263	1.663	1.684	--	1.634	1.671	1.619
2p-t26w1h0.75-t(1,2,3)	0.260	0.268	0.267	1.328	1.215	1.384	1.863	1.805	1.962
2p-t26w2h1.5-c(1,2,3)	0.376	0.363	0.370	--	1.066	--	1.361	1.264	1.325
2p-t26w2h1.5-ct(1,2,3)	0.363	0.370	0.366	1.295	--	1.401	1.526	1.598	1.537
2p-t26w2h1.5-t(1,2,3)	0.352	0.338	0.346	--	--	1.577	1.669	1.642	1.677
2p-t22w0.5h0.5-c(1,2,3)	0.404	n/a	0.383	1.569	n/a	1.592	2.225	2.323	2.674
2p-t22w0.5h0.5-ct(1,2,3)	n/a	0.430	n/a	1.782	1.832	n/a	2.784	2.823	n/a
2p-t22w0.5h0.5-t(1,2,3)	0.427	0.446	0.442	1.817	1.871	1.779	2.955	2.893	3.331
2p-t22w1h0.75-c(1,2,3)	0.205	n/a	0.408	--	--	--	1.133	2.061	1.648
2p-t22w1h0.75-ct(1,2,3)	n/a	n/a	0.418	1.696	1.852	1.637	1.870	1.895	1.885
2p-t22w1h0.75-t(1,2,3)	0.406	0.387	0.373	1.589	n/a	1.594	2.128	2.002	2.276
2p-t22w3h2-c(1,2,3)	0.332	0.316	0.317	--	1.102	--	1.328	1.146	1.118
2p-t22w3h2-ct(1,2,3)	0.330	0.331	0.334	1.299	1.336	1.357	1.434	1.368	1.409
2p-t22w3h2-t(1,2,3)	0.281	n/a	0.293	1.461	1.480	1.503	1.493	1.487	1.550
2p-t22w5.5h3-c(1,2,3)	0.466	0.479	0.473	1.357	--	--	1.367	1.344	1.378
2p-t22w5.5h3-ct(1,2,3)	0.459	0.465	0.465	--	--	1.501	1.516	1.535	1.597
2p-t22w5.5h3-t(1,2,3)	0.469	0.466	0.466	--	--	--	1.621	1.644	1.712

Note: 1 inch = 25.4 mm. "--" indicates no yielding. "n/a" indicates that data is not available.

Table 4.5.1 Maximum Compressive and Tensile Strains in the Same Section at Yielding in One-Point Loading Condition

Specimens	Thickness (in.)	Average w/t	Compressive Strain (Test 1)	Tensile Strain (Test 1)	Compressive Strain (Test 2)	Tensile Strain (Test 2)
1p-t26w0.5h0.5-ct(1,2)	0.017	31.33	5739	4813	4536	5739
1p-t26w0.5h0.5-t(1,2)	0.017	31.65	3729	5741	3743	5738
1p-t26w2h1.5-ct(1,2)	0.017	118.64	5739	3647	n/a	n/a
1p-t26w2h1.5-t(1,2)	0.017	118.86	5739	3417	5739	4122
1p-t22w0.5h0.5-ct(1,2)	0.029	18.35	5212	5282	4927	5282
1p-t22w0.5h0.5-t(1,2)	0.029	17.93	n/a	n/a	4348	5286
1p-t22w5.5h3-ct(1,2)	0.029	189.74	5282	3196	5280	3221
1p-t22w5.5h3-t(1,2)	0.029	189.95	5280	3558	--	--

Note: 1 inch = 25.4 mm. The yield strains for the 26 and 22 gage sheet steels are 5739 and 5282 microstrains, respectively. "--" indicates no yielding in section. "n/a" indicates that data is not available.

Table 4.5.2 Maximum Compressive and Tensile Strains in the Same Section at Failure of the Panels in One-Point Loading Condition

Specimens	Thickness (in.)	Average w/t	Compressive Strain (Test 1)	Tensile Strain (Test 1)	Compressive Strain (Test 2)	Tensile Strain (Test 2)
1p-t26w0.5h0.5-ct(1,2)	0.017	31.33	6365	5010	6498	9714
1p-t26w0.5h0.5-t(1,2)	0.017	31.65	4186	13166	4026	14342
1p-t26w2h1.5-ct(1,2)	0.017	118.64	7103	4358	6751	4179
1p-t26w2h1.5-t(1,2)	0.017	118.86	3417	5739	16288	4974
1p-t22w0.5h0.5-ct(1,2)	0.029	18.35	8375	14973	6808	14202
1p-t22w0.5h0.5-t(1,2)	0.029	17.93	7604	23162	7655	22624
1p-t22w5.5h3-ct(1,2)	0.029	189.74	6039	3310	7481	3468
1p-t22w5.5h3-t(1,2)	0.029	189.95	12040	3909	4209	3876

Note: 1 inch = 25.4 mm. The yield strains for the 26 and 22 gage sheet steels are 5739 and 5282 microstrains, respectively.

Table 4.5.3 Central Deflections at Service Load, at Yielding, and at Failure of the Panels in One-Point Loading Condition

Specimens	Deflection at Service Load (in.)		Deflection at Yielding (in.)		Deflection at Failure (in.)	
	Test 1	Test 2	Test 1	Test 2	Test 1	Test 2
1p-t26w0.5h0.5-ct(1,2)	0.050	0.049	0.258		0.286	0.280
1p-t26w0.5h0.5-t(1,2)	0.046	0.045	0.179	0.178	0.296	0.294
1p-t26w2h1.5-ct(1,2)	0.145	0.166	0.539	n/a	0.648	0.632
1p-t26w2h1.5-t(1,2)	0.148	0.134	0.668	0.571	0.640	0.703
1p-t22w0.5h0.5-ct(1,2)	0.064	0.065	0.228	0.240	0.354	0.362
1p-t22w0.5h0.5-t(1,2)	n/a	0.043	n/a	0.178	0.360	0.374
1p-t22w5.5h3-ct(1,2)	0.352	n/a	1.096	1.078	1.149	1.158
1p-t22w5.5h3-t(1,2)	0.340	0.340	1.169	--	1.262	1.288

Note: 1 inch = 25.4 mm. "--" indicates no yielding. "n/a" indicates that data is not available.

Table 5.1.1 Calculated Moments Using Specified 60 ksi Stress, 75% of Actual Yield Strength, and 100% of Actual Yield Strength of the Steel

Sections	Thickness (in.)	Average w/t	$M_{e,60ksi}$ (kips-in)	$M_{e,75\%Fy}$ (kips-in)	$M_{y,100\%Fy}$ (kips-in)	f_t/f_c ($100\%F_y$)
t28w1.5h1-c	0.015	103.13	1.68	2.16	2.78	0.81
t28w1.5h1-ct	0.015	103.52	1.38	1.91	2.44	1.05
t28w1.5h1-t	0.015	102.86	1.26	1.75	2.22	1.10
t26w0.5h0.5-c	0.017	31.43	1.08	1.43	1.80	0.84
t26w0.5h0.5-ct	0.017	31.33	0.90	1.27	1.69	1.00
t26w0.5h0.5-t	0.017	31.65	0.84	1.10	1.46	1.08
t26w1h0.75-c	0.017	61.07	1.38	1.77	2.25	0.83
t26w1h0.75-ct	0.017	60.38	1.14	1.60	2.03	1.00
t26w1h0.75-t	0.017	59.56	0.96	1.35	1.80	1.13
t26w2h1.5-c	0.017	120.41	3.42	4.47	5.40	0.84
t26w2h1.5-ct	0.017	118.64	2.94	4.05	5.18	0.98
t26w2h1.5-t	0.017	118.86	2.64	3.63	4.84	1.09
t22w0.5h0.5-c	0.029	18.13	1.86	2.42	3.22	0.84
t22w0.5h0.5-ct	0.029	18.35	1.68	2.18	2.91	1.00
t22w0.5h0.5-t	0.029	17.93	1.50	1.95	2.60	1.12
t22w1h0.75-c	0.029	35.06	3.00	3.66	4.57	0.80
t22w1h0.75-ct	0.029	35.40	2.64	3.43	4.47	1.00
t22w1h0.75-t	0.029	35.04	2.10	2.65	3.53	1.24
t22w3h2-c	0.029	103.33	6.00	7.40	9.35	0.80
t22w3h2-ct	0.029	103.00	5.28	6.70	8.73	1.00
t22w3h2-t	0.029	103.31	4.32	5.53	7.17	1.19
t22w5.5h3-c	0.029	188.98	10.68	13.17	14.86	0.79
t22w5.5h3-ct	0.029	189.74	9.18	11.69	15.07	0.99
t22w5.5h3-t	0.029	189.95	7.98	10.13	13.30	1.13

Note: 1 inch = 25.4 mm. 1 kip = 4.448 kN. $M_{e,60ksi}$ = Effective moment calculated by using 60 ksi stress. $M_{e,75\%Fy}$ = Moment calculated by using 75% of the actual yield strength of the steel. $M_{y,100\%Fy}$ = Yield moment calculated by using 100% of the actual yield strength of the steel. f_t/f_c = calculated tension to compression stress ratio. All the calculated moments are determined based on the AISI Specification (AISI 1986).

Table 5.1.2 Tested Ultimate Moments and Ratios of Tested Ultimate Moment to Calculated Effective Moment Using 60 ksi

Specimens	Thickness (in.)	Average w/t	$M_{u,test}$ (kips-in) (test 1)	$M_{u,test}$ (kips-in) (test 2)	$M_{u,test}$ (kips-in) (test 3)	$M_{u,test}/M_{e,60ksi}$ (test 1)	$M_{u,test}/M_{e,60ksi}$ (test 2)	$M_{u,test}/M_{e,60ksi}$ (test 3)
2p-t28w1.5h1-c(1,2,3)	0.015	103.13	2.41	2.40	2.37	1.43	1.43	1.41
2p-t28w1.5h1-ct(1,2,3)	0.015	103.52	2.32	2.35	2.32	1.68	1.70	1.68
2p-t28w1.5h1-t(1,2,3)	0.015	102.86	2.20	2.19	2.13	1.75	1.74	1.69
2p-t26w0.5h0.5-c(1,2,3)	0.017	31.43	1.79	1.83	1.85	1.66	1.69	1.71
2p-t26w0.5h0.5-ct(1,2,3)	0.017	31.33	1.80	1.97	1.78	2.00	2.19	1.98
2p-t26w0.5h0.5-t(1,2,3)	0.017	31.65	1.64	1.81	1.66	1.95	2.15	1.98
2p-t26w1h0.75-c(1,2,3)	0.017	61.07	2.32	2.33	2.35	1.68	1.69	1.70
2p-t26w1h0.75-ct(1,2,3)	0.017	60.38	2.33	2.23	2.25	2.04	1.96	1.97
2p-t26w1h0.75-t(1,2,3)	0.017	59.56	2.13	2.16	2.12	2.22	2.25	2.21
2p-t26w2h1.5-c(1,2,3)	0.017	120.41	4.50	4.54	4.59	1.32	1.33	1.34
2p-t26w2h1.5-ct(1,2,3)	0.017	118.64	4.46	4.41	4.50	1.52	1.50	1.53
2p-t26w2h1.5-t(1,2,3)	0.017	118.86	4.35	4.40	4.45	1.65	1.67	1.69
2p-t22w0.5h0.5-c(1,2,3)	0.029	18.13	3.65	3.85	3.67	1.96	2.07	1.97
2p-t22w0.5h0.5-ct(1,2,3)	0.029	18.35	3.42	3.29	3.58	2.04	1.96	2.13
2p-t22w0.5h0.5-t(1,2,3)	0.029	17.93	2.99	2.90	3.02	1.99	1.93	2.01
2p-t22w1h0.75-c(1,2,3)	0.029	35.06	4.86	4.78	4.78	1.62	1.59	1.59
2p-t22w1h0.75-ct(1,2,3)	0.029	35.40	4.44	4.34	4.55	1.68	1.64	1.72
2p-t22w1h0.75-t(1,2,3)	0.029	35.04	3.73	3.94	3.92	1.78	1.88	1.87
2p-t22w3h2-c(1,2,3)	0.029	103.33	8.04	8.25	8.34	1.34	1.38	1.39
2p-t22w3h2-ct(1,2,3)	0.029	103.00	7.38	7.47	7.54	1.40	1.41	1.43
2p-t22w3h2-t(1,2,3)	0.029	103.31	7.14	7.07	7.15	1.65	1.64	1.66
2p-t22w5.5h3-c(1,2,3)	0.029	188.98	12.89	12.98	13.24	1.21	1.22	1.24
2p-t22w5.5h3-ct(1,2,3)	0.029	189.74	12.31	12.43	12.13	1.34	1.35	1.32
2p-t22w5.5h3-t(1,2,3)	0.029	189.95	12.12	12.07	11.94	1.52	1.51	1.50

Note: 1 inch = 25.4 mm. 1 kip = 4.448 kN. $M_{u,test}$ = Tested ultimate moment. $M_{e,60ksi}$ = Calculated effective moment by using 60 ksi. All the calculated moments are determined based on the AISI Specification (AISI 1986).

Table 5.1.3 Tested Ultimate Moments and Ratios of Tested Ultimate Moment to Calculated Moment Using 75% of Actual Yield Strength of the Steel

Specimens	Thickness (in.)	Average w/t	$M_{u,test}$ (kips-in) (test 1)	$M_{u,test}$ (kips-in) (test 2)	$M_{u,test}$ (kips-in) (test 3)	$M_{u,test}/M_{e,75\%Fy}$ (test 1)	$M_{u,test}/M_{e,75\%Fy}$ (test 2)	$M_{u,test}/M_{e,75\%Fy}$ (test 3)
2p-t28w1.5h1-c(1,2,3)	0.015	103.13	2.41	2.40	2.37	1.11	1.11	1.09
2p-t28w1.5h1-ct(1,2,3)	0.015	103.52	2.32	2.35	2.32	1.21	1.23	1.21
2p-t28w1.5h1-t(1,2,3)	0.015	102.86	2.20	2.19	2.13	1.26	1.25	1.22
2p-t26w0.5h0.5-c(1,2,3)	0.017	31.43	1.79	1.83	1.85	1.25	1.28	1.29
2p-t26w0.5h0.5-ct(1,2,3)	0.017	31.33	1.80	1.97	1.78	1.42	1.56	1.41
2p-t26w0.5h0.5-t(1,2,3)	0.017	31.65	1.64	1.81	1.66	1.50	1.65	1.51
2p-t26w1h0.75-c(1,2,3)	0.017	61.07	2.32	2.33	2.35	1.31	1.31	1.33
2p-t26w1h0.75-ct(1,2,3)	0.017	60.38	2.33	2.23	2.25	1.45	1.39	1.40
2p-t26w1h0.75-t(1,2,3)	0.017	59.56	2.13	2.16	2.12	1.58	1.60	1.57
2p-t26w2h1.5-c(1,2,3)	0.017	120.41	4.50	4.54	4.59	1.01	1.02	1.03
2p-t26w2h1.5-ct(1,2,3)	0.017	118.64	4.46	4.41	4.50	1.10	1.09	1.11
2p-t26w2h1.5-t(1,2,3)	0.017	118.86	4.35	4.40	4.45	1.20	1.21	1.23
2p-t22w0.5h0.5-c(1,2,3)	0.029	18.13	3.65	3.85	3.67	1.51	1.59	1.52
2p-t22w0.5h0.5-ct(1,2,3)	0.029	18.35	3.42	3.29	3.58	1.57	1.51	1.64
2p-t22w0.5h0.5-t(1,2,3)	0.029	17.93	2.99	2.90	3.02	1.53	1.49	1.55
2p-t22w1h0.75-c(1,2,3)	0.029	35.06	4.86	4.78	4.78	1.33	1.31	1.31
2p-t22w1h0.75-ct(1,2,3)	0.029	35.40	4.44	4.34	4.55	1.29	1.27	1.33
2p-t22w1h0.75-t(1,2,3)	0.029	35.04	3.73	3.94	3.92	1.41	1.49	1.48
2p-t22w3h2-c(1,2,3)	0.029	103.33	8.04	8.25	8.34	1.09	1.11	1.13
2p-t22w3h2-ct(1,2,3)	0.029	103.00	7.38	7.47	7.54	1.10	1.11	1.13
2p-t22w3h2-t(1,2,3)	0.029	103.31	7.14	7.07	7.15	1.29	1.28	1.29
2p-t22w5.5h3-c(1,2,3)	0.029	188.98	12.89	12.98	13.24	0.98	0.99	1.01
2p-t22w5.5h3-ct(1,2,3)	0.029	189.74	12.31	12.43	12.13	1.05	1.06	1.04
2p-t22w5.5h3-t(1,2,3)	0.029	189.95	12.12	12.07	11.94	1.20	1.19	1.18

Note: 1 inch = 25.4 mm. 1 kip = 4.448 kN. $M_{u,test}$ = Tested ultimate moment. $M_{e,75\%Fy}$ = Calculated moment by using 75% of the actual yield strength of the steel. All the calculated moments are determined based on the AISI Specification (AISI 1986).

Table 5.1.4 Tested Ultimate Moments and Ratios of Tested Ultimate Moment to Calculated Yield Moment Using 100% of Actual Yield Strength of Steel

Specimens	Thickness (in.)	Average w/t	$M_{u,test}$ (kips-in) (test 1)	$M_{u,test}$ (kips-in) (test 2)	$M_{u,test}$ (kips-in) (test 3)	$M_{u,test}/M_{y,100\%Fy}$ (test 1)	$M_{u,test}/M_{y,100\%Fy}$ (test 2)	$M_{u,test}/M_{y,100\%Fy}$ (test 3)
2p-t28w1.5h1-c(1,2,3)	0.015	103.13	2.41	2.40	2.37	0.87	0.86	0.85
2p-t28w1.5h1-ct(1,2,3)	0.015	103.52	2.32	2.35	2.32	0.95	0.96	0.95
2p-t28w1.5h1-t(1,2,3)	0.015	102.86	2.20	2.19	2.13	0.99	0.99	0.96
2p-t26w0.5h0.5-c(1,2,3)	0.017	31.43	1.79	1.83	1.85	0.99	1.02	1.03
2p-t26w0.5h0.5-ct(1,2,3)	0.017	31.33	1.80	1.97	1.78	1.07	1.17	1.05
2p-t26w0.5h0.5-t(1,2,3)	0.017	31.65	1.64	1.81	1.66	1.12	1.24	1.14
2p-t26w1h0.75-c(1,2,3)	0.017	61.07	2.32	2.33	2.35	1.03	1.04	1.04
2p-t26w1h0.75-ct(1,2,3)	0.017	60.38	2.33	2.23	2.25	1.15	1.10	1.11
2p-t26w1h0.75-t(1,2,3)	0.017	59.56	2.13	2.16	2.12	1.18	1.20	1.18
2p-t26w2h1.5-c(1,2,3)	0.017	120.41	4.50	4.54	4.59	0.83	0.84	0.85
2p-t26w2h1.5-ct(1,2,3)	0.017	118.64	4.46	4.41	4.50	0.86	0.85	0.87
2p-t26w2h1.5-t(1,2,3)	0.017	118.86	4.35	4.40	4.45	0.90	0.91	0.92
2p-t22w0.5h0.5-c(1,2,3)	0.029	18.13	3.65	3.85	3.67	1.13	1.20	1.14
2p-t22w0.5h0.5-ct(1,2,3)	0.029	18.35	3.42	3.29	3.58	1.18	1.13	1.23
2p-t22w0.5h0.5-t(1,2,3)	0.029	17.93	2.99	2.90	3.02	1.15	1.12	1.16
2p-t22w1h0.75-c(1,2,3)	0.029	35.06	4.86	4.78	4.78	1.06	1.05	1.05
2p-t22w1h0.75-ct(1,2,3)	0.029	35.40	4.44	4.34	4.55	0.99	0.97	1.02
2p-t22w1h0.75-t(1,2,3)	0.029	35.04	3.73	3.94	3.92	1.06	1.12	1.11
2p-t22w3h2-c(1,2,3)	0.029	103.33	8.04	8.25	8.34	0.86	0.88	0.89
2p-t22w3h2-ct(1,2,3)	0.029	103.00	7.38	7.47	7.54	0.85	0.86	0.86
2p-t22w3h2-t(1,2,3)	0.029	103.31	7.14	7.07	7.15	1.00	0.99	1.00
2p-t22w5.5h3-c(1,2,3)	0.029	188.98	12.89	12.98	13.24	0.87	0.87	0.89
2p-t22w5.5h3-ct(1,2,3)	0.029	189.74	12.31	12.43	12.13	0.82	0.83	0.81
2p-t22w5.5h3-t(1,2,3)	0.029	189.95	12.12	12.07	11.94	0.91	0.91	0.90

Note: 1 inch = 25.4 mm. 1 kip = 4.448 kN. $M_{u,test}$ = Tested ultimate moment. $M_{y,100\%Fy}$ = Calculated yield moment by using 100% of the actual yield strength of the steel. All the calculated moments are determined based on the AISI Specification (AISI 1986).

Table 5.1.5 Tested Yield Moments and Ratios of Tested Yield Moment to Calculated Yield Moment

Specimens	Thickness (in.)	Average w/t	$M_{y,test}$ (kips-in) (test 1)	$M_{y,test}$ (kips-in) (test 2)	$M_{y,test}$ (kips-in) (test 3)	$M_{y,test}/M_{y,100\%Fy}$ (test 1)	$M_{y,test}/M_{y,100\%Fy}$ (test 2)	$M_{y,test}/M_{y,100\%Fy}$ (test 3)
2p-t28w1.5h1-c(1,2,3)	0.015	103.13	--	--	2.35	--	--	0.85
2p-t28w1.5h1-ct(1,2,3)	0.015	103.52	n/a	2.35	2.21	n/a	0.96	0.90
2p-t28w1.5h1-t(1,2,3)	0.015	102.86	2.16	--	2.10	0.97	--	0.95
2p-t26w0.5h0.5-c(1,2,3)	0.017	31.43	1.78	1.72	1.75	0.99	0.96	0.97
2p-t26w0.5h0.5-ct(1,2,3)	0.017	31.33	1.72	1.92	1.77	1.02	1.14	1.05
2p-t26w0.5h0.5-t(1,2,3)	0.017	31.65	1.63	1.80	1.65	1.11	1.23	1.13
2p-t26w1h0.75-c(1,2,3)	0.017	61.07	2.16	--	--	0.96	--	--
2p-t26w1h0.75-ct(1,2,3)	0.017	60.38	2.31	2.23	--	1.14	1.10	--
2p-t26w1h0.75-t(1,2,3)	0.017	59.56	2.02	1.96	2.03	1.12	1.09	1.13
2p-t26w2h1.5-c(1,2,3)	0.017	120.41	--	4.34	--	--	0.80	--
2p-t26w2h1.5-ct(1,2,3)	0.017	118.64	4.26	--	4.42	0.82	--	0.85
2p-t26w2h1.5-t(1,2,3)	0.017	118.86	--	--	4.41	--	--	0.91
2p-t22w0.5h0.5-c(1,2,3)	0.029	18.13	3.44	n/a	3.29	1.07	n/a	1.02
2p-t22w0.5h0.5-ct(1,2,3)	0.029	18.35	3.09	3.07	n/a	1.06	1.06	n/a
2p-t22w0.5h0.5-t(1,2,3)	0.029	17.93	2.86	2.79	2.85	1.10	1.07	1.10
2p-t22w1h0.75-c(1,2,3)	0.029	35.06	--	--	--	--	--	--
2p-t22w1h0.75-ct(1,2,3)	0.029	35.40	4.44	4.29	4.54	0.99	0.96	1.02
2p-t22w1h0.75-t(1,2,3)	0.029	35.04	3.66	n/a	3.72	1.04	n/a	1.05
2p-t22w3h2-c(1,2,3)	0.029	103.33	--	8.16	--	--	0.87	--
2p-t22w3h2-ct(1,2,3)	0.029	103.00	7.29	7.45	7.51	0.84	0.85	0.86
2p-t22w3h2-t(1,2,3)	0.029	103.31	7.14	7.07	7.15	1.00	0.99	1.00
2p-t22w5.5h3-c(1,2,3)	0.029	188.98	12.89	--	--	0.87	--	--
2p-t22w5.5h3-ct(1,2,3)	0.029	189.74	--	--	12.13	--	--	0.81
2p-t22w5.5h3-t(1,2,3)	0.029	189.95	--	--	--	--	--	--

Note: 1 inch = 25.4 mm. 1 kip = 4.448 kN. $M_{y,test}$ = Tested yield moment. $M_{y,100\%Fy}$ = Calculated yield moment by using 100% of the actual yield strength of the steel. "--" = Panel did not yield in the section according to the recorded strains. "n/a" = Data not available. All the calculated moments are determined based on the AISI Specification (AISI 1986).

Table 5.1.6 Tested Yield Moments and Ratios of Tested Yield Moment to Calculated Moment Using Pan's Yield Strength Reduction Factor

Specimens	Thickness (in.)	Average w/t	$M_{y,test}$ (kips-in) (test 1)	$M_{y,test}$ (kips-in) (test 2)	$M_{y,test}$ (kips-in) (test 3)	$M_{y,test}/M_{e,Pan}$ (test 1)	$M_{y,test}/M_{e,Pan}$ (test 2)	$M_{y,test}/M_{e,Pan}$ (test 3)
2p-t28w1.5h1-c(1,2,3)	0.015	103.13	--	--	2.35	--	--	0.93
2p-t28w1.5h1-ct(1,2,3)	0.015	103.52	n/a	2.35	2.21	n/a	1.05	0.99
2p-t26w0.5h0.5-c(1,2,3)	0.017	31.43	1.78	1.72	1.75	1.06	1.03	1.04
2p-t26w0.5h0.5-ct(1,2,3)	0.017	31.33	1.72	1.92	1.77	1.09	1.22	1.13
2p-t26w1h0.75-c(1,2,3)	0.017	61.07	2.16	--	--	1.01	--	--
2p-t26w1h0.75-ct(1,2,3)	0.017	60.38	2.31	2.23	--	1.26	1.22	--
2p-t26w2h1.5-c(1,2,3)	0.017	120.41	--	4.34	--	--	0.88	--
2p-t26w2h1.5-ct(1,2,3)	0.017	118.64	4.26	--	4.42	0.91	--	0.95
2p-t22w0.5h0.5-c(1,2,3)	0.029	18.13	3.44	n/a	3.29	1.12	n/a	1.08
2p-t22w0.5h0.5-ct(1,2,3)	0.029	18.35	3.09	3.07	n/a	1.12	1.11	n/a
2p-t22w1h0.75-c(1,2,3)	0.029	35.06	--	--	--	--	--	--
2p-t22w1h0.75-ct(1,2,3)	0.029	35.40	4.44	4.29	4.54	1.07	1.03	1.09
2p-t22w3h2-c(1,2,3)	0.029	103.33	--	8.16	--	--	0.97	--
2p-t22w3h2-ct(1,2,3)	0.029	103.00	7.29	7.45	7.51	0.93	0.96	0.97
2p-t22w5.5h3-c(1,2,3)	0.029	188.98	12.89	--	--	0.94	--	--
2p-t22w5.5h3-ct(1,2,3)	0.029	189.74	--	--	12.13	--	--	0.94

Note: 1 inch = 25.4 mm. 1 kip = 4.448 kN. $M_{y,test}$ = Tested yield moment. $M_{e,Pan}$ = Calculated moment by using Pan's yield strength reduction factor. "--" = Panel did not yield in the section according to the recorded strains. "n/a" = Data not available. All the calculated moments are determined based on the AISI Specification (AISI 1986).

Table 5.1.7 Ratios of Tested Central Deflection to Calculated Central Deflection at Service Load

Specimens	Tested Central Deflection (in.)			Calculated Central Deflection (E=29,500 ksi) (in.)	Tested Central Deflection to Calculated Central Deflection		
	Test 1	Test 2	Test 3		Test 1	Test 2	Test 3
2p-t28w1.5h1-c(1,2,3)	0.289	0.272	0.292	0.323	0.90	0.84	0.91
2p-t28w1.5h1-ct(1,2,3)	0.259	0.263	0.259	0.326	0.79	0.81	0.79
2p-t28w1.5h1-t(1,2,3)	0.269	n/a	0.280	0.298	0.90	n/a	0.94
2p-t26w0.5h0.5-c(1,2,3)	0.473	0.453	0.444	0.475	1.00	0.95	0.93
2p-t26w0.5h0.5-ct(1,2,3)	0.409	0.384	0.397	0.495	0.83	0.78	0.80
2p-t26w0.5h0.5-t(1,2,3)	0.469	0.413	0.454	0.462	1.02	0.89	0.98
2p-t26w1h0.75-c(1,2,3)	0.289	0.276	0.278	0.303	0.95	0.91	0.92
2p-t26w1h0.75-ct(1,2,3)	0.261	0.266	0.263	0.313	0.83	0.85	0.84
2p-t26w1h0.75-t(1,2,3)	0.260	0.268	0.267	0.302	0.86	0.89	0.89
2p-t26w2h1.5-c(1,2,3)	0.376	0.363	0.370	0.446	0.84	0.81	0.83
2p-t26w2h1.5-ct(1,2,3)	0.363	0.370	0.366	0.430	0.84	0.86	0.85
2p-t26w2h1.5-t(1,2,3)	0.352	0.338	0.346	0.428	0.82	0.79	0.81
2p-t22w0.5h0.5-c(1,2,3)	0.404	n/a	0.383	0.409	0.99	n/a	0.94
2p-t22w0.5h0.5-ct(1,2,3)	n/a	0.430	n/a	0.462	n/a	0.93	n/a
2p-t22w0.5h0.5-t(1,2,3)	0.427	0.446	0.442	0.471	0.91	0.95	0.94
2p-t22w1h0.75-c(1,2,3)	0.461	n/a	0.408	0.439	1.05	n/a	0.93
2p-t22w1h0.75-ct(1,2,3)	n/a	n/a	0.418	0.451	n/a	n/a	0.93
2p-t22w1h0.75-t(1,2,3)	0.406	0.387	0.373	0.430	0.94	0.90	0.87
2p-t22w3h2-c(1,2,3)	0.332	0.316	0.317	0.381	0.87	0.83	0.83
2p-t22w3h2-ct(1,2,3)	0.330	0.331	0.334	0.390	0.85	0.85	0.86
2p-t22w3h2-t(1,2,3)	0.281	n/a	0.293	0.353	0.80	n/a	0.83
2p-t22w5.5h3-c(1,2,3)	0.466	0.479	0.473	0.559	0.83	0.86	0.84
2p-t22w5.5h3-ct(1,2,3)	0.459	0.465	0.465	0.551	0.83	0.84	0.84
2p-t22w5.5h3-t(1,2,3)	0.469	0.466	0.466	0.523	0.90	0.89	0.89

Note: 1 inch = 25.4 mm. "n/a" indicates that data is not available.

Table 5.1.8 Ratios of Tested Central Deflection to Calculated Central Deflection at Service Load Using Actual Modulus of Elasticity

Specimens	Tested Central Deflection at Service Load (in.)			Calculated Central Deflection (Using Actual E) (in.)	Tested Central Deflection to Calculated Central Deflection		
	Test 1	Test 2	Test 3		Test 1	Test 2	Test 3
2p-t28w1.5h1-c(1,2,3)	0.289	0.272	0.292	0.314	0.92	0.87	0.93
2p-t28w1.5h1-ct(1,2,3)	0.259	0.263	0.259	0.317	0.82	0.83	0.82
2p-t28w1.5h1-t(1,2,3)	0.269	n/a	0.280	0.289	0.93	n/a	0.97
2p-t26w0.5h0.5-c(1,2,3)	0.473	0.453	0.444	0.459	1.03	0.99	0.97
2p-t26w0.5h0.5-ct(1,2,3)	0.409	0.384	0.397	0.478	0.86	0.80	0.83
2p-t26w0.5h0.5-t(1,2,3)	0.469	0.413	0.454	0.446	1.05	0.93	1.02
2p-t26w1h0.75-c(1,2,3)	0.289	0.276	0.278	0.293	0.99	0.94	0.95
2p-t26w1h0.75-ct(1,2,3)	0.261	0.266	0.263	0.303	0.86	0.88	0.87
2p-t26w1h0.75-t(1,2,3)	0.260	0.268	0.267	0.291	0.89	0.92	0.92
2p-t26w2h1.5-c(1,2,3)	0.376	0.363	0.370	0.431	0.87	0.84	0.86
2p-t26w2h1.5-ct(1,2,3)	0.363	0.370	0.366	0.415	0.87	0.89	0.88
2p-t26w2h1.5-t(1,2,3)	0.352	0.338	0.346	0.413	0.85	0.82	0.84
2p-t22w0.5h0.5-c(1,2,3)	0.404	n/a	0.383	0.380	1.06	n/a	1.01
2p-t22w0.5h0.5-ct(1,2,3)	n/a	0.430	n/a	0.429	n/a	1.00	n/a
2p-t22w0.5h0.5-t(1,2,3)	0.427	0.446	0.442	0.438	0.98	1.02	1.01
2p-t22w1h0.75-c(1,2,3)	0.461	n/a	0.408	0.408	1.03	n/a	1.00
2p-t22w1h0.75-ct(1,2,3)	n/a	n/a	0.418	0.419	n/a	n/a	1.00
2p-t22w1h0.75-t(1,2,3)	0.406	0.387	0.373	0.400	1.02	0.97	0.93
2p-t22w3h2-c(1,2,3)	0.332	0.316	0.317	0.354	0.94	0.89	0.90
2p-t22w3h2-ct(1,2,3)	0.330	0.331	0.334	0.362	0.91	0.91	0.92
2p-t22w3h2-t(1,2,3)	0.281	n/a	0.293	0.328	0.86	n/a	0.89
2p-t22w5.5h3-c(1,2,3)	0.466	0.479	0.473	0.519	0.90	0.92	0.91
2p-t22w5.5h3-ct(1,2,3)	0.459	0.465	0.465	0.512	0.90	0.91	0.91
2p-t22w5.5h3-t(1,2,3)	0.469	0.466	0.466	0.486	0.97	0.96	0.96

Note: 1 inch = 25.4 mm. "n/a" indicates that data is not available.

Table 5.1.9 Ratios of Tested Central Deflection to Calculated Central Deflection at Yielding

Specimens	Tested Central Deflection at Yielding (in.)			Calculated Central Deflection Using Tested Yield Moment (E=29,500 ksi) (in.)			Tested Central Deflection to Calculated Central Deflection		
	Test 1	Test 2	Test 3	Test 1	Test 2	Test 3	Test 1	Test 2	Test 3
2p-t28w1.5h1-c(1,2,3)	--	--	1.181	--	--	0.927	--	--	1.27
2p-t28w1.5h1-ct(1,2,3)	n/a	1.451	1.141	n/a	1.096	1.031	n/a	1.32	1.11
2p-t28w1.5h1-t(1,2,3)	1.290	--	1.345	1.108	--	1.077	1.16	--	1.25
2p-t26w0.5h0.5-c(1,2,3)	1.825	1.517	1.571	1.307	1.263	1.285	1.40	1.20	1.22
2p-t26w0.5h0.5-ct(1,2,3)	1.715	2.063	2.207	1.579	1.763	1.625	1.09	1.17	1.36
2p-t26w0.5h0.5-t(1,2,3)	1.990	1.997	2.083	1.496	1.653	1.515	1.33	1.21	1.38
2p-t26w1h0.75-c(1,2,3)	0.981	--	--	0.992	--	--	0.99	--	--
2p-t26w1h0.75-ct(1,2,3)	1.663	1.684	--	1.212	1.170	--	1.37	1.44	--
2p-t26w1h0.75-t(1,2,3)	1.328	1.215	1.384	1.236	1.200	1.242	1.07	1.01	1.11
2p-t26w2h1.5-c(1,2,3)	--	1.066	--	--	1.143	--	--	0.93	--
2p-t26w2h1.5-ct(1,2,3)	1.295	--	1.401	1.254	--	1.301	1.03	--	1.08
2p-t26w2h1.5-t(1,2,3)	--	--	1.577	--	--	1.380	--	--	1.14
2p-t22w0.5h0.5-c(1,2,3)	1.569	n/a	1.592	1.263	n/a	1.208	1.24	n/a	1.32
2p-t22w0.5h0.5-ct(1,2,3)	1.782	1.832	n/a	1.418	1.409	n/a	1.26	1.30	n/a
2p-t22w0.5h0.5-t(1,2,3)	1.817	1.871	1.779	1.500	1.464	1.495	1.21	1.28	1.19
2p-t22w1h0.75-c(1,2,3)	--	--	--	--	--	--	--	--	--
2p-t22w1h0.75-ct(1,2,3)	1.696	1.852	1.637	1.424	1.375	1.456	1.19	1.34	1.12
2p-t22w1h0.75-t(1,2,3)	1.589	n/a	1.594	1.341	n/a	1.363	1.18	n/a	1.17
2p-t22w3h2-c(1,2,3)	--	1.102	--	--	1.027	--	--	1.07	--
2p-t22w3h2-ct(1,2,3)	1.299	1.336	1.357	1.066	1.094	1.103	1.22	1.22	1.23
2p-t22w3h2-t(1,2,3)	1.461	1.480	1.503	1.152	1.141	1.154	1.27	1.30	1.30
2p-t22w5.5h3-c(1,2,3)	1.357	--	--	1.411	--	--	0.96	--	--
2p-t22w5.5h3-ct(1,2,3)	--	--	1.501	--	--	1.455	--	--	1.03
2p-t22w5.5h3-t(1,2,3)	--	--	--	--	--	--	--	--	--

Note: 1 inch = 25.4 mm. "--" indicates no yielding. "n/a" indicates that data is not available.

Table 5.2.1 Tested Ultimate Moments and Ratios of Tested Ultimate Moment to Calculated Moment in One-Point Loading Condition

Specimens	Thickness (in.)	Average w/t	$M_{u,test}$ (kips-in) (test 1)	$M_{u,test}$ (kips-in) (test 2)	$M_{u,test}/M_{e,60ksi}$ (test 1)	$M_{u,test}/M_{e,60ksi}$ (test 2)	$M_{u,test}/M_{e,75\%Fy}$ (test 1)	$M_{u,test}/M_{e,75\%Fy}$ (test 2)
1p-t26w0.5h0.5-ct(1,2)	0.017	31.33	2.16	2.26	2.40	2.51	1.71	1.79
1p-t26w0.5h0.5-t(1,2)	0.017	31.65	2.07	2.05	2.46	2.44	1.89	1.87
1p-t26w2h1.5-ct(1,2)	0.017	118.64	4.54	4.42	1.54	1.50	1.12	1.09
1p-t26w2h1.5-t(1,2)	0.017	118.86	4.27	4.61	1.62	1.75	1.18	1.27
1p-t22w0.5h0.5-ct(1,2)	0.029	18.35	4.50	4.59	2.68	2.73	2.06	2.10
1p-t22w0.5h0.5-t(1,2)	0.029	17.93	4.01	4.13	2.67	2.75	2.06	2.12
1p-t22w5.5h3-ct(1,2)	0.029	189.74	13.22	12.76	1.44	1.39	1.13	1.09
1p-t22w5.5h3-t(1,2)	0.029	189.95	12.88	13.06	1.61	1.64	1.27	1.29

Note: 1 inch = 25.4 mm. 1 kip = 4.448 kN. $M_{u,test}$ = Tested ultimate moment. $M_{e,60ksi}$ = Calculated moment using specified 60 ksi. $M_{e,75\%Fy}$ = Calculated moment by using 75% of the actual yield strength of the Structural Grade 80 steel. All the calculated moments are determined based on the AISI Specification (AISI 1986).

Table 5.2.2 Tested Ultimate Moments and Ratios of Tested Ultimate Moment to Calculated Yield Moment in One-Point Loading Condition

Specimens	Thickness (in.)	Average w/t	$M_{u,test}$ (kips-in) (test 1)	$M_{u,test}$ (kips-in) (test 2)	$M_{u,test}/M_{y,100\%Fy}$ (test 1)	$M_{u,test}/M_{y,100\%Fy}$ (test 2)
1p-t26w0.5h0.5-ct(1,2)	0.017	31.33	2.16	2.26	1.28	1.34
1p-t26w0.5h0.5-t(1,2)	0.017	31.65	2.07	2.05	1.42	1.40
1p-t26w2h1.5-ct(1,2)	0.017	118.64	4.54	4.42	0.88	0.85
1p-t26w2h1.5-t(1,2)	0.017	118.86	4.27	4.61	0.88	0.95
1p-t22w0.5h0.5-ct(1,2)	0.029	18.35	4.50	4.59	1.55	1.58
1p-t22w0.5h0.5-t(1,2)	0.029	17.93	4.01	4.13	1.54	1.59
1p-t22w5.5h3-ct(1,2)	0.029	189.74	13.22	12.76	0.88	0.85
1p-t22w5.5h3-t(1,2)	0.029	189.95	12.88	13.06	0.97	0.98

Note: 1 inch = 25.4 mm. 1 kip = 4.448 kN. $M_{u,test}$ = Tested ultimate moment. $M_{y,100\%Fy}$ = Calculated moment by using 100% of the actual yield strength of the steel. All the calculated moments are determined based on the AISI Specification (AISI 1986).

Table 5.2.3 Tested Yield Moments and Ratios of Tested Yield Moment to Calculated Yield Moment in One-Point Loading Condition

Specimens	Thickness (in.)	Average w/t	$M_{y,test}$ (kips-in) (test 1)	$M_{y,test}$ (kips-in) (test 2)	$M_{y,test}/M_{y,100\%Fy}$ (test 1)	$M_{y,test}/M_{y,100\%Fy}$ (test 2)
1p-t26w0.5h0.5-ct(1,2)	0.017	31.33	2.12	2.01	1.26	1.19
1p-t26w0.5h0.5-t(1,2)	0.017	31.65	1.69	1.68	1.16	1.15
1p-t26w2h1.5-ct(1,2)	0.017	118.64	4.31	n/a	0.83	n/a
1p-t26w2h1.5-t(1,2)	0.017	118.86	4.09	4.31	0.85	0.89
1p-t22w0.5h0.5-ct(1,2)	0.029	18.35	3.84	3.99	1.32	1.37
1p-t22w0.5h0.5-t(1,2)	0.029	17.93	n/a	3.09	n/a	1.19
1p-t22w5.5h3-ct(1,2)	0.029	189.74	13.14	12.60	0.87	0.84
1p-t22w5.5h3-t(1,2)	0.029	189.95	12.62	--	0.95	--

Note: 1 inch = 25.4 mm. 1 kip = 4.448 kN. $M_{y,test}$ = Tested yield moment. $M_{y,100\%Fy}$ = Calculated moment by using 100% of the actual yield strength of the steel. All the calculated moments are determined based on the AISI Specification (AISI 1986). "--" indicates no yielding. "n/a" indicates that data is not available.

Table 5.2.4 Tested Yield Moments and Ratios of Tested Yield Moment to Calculated Moment Using Pan's Yield Strength Reduction Factor in One-Point Loading Condition

Specimens	Thickness (in.)	Average w/t	$M_{y,test}$ (kips-in) (test 1)	$M_{y,test}$ (kips-in) (test 2)	$M_{y,test}/M_{e,Pan}$ (test 1)	$M_{y,test}/M_{e,Pan}$ (test 2)
1p-t26w0.5h0.5-ct(1,2)	0.017	31.33	2.12	2.01	1.35	1.28
1p-t26w2h1.5-ct(1,2)	0.017	118.64	4.31	n/a	0.92	n/a
1p-t22w0.5h0.5-ct(1,2)	0.029	18.35	3.84	3.99	1.39	1.44
1p-t22w5.5h3-ct(1,2)	0.029	189.74	13.14	12.60	1.01	0.97

Note: 1 inch = 25.4 mm. 1 kip = 4.448 kN. $M_{y,test}$ = Tested yield moment. $M_{e,Pan}$ = Calculated moment by using Pan's yield strength reduction factor. All the calculated moments are determined based on the AISI Specification (AISI 1986). "n/a" indicates that data is not available.

Table 5.2.5 Ratios of Tested Central Deflection to Calculated Central Deflection at Service Load in One-Point Loading Condition

Specimens	Thickness (in.)	Average w/t	Calculated Central Deflection (E=29,500 ksi) (in.)	Tested Central Deflection at Service Load (in.)		Tested Central Deflection to Calculated Central Deflection	
				Test 1	Test 2	Test 1	Test 2
1p-t26w0.5h0.5-ct(1,2)	0.017	31.33	0.055	0.050	0.049	0.91	0.89
1p-t26w0.5h0.5-t(1,2)	0.017	31.65	0.051	0.046	0.045	0.90	0.88
1p-t26w2h1.5-ct(1,2)	0.017	118.64	0.194	0.145	0.166	0.75	0.86
1p-t26w2h1.5-t(1,2)	0.017	118.86	0.193	0.148	0.134	0.77	0.69
1p-t22w0.5h0.5-ct(1,2)	0.029	18.35	0.051	0.064	0.065	1.25	1.27
1p-t22w0.5h0.5-t(1,2)	0.029	17.93	0.052	n/a	0.043	n/a	0.82
1p-t22w5.5h3-ct(1,2)	0.029	189.74	0.418	0.352	n/a	0.84	n/a
1p-t22w5.5h3-t(1,2)	0.029	189.95	0.396	0.340	0.340	0.86	0.86

Note: 1 inch = 25.4 mm. 1 kip = 4.448 kN. "n/a" = Data not available.

Table 5.2.6 Ratios of Tested Central Deflection to Calculated Central Deflection at Yielding in One-Point Loading Condition

Specimens	Thickness (in.)	Average w/t	Calculated Central Deflection Using Tested Yield Moment (in.)		Tested Central Deflection at Yielding (in.)		Tested Central Deflection to Calculated Central Deflection	
			Test 1	Test 2	Test 1	Test 2	Test 1	Test 2
1p-t26w0.5h0.5-ct(1,2)	0.017	31.33	0.216	0.204	0.258		1.20	
1p-t26w0.5h0.5-t(1,2)	0.017	31.65	0.172	0.171	0.179	0.178	1.04	1.04
1p-t26w2h1.5-ct(1,2)	0.017	118.64	0.573	n/a	0.539	n/a	0.94	n/a
1p-t26w2h1.5-t(1,2)	0.017	118.86	0.578	0.609	0.668	0.571	1.16	0.94
1p-t22w0.5h0.5-ct(1,2)	0.029	18.35	0.195	0.203	0.228	0.240	1.17	1.18
1p-t22w0.5h0.5-t(1,2)	0.029	17.93	n/a	0.180	n/a	0.178	n/a	0.99
1p-t22w5.5h3-ct(1,2)	0.029	189.74	1.194	1.145	1.096	1.078	0.92	0.94
1p-t22w5.5h3-t(1,2)	0.029	189.95	1.233	--	1.169	--	0.95	--

Note: 1 inch = 25.4 mm. 1 kip = 4.448 kN. "n/a" = Data not available. "--" indicates no yielding.

Table 5.3.1 Ratios of Tested Moment for One-Point Loading Condition to Tested Moment for Two-Point Loading Condition

Specimens	Thickness (in.)	Average w/t	Average $M_{y,test\text{-}1p}$ (kips-in)	Average $M_{y,test\text{-}2p}$ (kips-in)	$M_{y,test\text{-}1p}$ to $M_{y,test\text{-}2p}$	Average $M_{u,test\text{-}1p}$ (kips-in)	Average $M_{u,test\text{-}2p}$ (kips-in)	$M_{u,test\text{-}1p}$ to $M_{u,test\text{-}2p}$
1p-t26w0.5h0.5-ct(1,2)	0.017	31.33	2.07	1.80	1.15	2.21	1.85	1.19
1p-t26w0.5h0.5-t(1,2)	0.017	31.65	1.69	1.69	1.00	2.06	1.70	1.21
1p-t26w2h1.5-ct(1,2)	0.017	118.64	4.31	4.34	0.99	4.48	4.46	1.00
1p-t26w2h1.5-t(1,2)	0.017	118.86	4.20	4.41	0.95	4.44	4.40	1.01
1p-t22w0.5h0.5-ct(1,2)	0.029	18.35	3.92	3.08	1.27	4.55	3.43	1.33
1p-t22w0.5h0.5-t(1,2)	0.029	17.93	3.09	2.83	1.09	4.07	2.97	1.37
1p-t22w5.5h3-ct(1,2)	0.029	189.74	12.87	12.13	1.06	12.99	12.29	1.06
1p-t22w5.5h3-t(1,2)	0.029	189.95	12.62	--	n/a	12.97	12.04	1.08

Note: 1 inch = 25.4 mm. 1 kip = 4.448 kN. $M_{u,test\text{-}1p}$ = Tested ultimate moment for one-point loading condition. $M_{u,test\text{-}2p}$= Tested ultimate moment for two-point loading condition. $M_{y,test\text{-}1p}$ = Tested yield moment for one-point loading condition. $M_{y,test\text{-}2p}$ = Tested yield moment for two-point loading condition.

Table 5.3.2 Ratio of Maximum Tested Shear at Failure to Calculated Shear Capacity in Both Two-Point and One-Point Loading Conditions

Specimens	Average w/t	$V_{u,test}$ (lb) (Test 1)	$V_{u,test}$ (lb) (Test 2)	$V_{u,test}$ (lb) (Test 3)	V_{calc} (lb)	$V_{u,test}$ to V_{calc} (kips-in) (Test 1)	$V_{u,test}$ to V_{calc} (kips-in) (Test 2)	$V_{u,test}$ to V_{calc} (kips-in) (Test 3)
1p-t26w0.5h0.5-ct(1,2)	31.33	360	377	--	3023	0.12	0.12	--
1p-t26w0.5h0.5-t(1,2)	31.65	346	341	--	2960	0.12	0.12	--
1p-t26w2h1.5-ct(1,2)	118.64	227	221	--	1596	0.14	0.14	--
1p-t26w2h1.5-t(1,2)	118.86	214	231	--	1622	0.13	0.14	--
1p-t22w0.5h0.5-ct(1,2)	18.35	750	765	--	4623	0.16	0.17	--
1p-t22w0.5h0.5-t(1,2)	17.93	668	688	--	4690	0.14	0.15	--
1p-t22w5.5h3-ct(1,2)	189.74	331	319	--	2004	0.17	0.16	--
1p-t22w5.5h3-t(1,2)	189.95	322	327	--	2017	0.16	0.16	--
2p-t26w0.5h0.5-ct(1,2,3)	31.33	360	394	355	3023	0.12	0.13	0.12
2p-t26w0.5h0.5-t(1,2,3)	31.65	328	361	333	2960	0.11	0.12	0.11
2p-t26w2h1.5-ct(1,2,3)	118.64	279	276	282	1596	0.17	0.17	0.18
2p-t26w2h1.5-t(1,2,3)	118.86	272	275	278	1622	0.17	0.17	0.17
2p-t22w0.5h0.5-ct(1,2,3)	18.35	683	657	716	4623	0.15	0.14	0.15
2p-t22w0.5h0.5-t(1,2,3)	17.93	598	579	604	4690	0.13	0.12	0.13
2p-t22w5.5h3-ct(1,2,3)	189.74	513	518	506	2004	0.26	0.26	0.25
2p-t22w5.5h3-t(1,2,3)	189.95	505	503	498	2017	0.25	0.25	0.25

Note: 1 inch = 25.4 mm. 1 kip = 4.448 kN. $V_{u,test}$ = Tested maximum shear at failure. V_{calc}= Calculated shear capacity.

Table 5.4.1 Comparison of Tested Moments of the Panels with Screws and Tested Moments of the Panels without Screws

Panel Specimen	w/t Ratio	With Screws		Without Screws		$M_{y,screw}/M_{y,no\ screw}$	$M_{u,screw}/M_{u,no\ screw}$
		$M_{y,screw}$ (kips-in)	$M_{u,screw}$ (kips-in)	$M_{y,no\ screw}$ (kips-in)	$M_{u,no\ screw}$ (kips-in)		
t26w0.5h0.5-c	31.43	1.88	1.96	1.75	1.82	1.07	1.08
t26w2h1.5-c	120.41	--	4.37	4.34	4.54	--	0.96
t22w0.5h0.5-c	18.13	3.64	4.05	3.37	3.72	1.08	1.09
t22w0.5h0.5-t	17.93	2.96	3.09	2.83	2.97	1.05	1.04
t22w5.5h3-c	188.98	13.33	13.38	12.89	13.04	1.03	1.03

Note: The tested yield and ultimate moments of the panels without screws are the average moments of three test specimens. 1 inch = 25.4 mm. 1 kips = 4.448 kN. $M_{y,screw}$ = Tested yield moment for panels with screws. $M_{u,screw}$ = Tested ultimate moment for panels with screws. $M_{y,no\ screw}$ = Tested yield moment for panels without screws. $M_{u,no\ screw}$ = Tested ultimate moment for panels without screws.

Table 5.4.2 Comparison of Tested Ultimate Displacements of the Panels with Screws and Tested Ultimate Displacements of the Panels without Screws

Panel Specimen	w/t Ratio	With Screws	Without Screws	$d_{u,screw}/d_{u,no\ screw}$
		$d_{u,screw}$ (in.)	$d_{u,no\ screw}$ (in.)	
t26w0.5h0.5-c	31.43	1.987	1.922	1.03
t26w2h1.5-c	120.41	1.329	1.326	1.00
t22w0.5h0.5-c	18.13	2.779	2.407	1.15
t22w0.5h0.5-t	17.93	2.951	3.060	0.96
t22w5.5h3-c	188.98	1.399	1.363	1.03

Note: The tested ultimate displacements of the panels without screws are the average displacements of three test specimens. 1 inch = 25.4 mm. $d_{u,screw}$ = Tested ultimate displacement for panels with screws. $d_{u,no\ screw}$ = Tested ultimate displacement for panels without screws.

Table 6.2.1 Ratios of Tested Average Ultimate Compressive Stress to Yield Strength for Panels Tested in Two-Point Loading Condition

Specimen	Thickness (in.)	Average w/t	f_c/F_y (test 1)	f_c/F_y (test 2)	f_c/F_y (test 3)
2p-t28w1.5h1-c(1,2,3)	0.015	103.13	0.894	0.894	0.949
2p-t28w1.5h1-ct(1,2,3)	0.015	103.52	0.964	0.953	0.987
2p-t28w1.5h1-t(1,2,3)	0.015	102.86	0.966	0.913	0.965
2p-t26w0.5h0.5-c(1,2,3)	0.017	31.43	0.987	1.001	1.012
2p-t26w0.5h0.5-ct(1,2,3)	0.017	31.33	1.005	0.983	0.863
2p-t26w0.5h0.5-t(1,2,3)	0.017	31.65	0.980	0.995	0.995
2p-t26w1h0.75-c(1,2,3)	0.017	61.07	1.014	0.948	--
2p-t26w1h0.75-ct(1,2,3)	0.017	60.38	0.973	0.963	0.930
2p-t26w1h0.75-t(1,2,3)	0.017	59.56	1.010	1.007	1.017
2p-t26w2h1.5-c(1,2,3)	0.017	120.41	0.843	0.913	0.929
2p-t26w2h1.5-ct(1,2,3)	0.017	118.64	1.003	0.943	0.958
2p-t26w2h1.5-t(1,2,3)	0.017	118.86	0.943	0.934	0.961
2p-t22w0.5h0.5-c(1,2,3)	0.029	18.13	1.018	1.018	1.020
2p-t22w0.5h0.5-ct(1,2,3)	0.029	18.35	1.018	1.019	1.017
2p-t22w0.5h0.5-t(1,2,3)	0.029	17.93	1.016	1.015	1.019
2p-t22w1h0.75-c(1,2,3)	0.029	35.06	0.940	0.971	0.931
2p-t22w1h0.75-ct(1,2,3)	0.029	35.40	0.988	0.983	0.992
2p-t22w1h0.75-t(1,2,3)	0.029	35.04	0.910	1.009	0.945
2p-t22w3h2-c(1,2,3)	0.029	103.33	0.975	0.993	0.923
2p-t22w3h2-ct(1,2,3)	0.029	103.00	1.013	0.995	1.009
2p-t22w3h2-t(1,2,3)	0.029	103.31	0.975	0.971	0.980
2p-t22w5.5h3-c(1,2,3)	0.029	188.98	0.990	0.957	0.890
2p-t22w5.5h3-ct(1,2,3)	0.029	189.74	0.953	0.886	0.972
2p-t22w5.5h3-t(1,2,3)	0.029	189.95	0.925	0.913	0.946

Note: 1 inch = 25.4 mm. 1 kip = 4.448 kN. f_c = Tested average ultimate compressive stress of the panels. F_y = Actual yield strength of the steel.

Table 6.2.2 Ratios of Tested Average Ultimate Tensile Stress to Yield Strength for Panels Tested in Two-Point Loading Condition

Specimen	Thickness (in.)	Average w/t	f_t/F_y (test 1)	f_t/F_y (test 2)	f_t/F_y (test 3)
2p-t28w1.5h1-c(1,2,3)	0.015	103.13	0.750	0.740	0.759
2p-t28w1.5h1-ct(1,2,3)	0.015	103.52	0.962	0.957	0.953
2p-t28w1.5h1-t(1,2,3)	0.015	102.86	0.994	0.985	0.977
2p-t26w0.5h0.5-c(1,2,3)	0.017	31.43	0.886	0.890	0.918
2p-t26w0.5h0.5-ct(1,2,3)	0.017	31.33	0.992	0.990	0.995
2p-t26w0.5h0.5-t(1,2,3)	0.017	31.65	1.000	1.003	1.007
2p-t26w1h0.75-c(1,2,3)	0.017	61.07	0.862	0.848	0.868
2p-t26w1h0.75-ct(1,2,3)	0.017	60.38	0.995	0.992	0.990
2p-t26w1h0.75-t(1,2,3)	0.017	59.56	1.011	1.010	1.016
2p-t26w2h1.5-c(1,2,3)	0.017	120.41	0.669	0.653	0.663
2p-t26w2h1.5-ct(1,2,3)	0.017	118.64	0.883	0.888	0.878
2p-t26w2h1.5-t(1,2,3)	0.017	118.86	0.946	0.945	0.937
2p-t22w0.5h0.5-c(1,2,3)	0.029	18.13	0.956	0.972	0.983
2p-t22w0.5h0.5-ct(1,2,3)	0.029	18.35	1.014	1.013	1.012
2p-t22w0.5h0.5-t(1,2,3)	0.029	17.93	1.018	1.019	1.021
2p-t22w1h0.75-c(1,2,3)	0.029	35.06	0.921	0.952	0.913
2p-t22w1h0.75-ct(1,2,3)	0.029	35.40	1.005	0.994	1.002
2p-t22w1h0.75-t(1,2,3)	0.029	35.04	1.012	1.015	1.014
2p-t22w3h2-c(1,2,3)	0.029	103.33	0.765	0.801	0.753
2p-t22w3h2-ct(1,2,3)	0.029	103.00	0.972	0.957	0.962
2p-t22w3h2-t(1,2,3)	0.029	103.31	0.994	0.993	0.999
2p-t22w5.5h3-c(1,2,3)	0.029	188.98	0.699	0.682	0.695
2p-t22w5.5h3-ct(1,2,3)	0.029	189.74	0.839	0.832	0.853
2p-t22w5.5h3-t(1,2,3)	0.029	189.95	0.904	0.893	0.921

Note: 1 inch = 25.4 mm. 1 kip = 4.448 kN. f_t = Tested average ultimate tensile stress of the panels. F_y = Actual yield strength of the steel.

Table 6.3.1 Comparison of Tested Moments with Calculated Moment Using the Modified Yield Strength Reduction Factor

Specimens	Thickness (in.)	Average w/t	$M_{u,test}$ (kips-in)	$M_{y,test}$ (kips-in)	$M_{reduced\ Fy}$ (kips-in)	$M_{u,test}/M_{reduced\ Fy}$	$M_{y,test}/M_{reduced\ Fy}$
2p-t28w1.5h1-c(1,2,3)	0.015	103.13	2.39	2.35	2.39	1.000	0.983
2p-t28w1.5h1-ct(1,2,3)	0.015	103.52	2.33	2.28	2.10	1.110	1.086
2p-t28w1.5h1-t(1,2,3)	0.015	102.86	2.17	2.13	1.90	1.142	1.121
2p-t26w0.5h0.5-c(1,2,3)	0.017	31.43	1.82	1.75	1.71	1.064	1.023
2p-t26w0.5h0.5-ct(1,2,3)	0.017	31.33	1.85	1.80	1.52	1.217	1.184
2p-t26w0.5h0.5-t(1,2,3)	0.017	31.65	1.70	1.69	1.36	1.250	1.243
2p-t26w1h0.75-c(1,2,3)	0.017	61.07	2.33	2.16	2.04	1.142	1.059
2p-t26w1h0.75-ct(1,2,3)	0.017	60.38	2.27	2.27	1.82	1.247	1.247
2p-t26w1h0.75-t(1,2,3)	0.017	59.56	2.14	2.00	1.54	1.390	1.299
2p-t26w2h1.5-c(1,2,3)	0.017	120.41	4.54	4.34	4.76	0.954	0.912
2p-t26w2h1.5-ct(1,2,3)	0.017	118.64	4.46	4.34	4.41	1.011	0.984
2p-t26w2h1.5-t(1,2,3)	0.017	118.86	4.40	4.41	3.99	1.103	1.105
2p-t22w0.5h0.5-c(1,2,3)	0.029	18.13	3.72	3.37	3.23	1.152	1.043
2p-t22w0.5h0.5-ct(1,2,3)	0.029	18.35	3.43	3.08	2.93	1.171	1.051
2p-t22w0.5h0.5-t(1,2,3)	0.029	17.93	2.97	2.83	2.57	1.156	1.101
2p-t22w1h0.75-c(1,2,3)	0.029	35.06	4.81	--	4.32	1.113	--
2p-t22w1h0.75-ct(1,2,3)	0.029	35.40	4.44	4.42	4.13	1.075	1.070
2p-t22w1h0.75-t(1,2,3)	0.029	35.04	3.86	3.69	3.23	1.195	1.142
2p-t22w3h2-c(1,2,3)	0.029	103.33	8.21	8.16	8.10	1.014	1.007
2p-t22w3h2-ct(1,2,3)	0.029	103.00	7.46	7.41	7.46	1.000	0.993
2p-t22w3h2-t(1,2,3)	0.029	103.31	7.12	7.12	6.12	1.163	1.163
2p-t22w5.5h3-c(1,2,3)	0.029	188.98	13.04	12.89	13.42	0.972	0.961
2p-t22w5.5h3-ct(1,2,3)	0.029	189.74	12.29	12.13	12.25	1.003	0.990
2p-t22w5.5h3-t(1,2,3)	0.029	189.95	12.04	--	10.62	1.134	--
Average						1.116	1.080
Standard Deviation						0.102	0.099

Note: 1 inch = 25.4 mm. 1 kip = 4.448 kN. $M_{u,test}$ = Tested ultimate moment. $M_{y,test}$ = Tested yield moment. "--" indicates that section did not yield in three panel specimens. $M_{reduced\ Fy}$ = Calculated moment using the modified yield strength reduction factor and the AISI Specification (AISI 1986).

Table 6.3.2 Comparison of Tested Moments with Calculated Moment Using the Modified Yield Strength Reduction Factor for Beams with Stiffened Compression Flanges Tested by Pan

Specimens	Thickness (in.)	Average w/t	$M_{u,test}$ (kips-in)	$M_{y,test}$ (kips-in)	$M_{reduced\ Fy}$ (kips-in)	$M_{u,test}/M_{reduced\ Fy}$	$M_{y,test}/M_{reduced\ Fy}$
80XFA3A	0.0840	80.96	91.13	73.42	73.93	1.233	0.993
80XFA3B	0.0860	78.67	91.88	74.01	76.19	1.206	0.971
80XFA4A	0.0850	61.97	59.85	51.65	53.97	1.109	0.957
80XFA4B	0.0850	61.97	63.98	53.05	54.11	1.182	0.980
80XFA5A	0.0835	44.08	43.35	37.04	36.17	1.199	1.024
80XFA5B	0.0830	44.63	41.48	35.12	36.03	1.151	0.975
100XFA1A	0.0640	100.79	68.96	67.13	58.01	1.189	1.157
100XFA1B	0.0640	109.82	68.06	--	57.95	1.175	--
100XFA3A	0.0620	72.11	50.19	42.70	37.41	1.342	1.141
100XFA3B	0.0640	69.00	50.74	42.58	38.91	1.304	1.094
100XFA4A	0.0635	54.45	36.09	34.14	28.70	1.258	1.190
100XFA4B	0.0640	54.97	36.09	31.32	28.82	1.252	1.087
Average						1.217	1.052
Standard Deviation						0.062	0.085

Note: 1 inch = 25.4 mm. 1 kip = 4.448 kN. $M_{u,test}$ = Tested ultimate moment. $M_{y,test}$ = Tested yield moment. "--" indicates that data is not available.
$M_{reduced\ Fy}$ = Calculated moment using the modified yield strength reduction factor and the AISI Specification (AISI 1986).

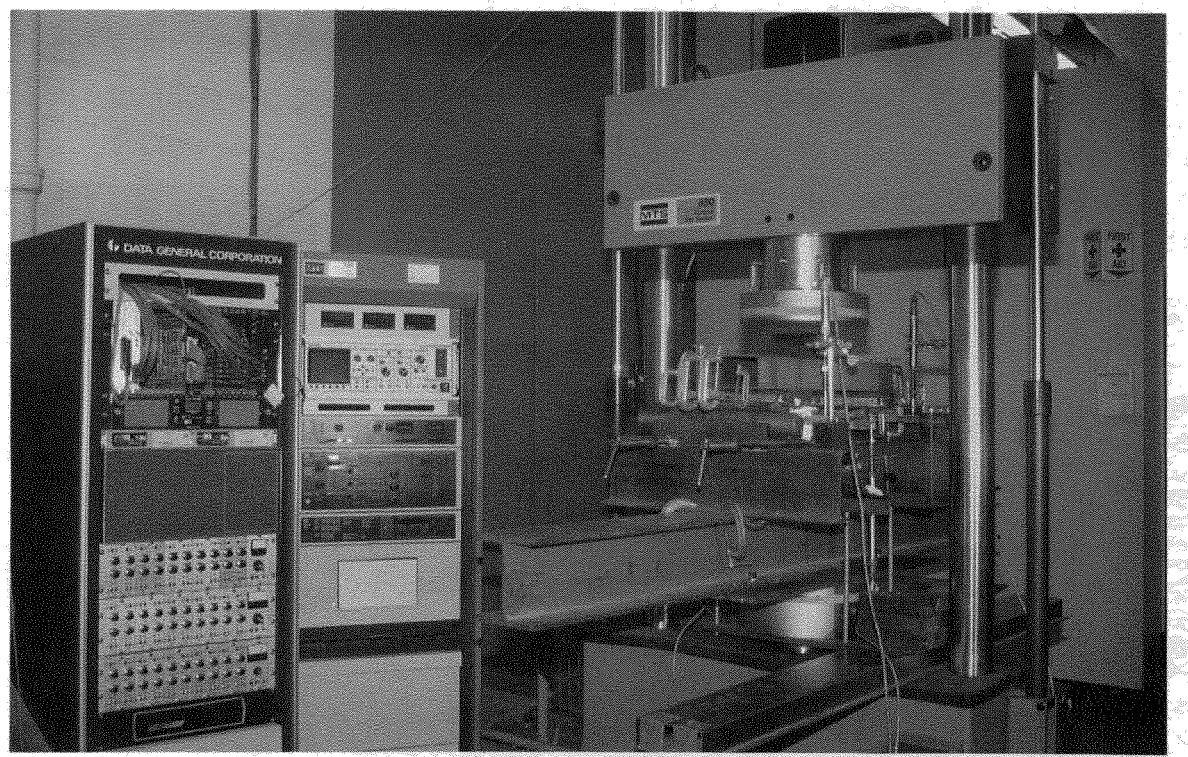

Fig. 4.1.1 Test Setup for Deck Panel Tests

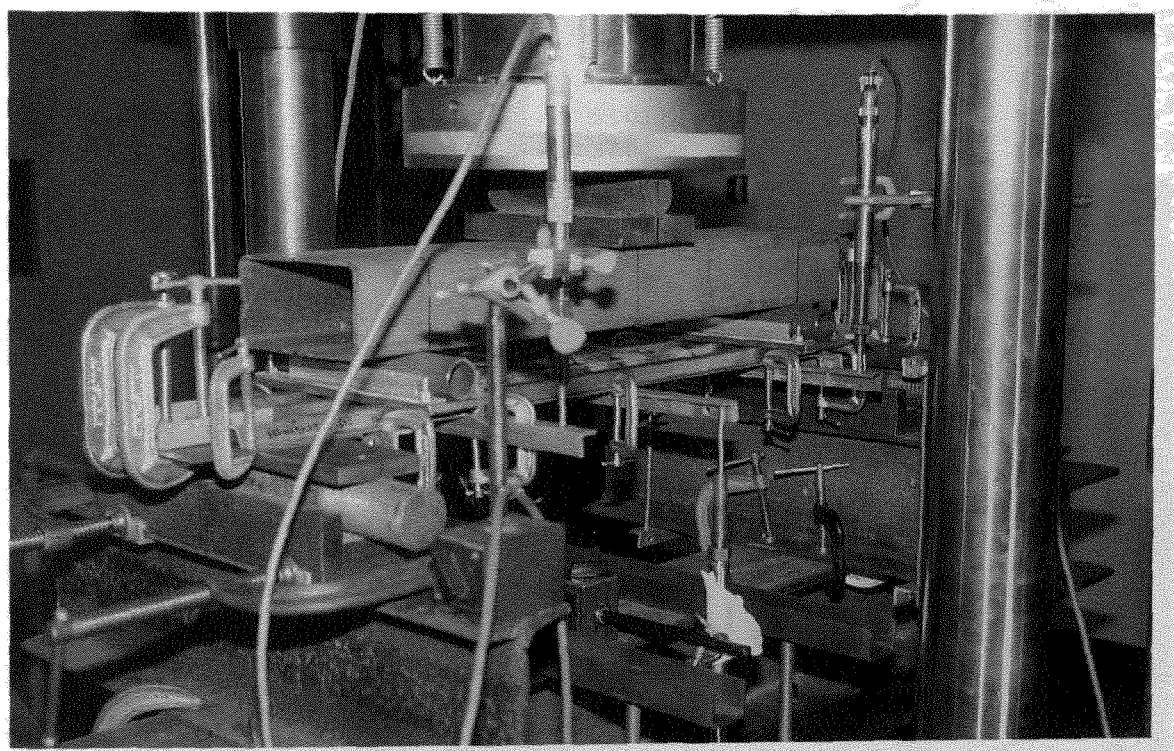

Fig. 4.1.2 Test Setup for Deck Panel Tests (Continued)

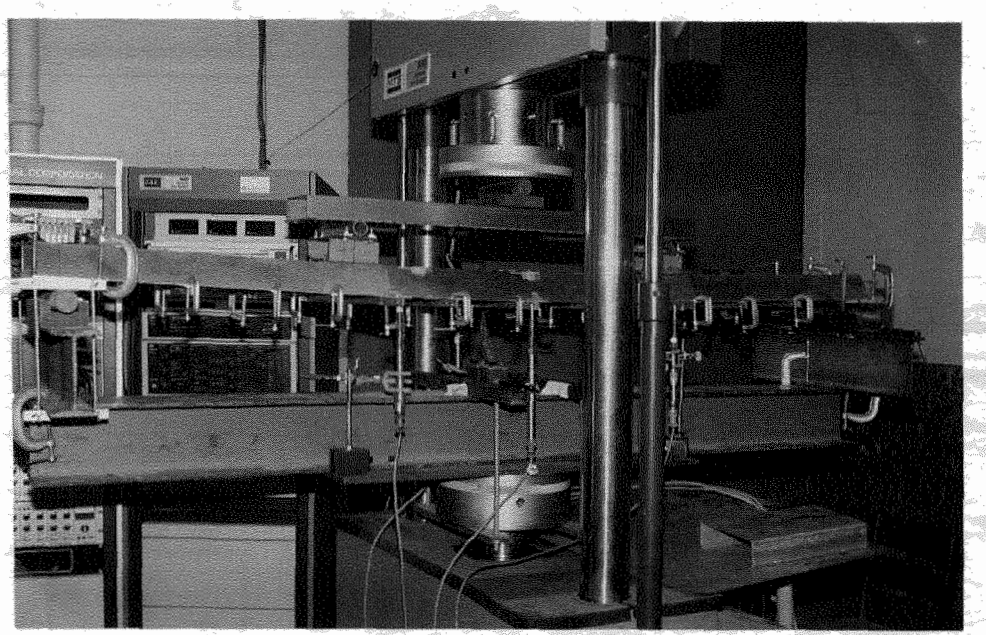

Fig. 4.1.3 Test Setup for Deck Panel Tests (Continued)

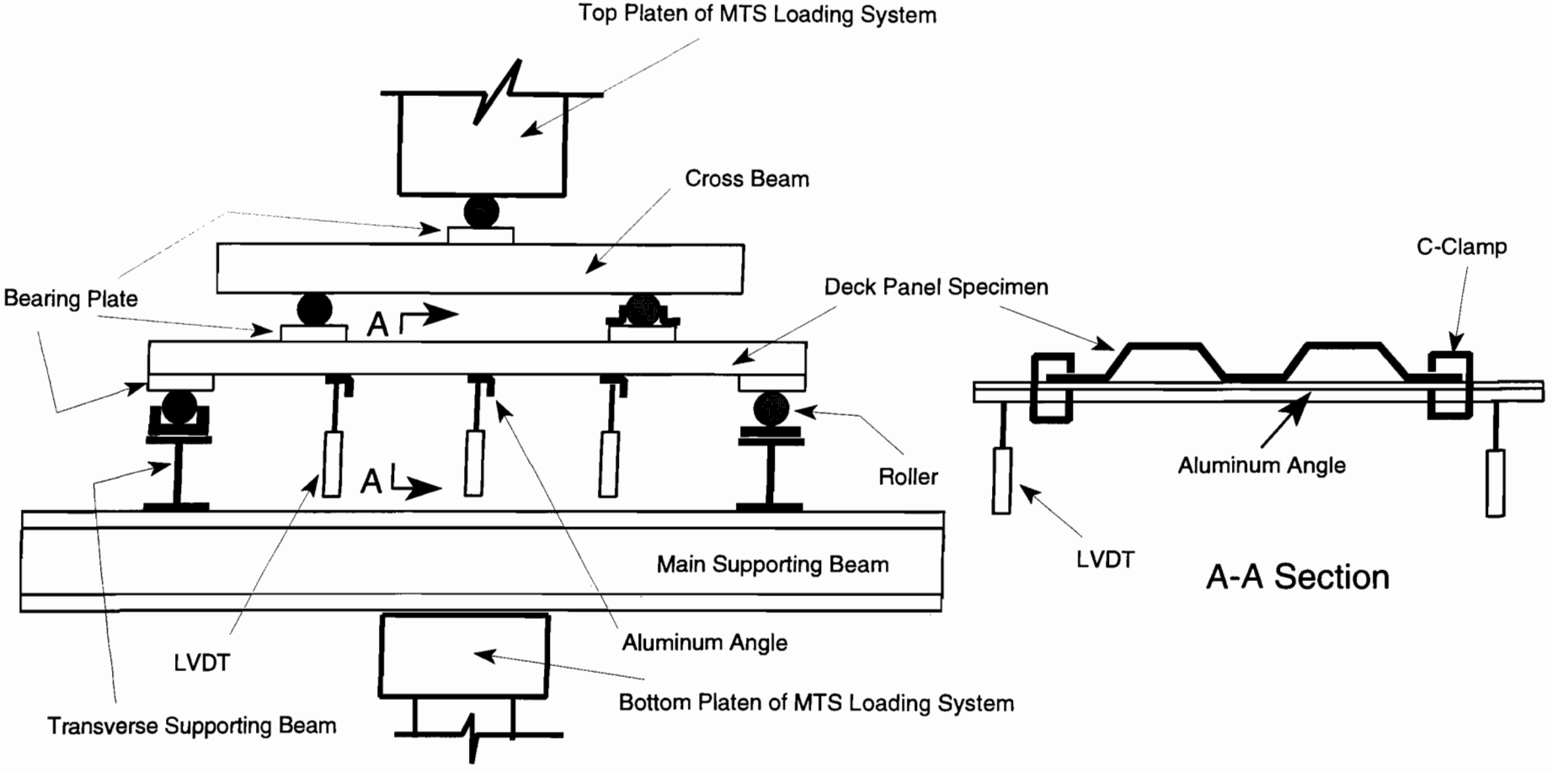

Fig. 4.1.4 Test Setup for Deck Panels with Two-Point Loading Condition

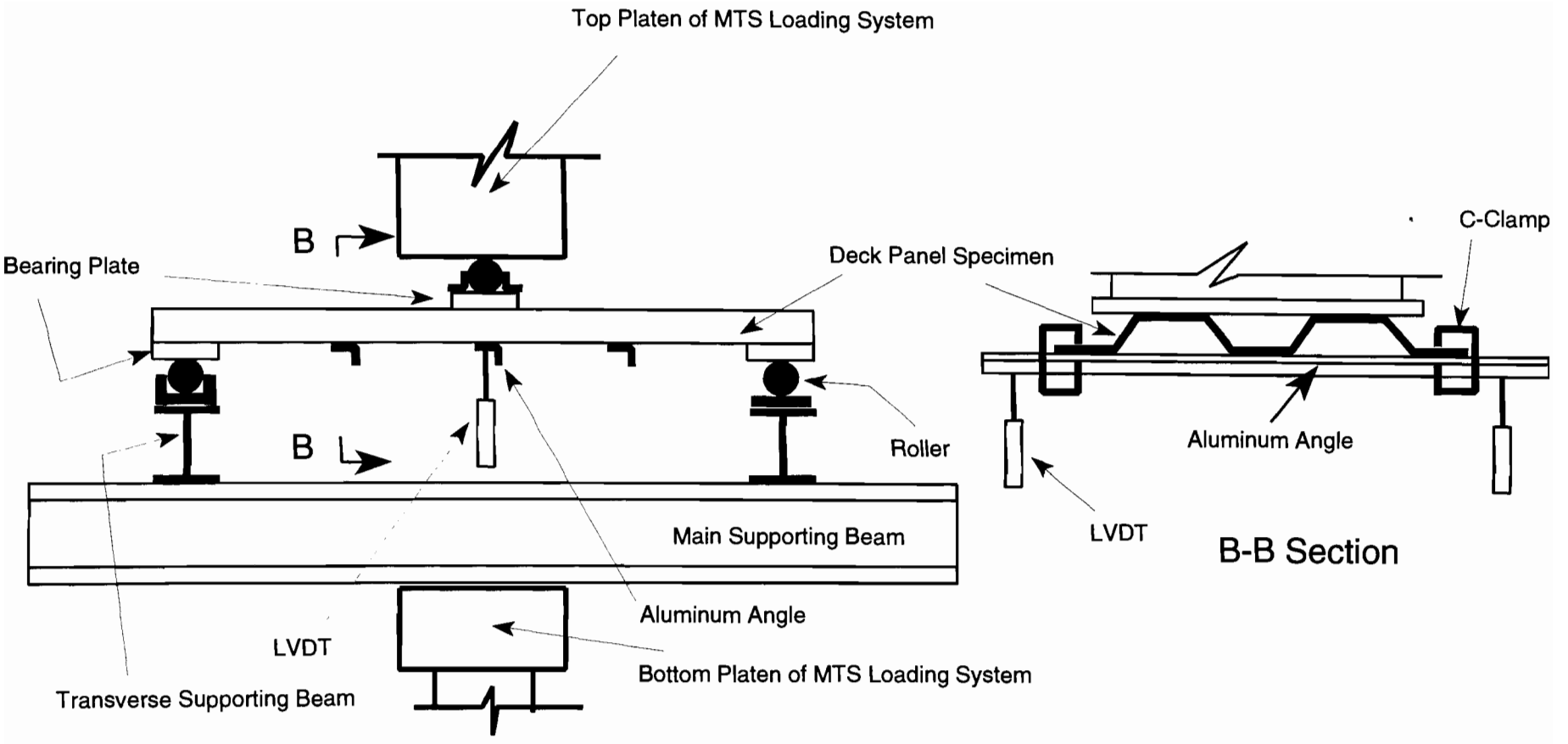

Fig. 4.1.5 Test Setup for Deck Panels with One-Point Loading Condition

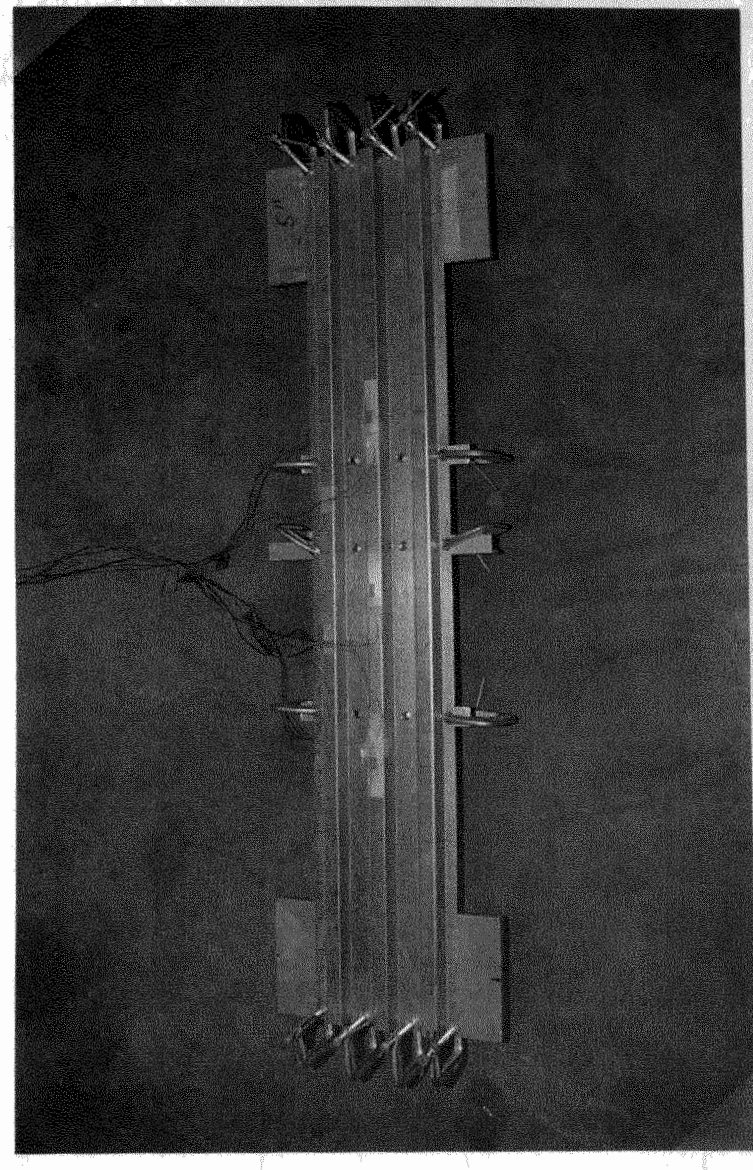

Fig. 4.1.6 Specimen with Screws Penetrating through Tension Flanges

Fig. 4.1.7 Specimen with Screws Penetrating through Tension Flanges (Continued)

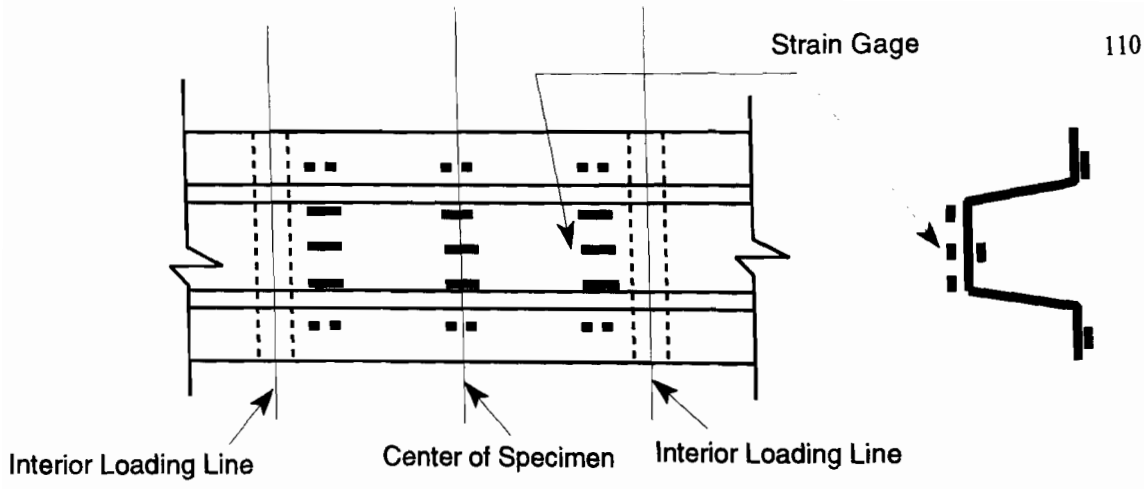

Fig. 4.2.1 Location of Strain Gages for Panels with Two-Point Loading Condition

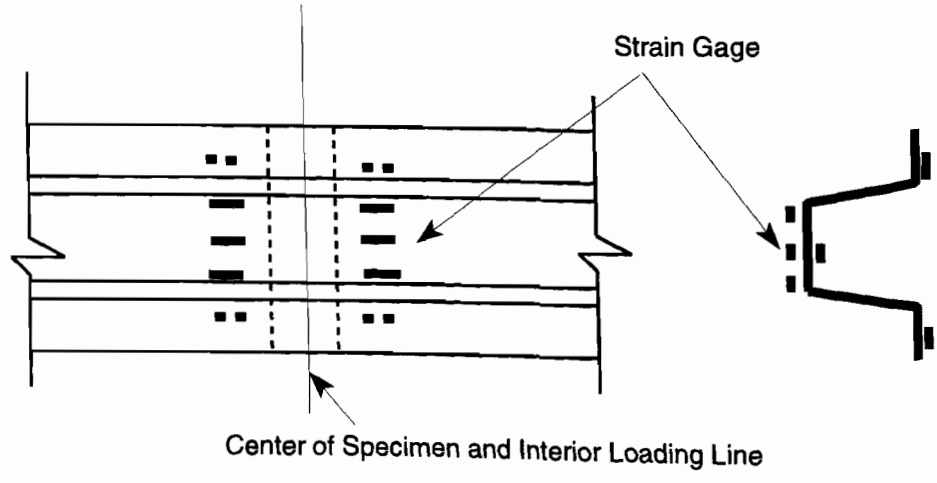

Fig. 4.2.2 Location of Strain Gages for Panels with One-Point Loading Condition

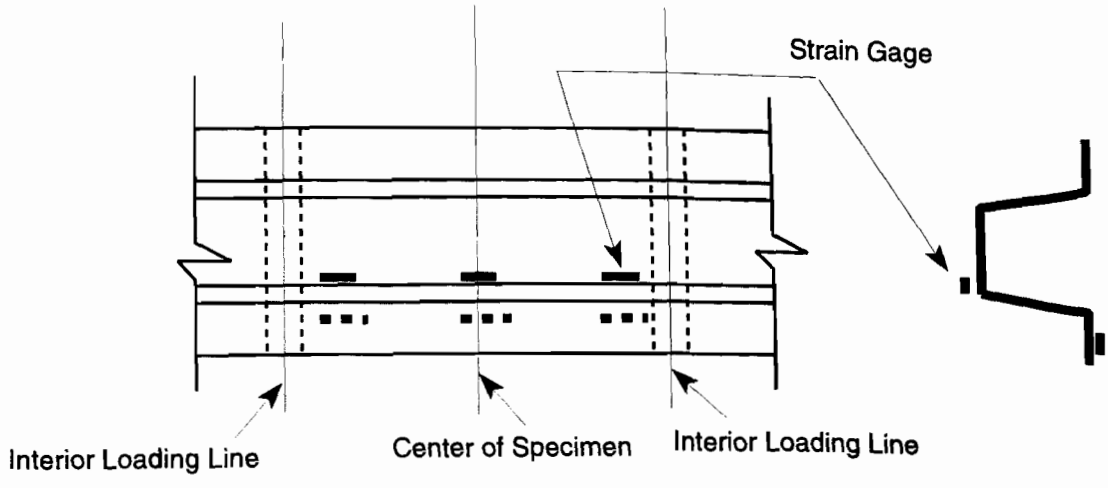

Fig. 4.2.3 Location of Strain Gages for Panels with Screws and Two-Point Loading Condition

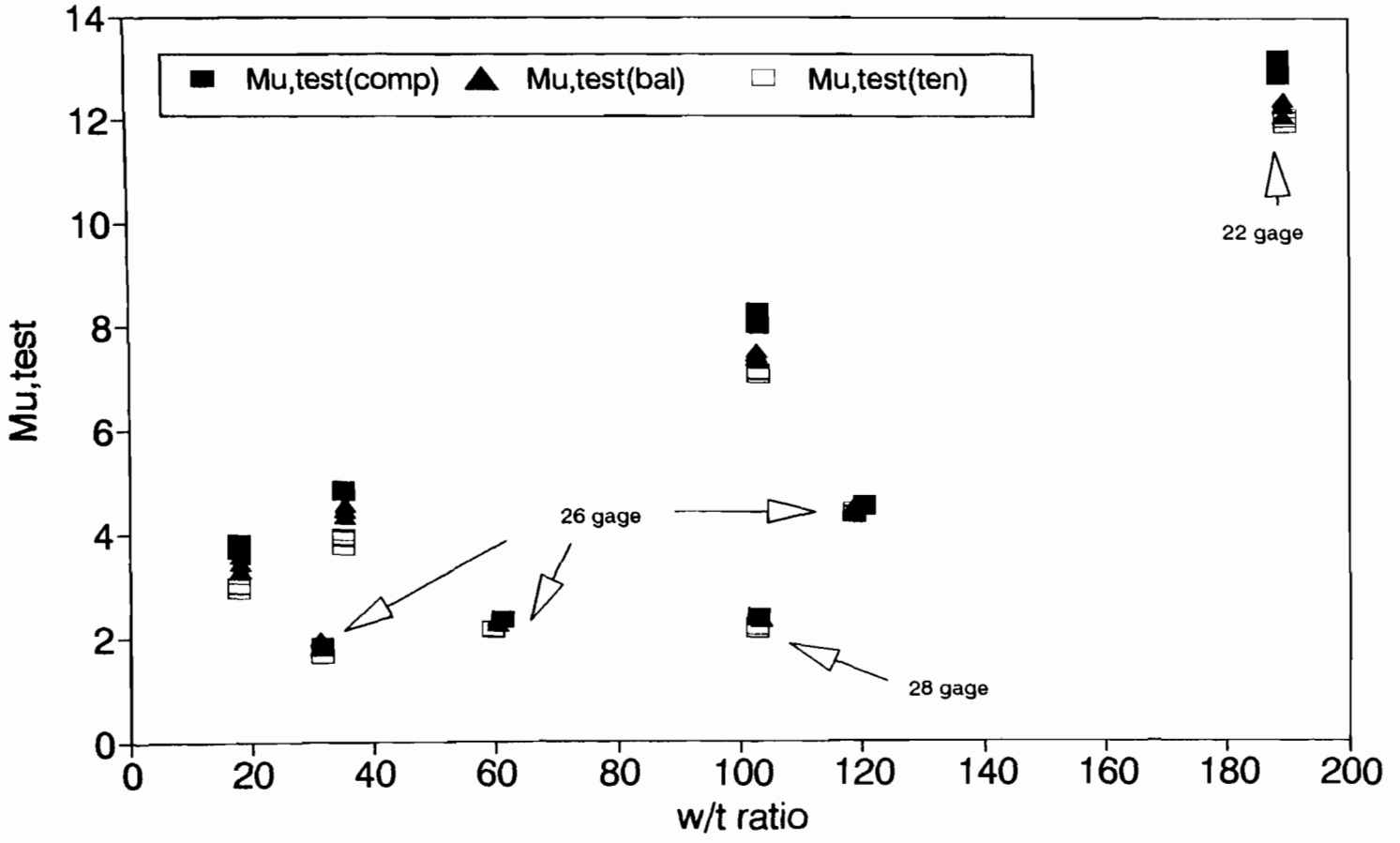

Fig. 4.4.1 Tested Ultimate Moment vs. w/t Ratio of Panels in Two-Point Loading Condition

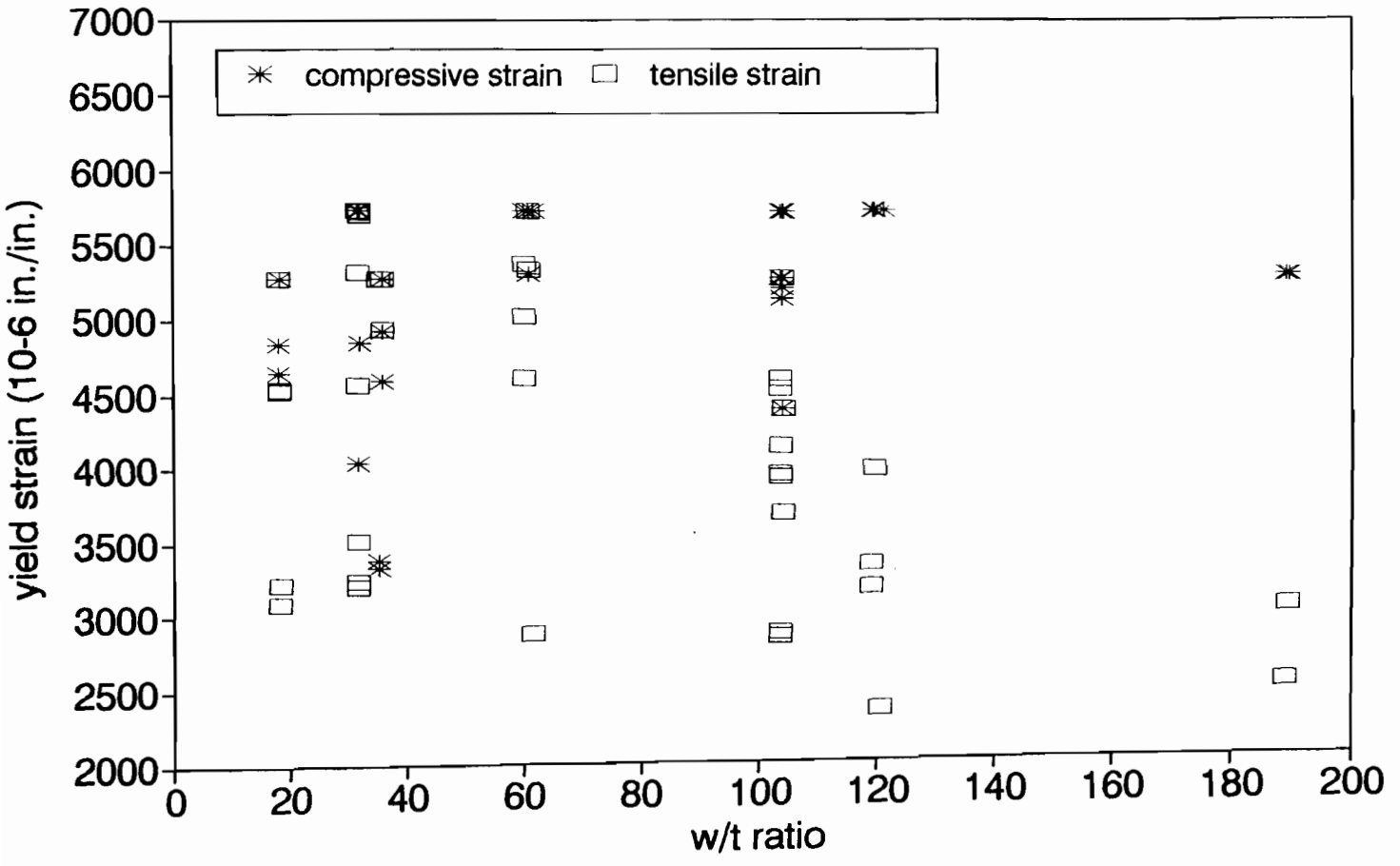

Fig. 4.4.2 Tested Yield Strain vs. w/t Ratio of Panels in Two-Point Loading Condition

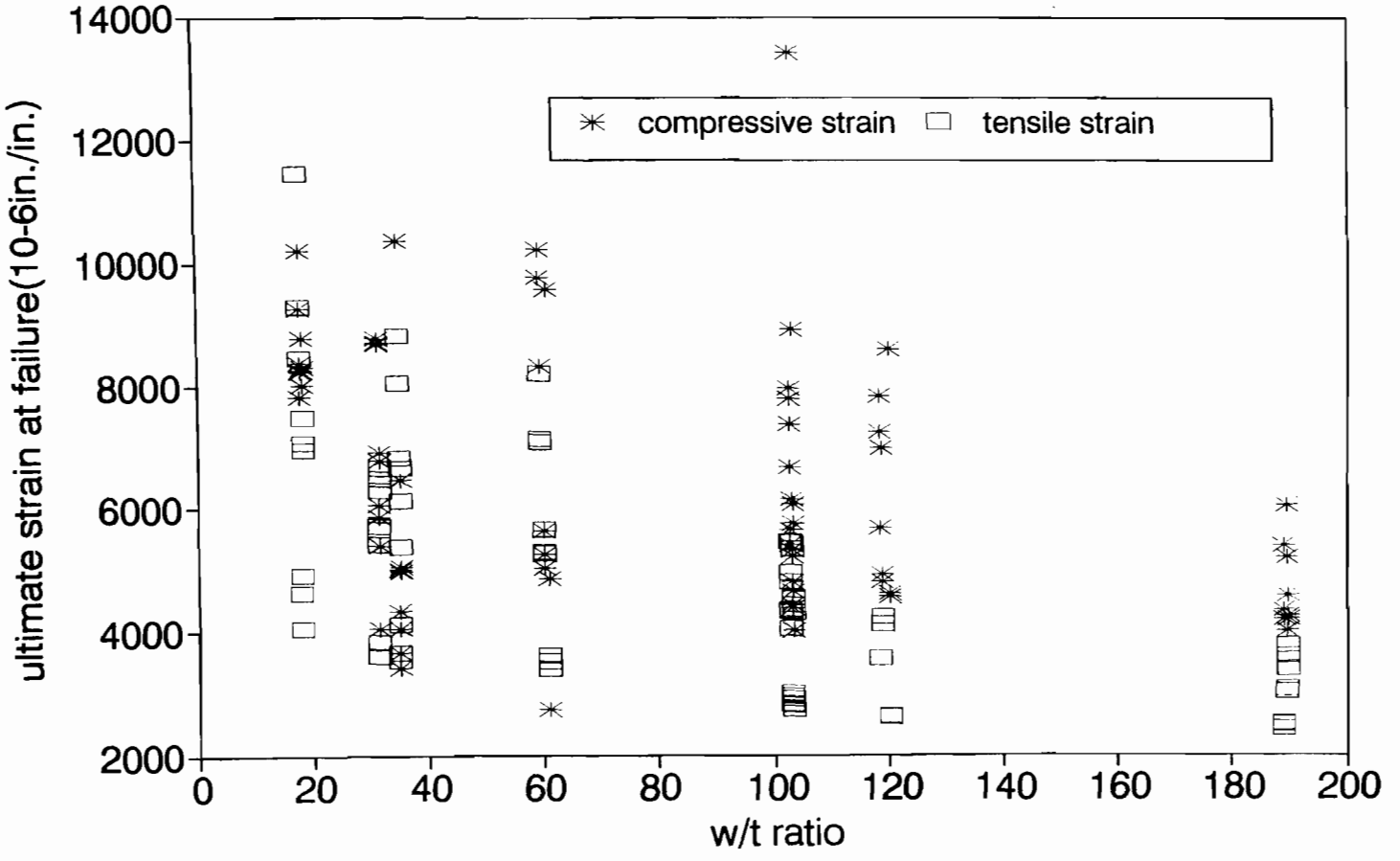

Fig. 4.4.3 Tested Ultimate Strain vs. w/t Ratio of Panels in Two-Point Loading Condition

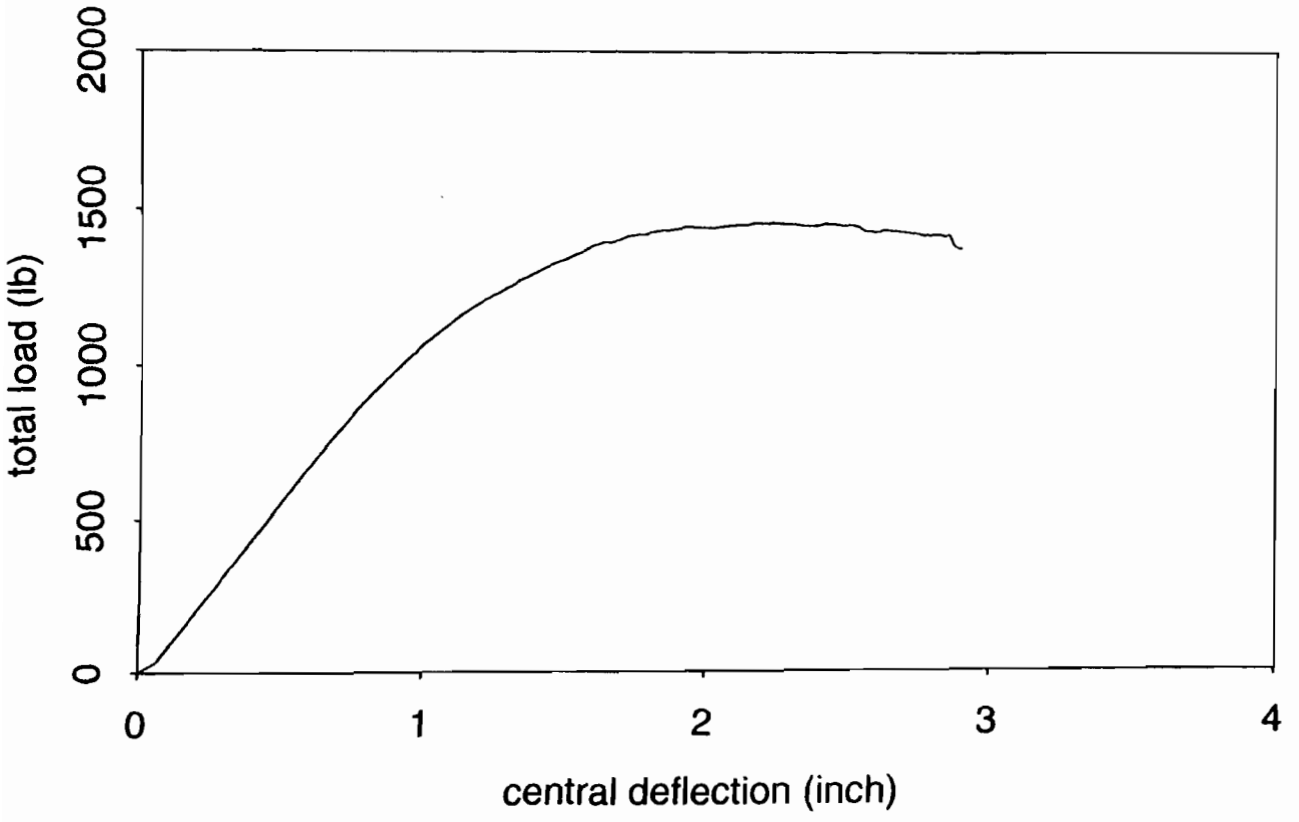

Fig. 4.4.4 Load-Central Displacement Relationship of Specimen 2p-t22w0.5h0.5-c(1)

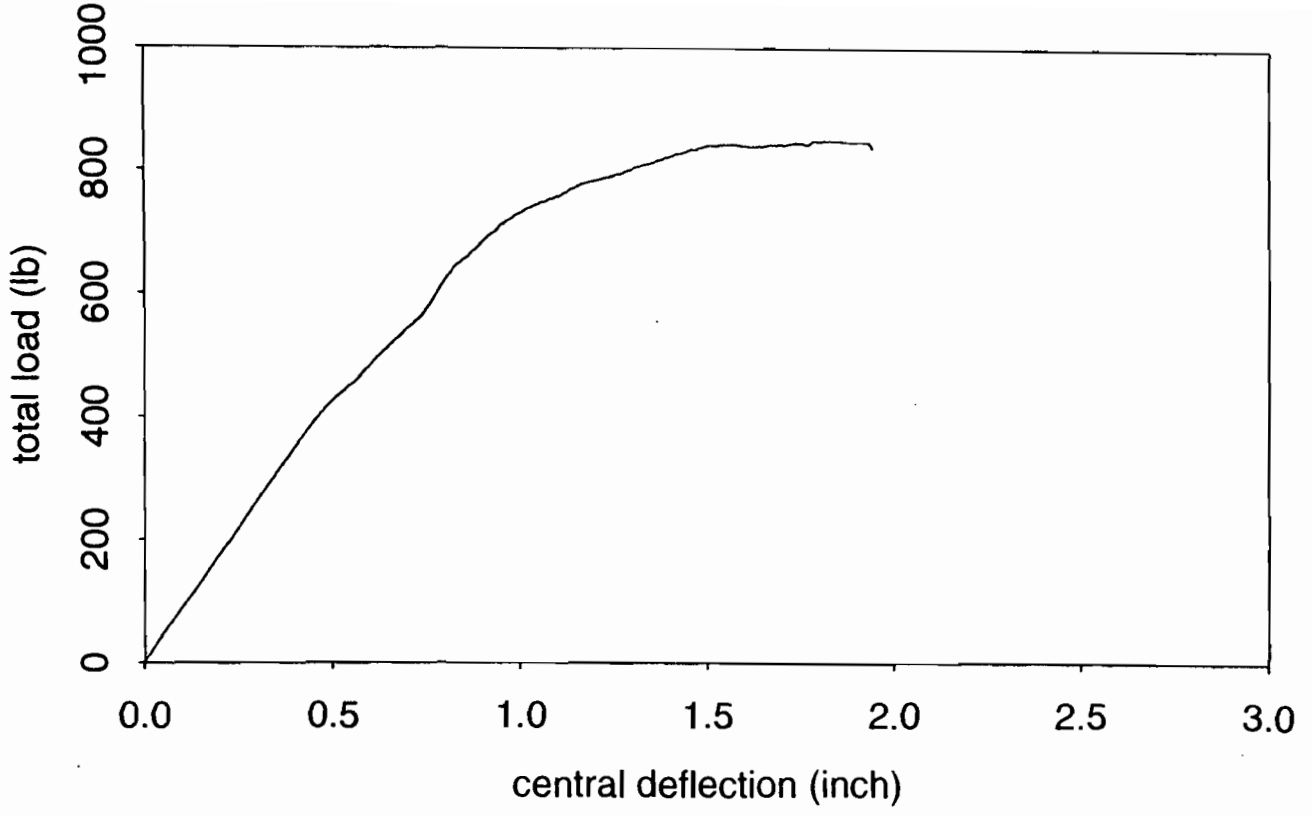

Fig. 4.4.5 Load-Central Displacement Relationship of Specimen 2p-t26w1.0h0.75-t(1)

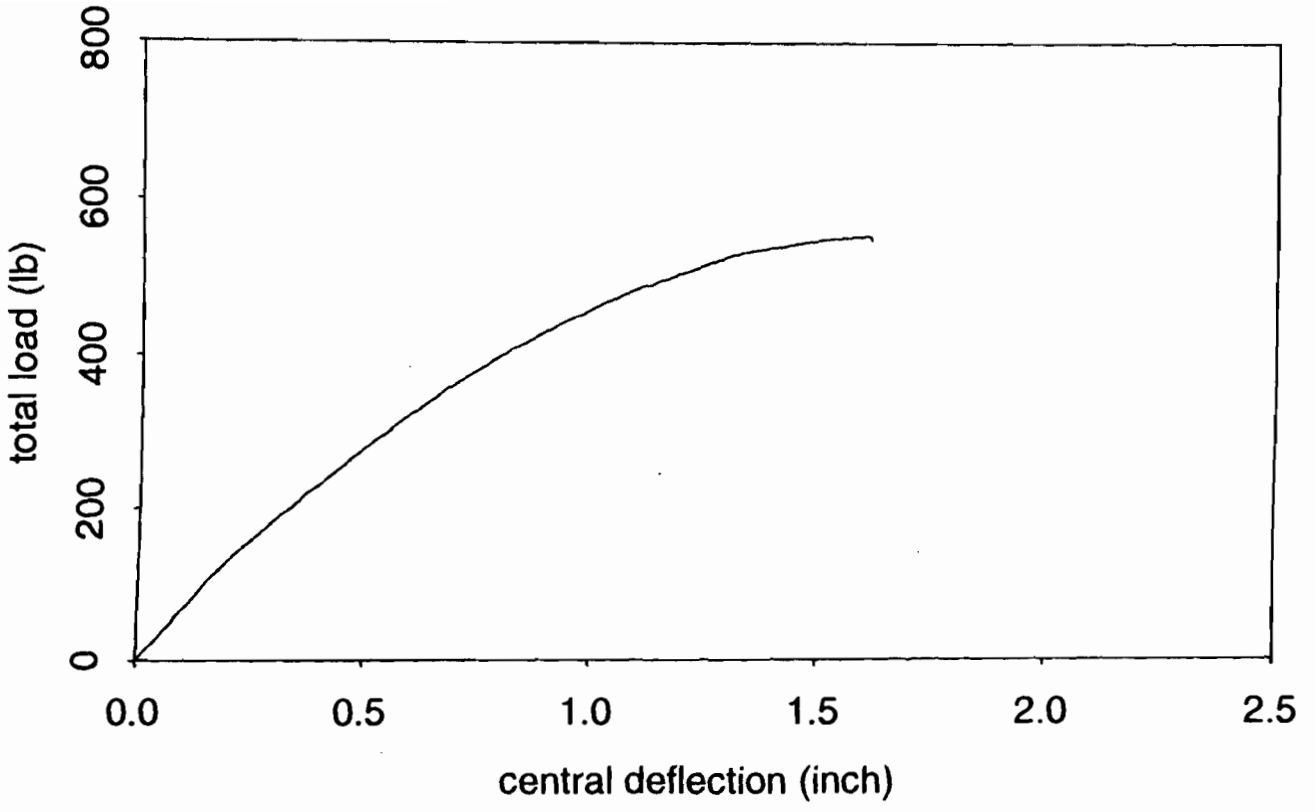

Fig. 4.4.6 Load-Central Displacement Relationship of Specimen 2p-t26w2.0h1.5-ct(2)

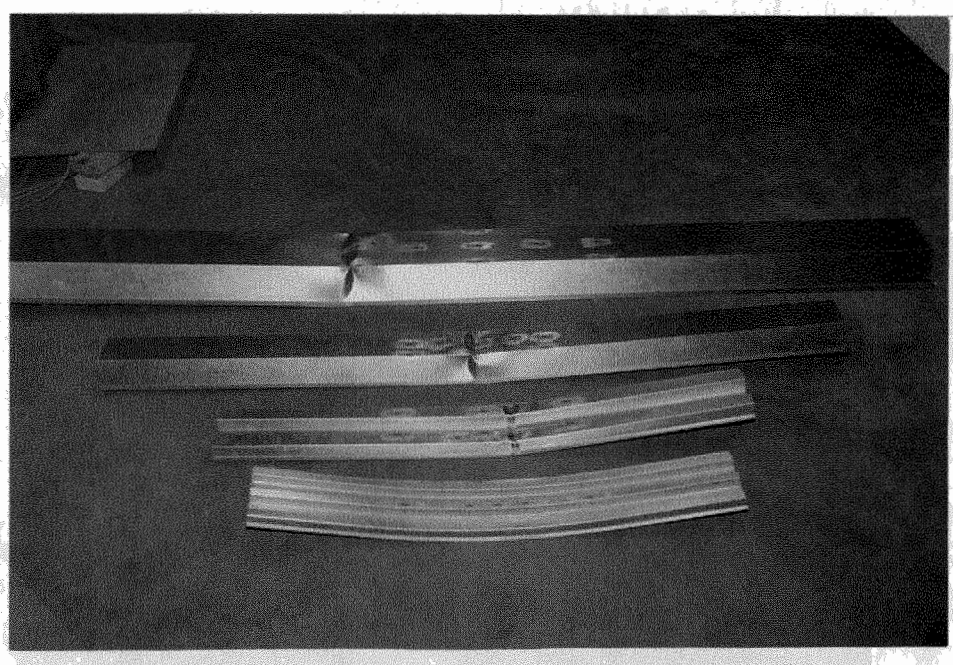

Fig. 4.4.7 Failure Mode of Panels in Two-Point Loading Condition

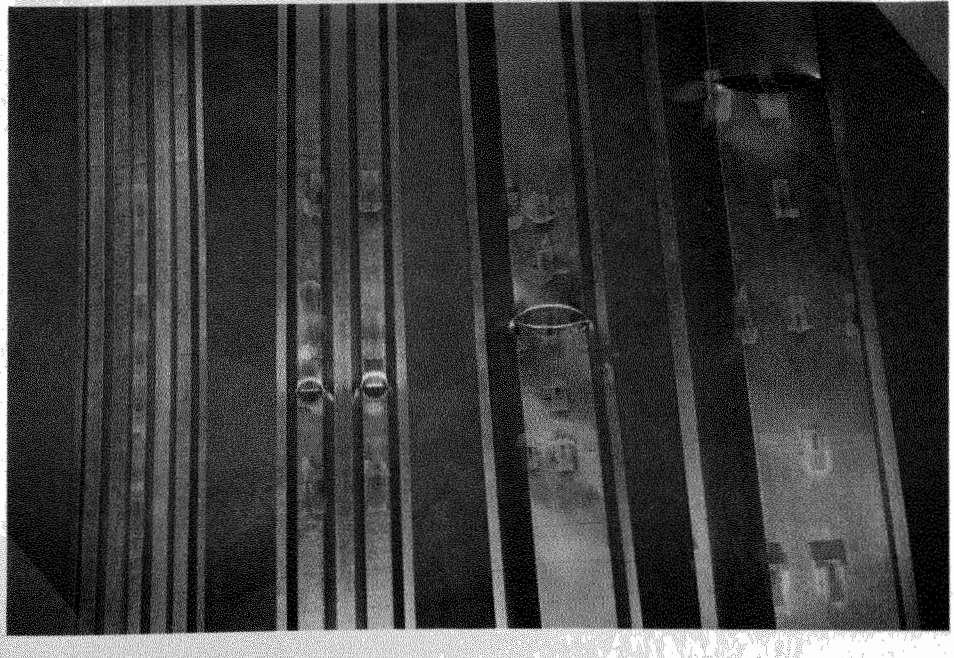

Fig. 4.4.8 Failure Mode of Panels in Two-Point Loading Condition (Continued)

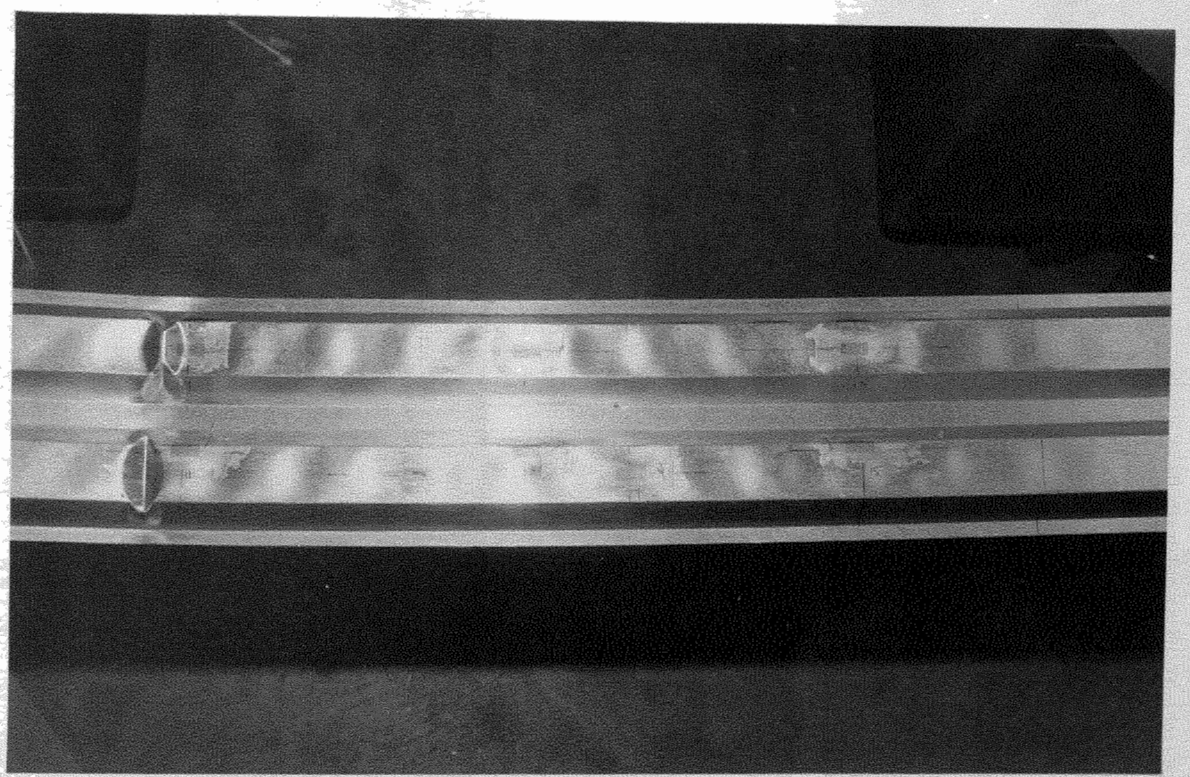

Fig. 4.4.9 Failure Mode of Panels in Two-Point Loading Condition (Continued)

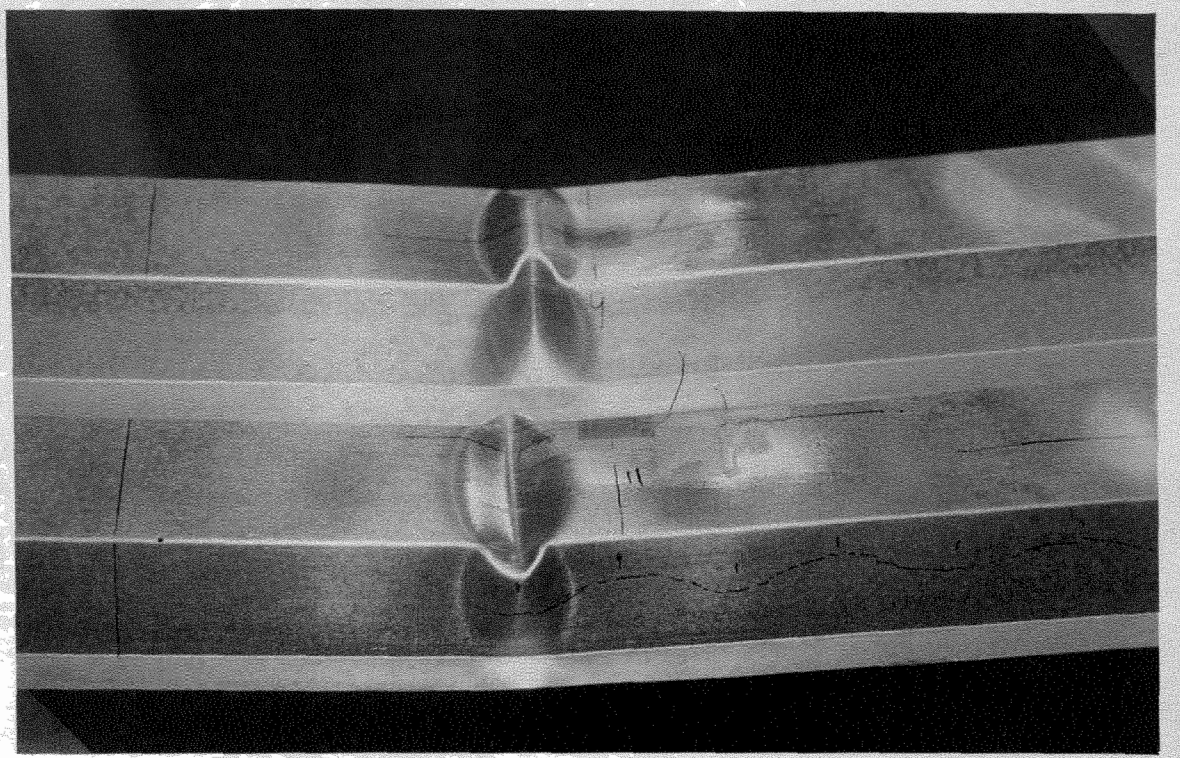

Fig. 4.4.10 Failure Mode of Panels in Two-Point Loading Condition (Continued)

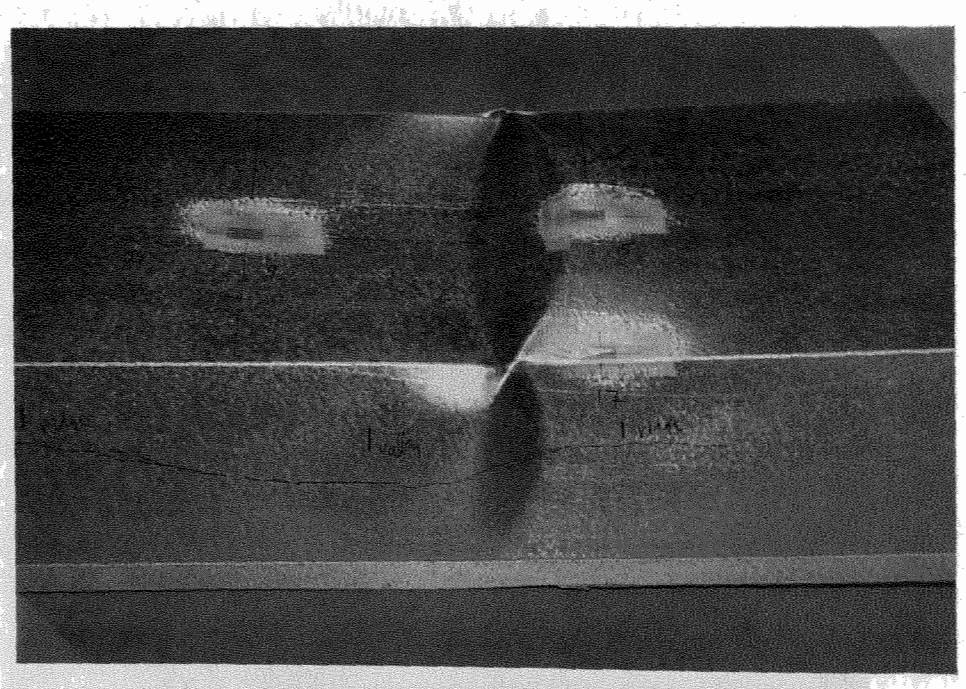

Fig. 4.4.11 Failure Mode of Panels in Two-Point Loading Condition (Continued)

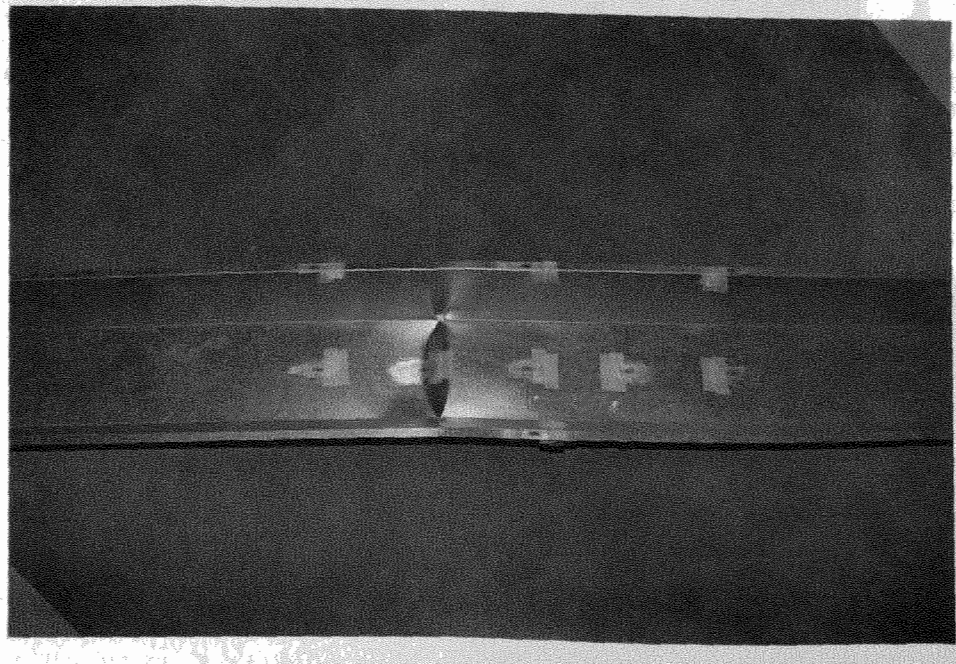

Fig. 4.4.12 Failure Mode of Panels in Two-Point Loading Condition (Continued)

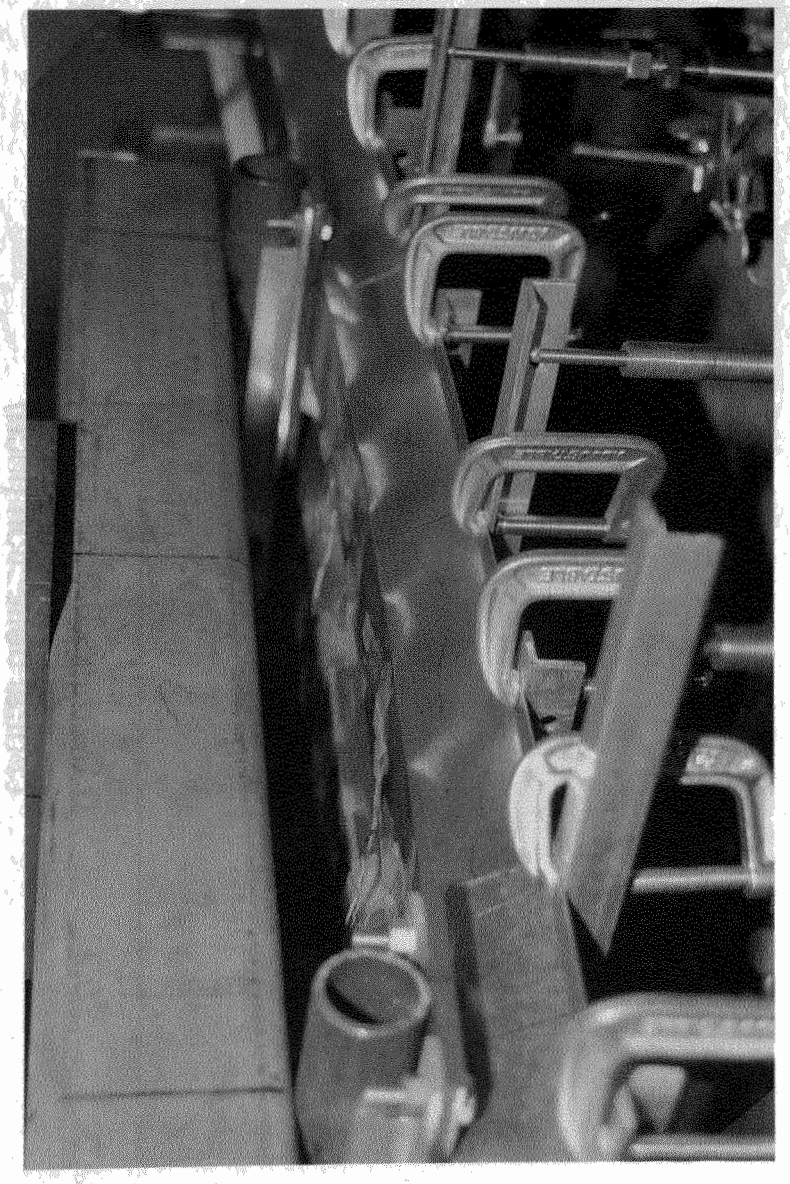

Fig. 4.4.13 Deformation of Web Near Failure

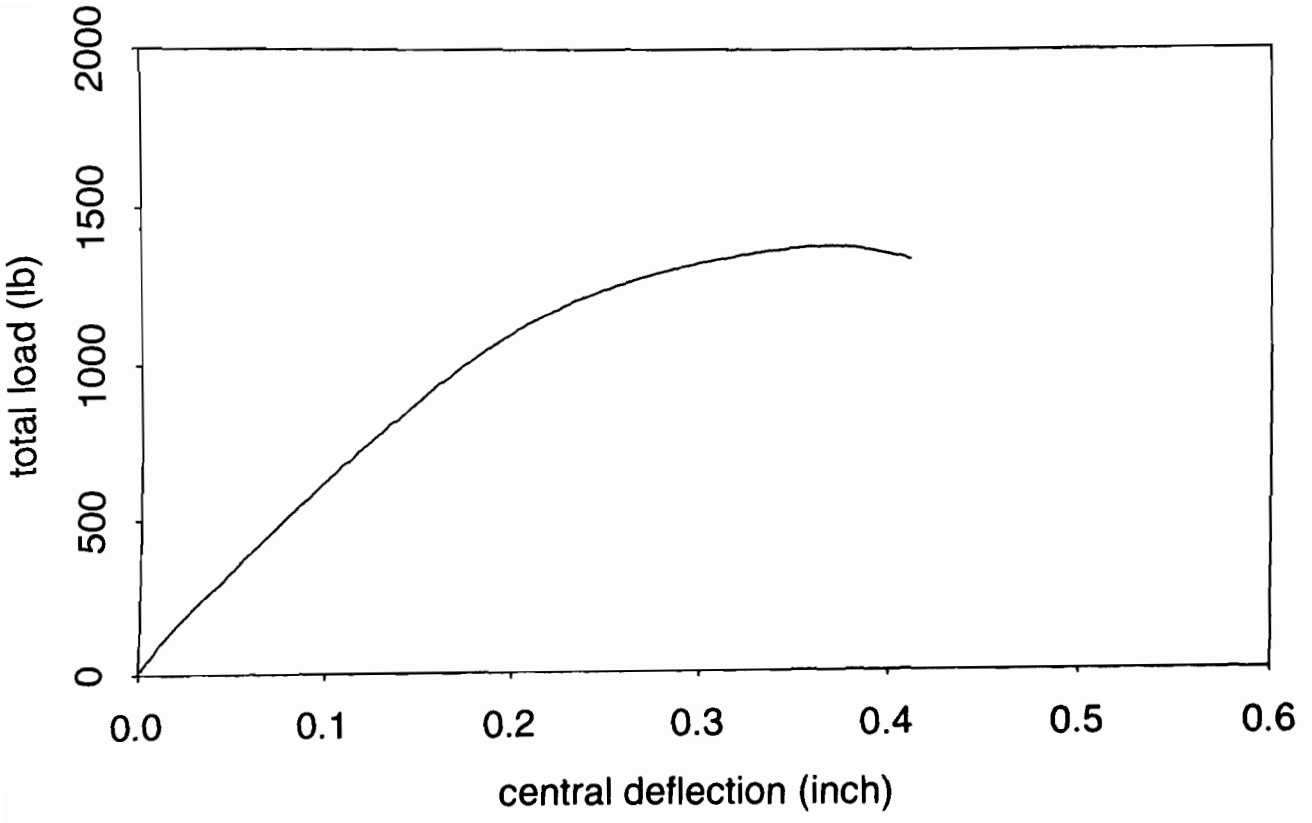

Fig. 4.5.1 Load-Central Displacement Relationship of Specimen 1p-t22w0.5h0.5-t(2)

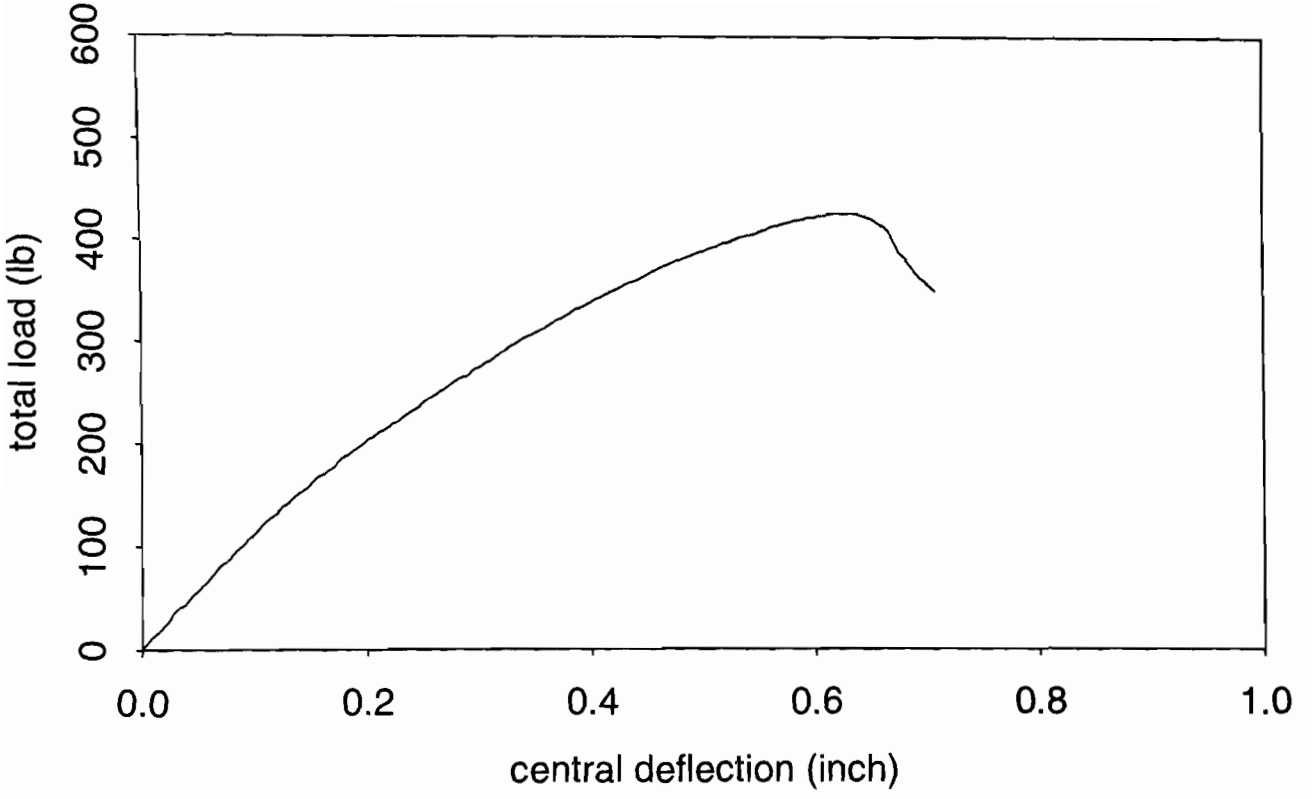

Fig. 4.5.2 Load-Central Displacement Relationship of Specimen 1p-t26w2.0h1.5-t(1)

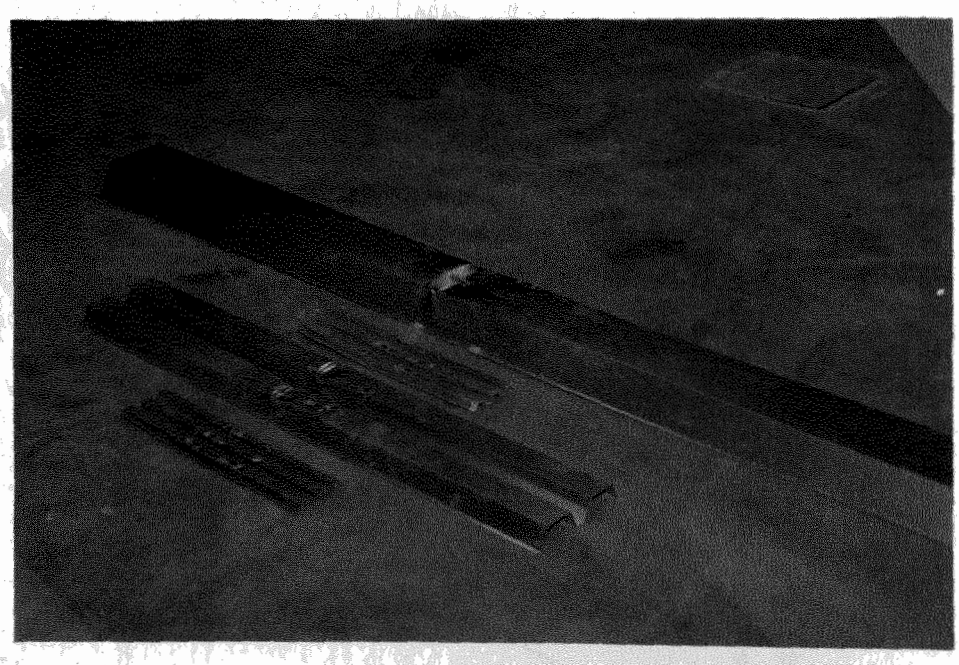

Fig. 4.5.3 Failure Mode of Panels in One-Point Loading Condition

Fig. 4.5.4 Failure Mode of Panels in One-Point Loading Condition (Continued)

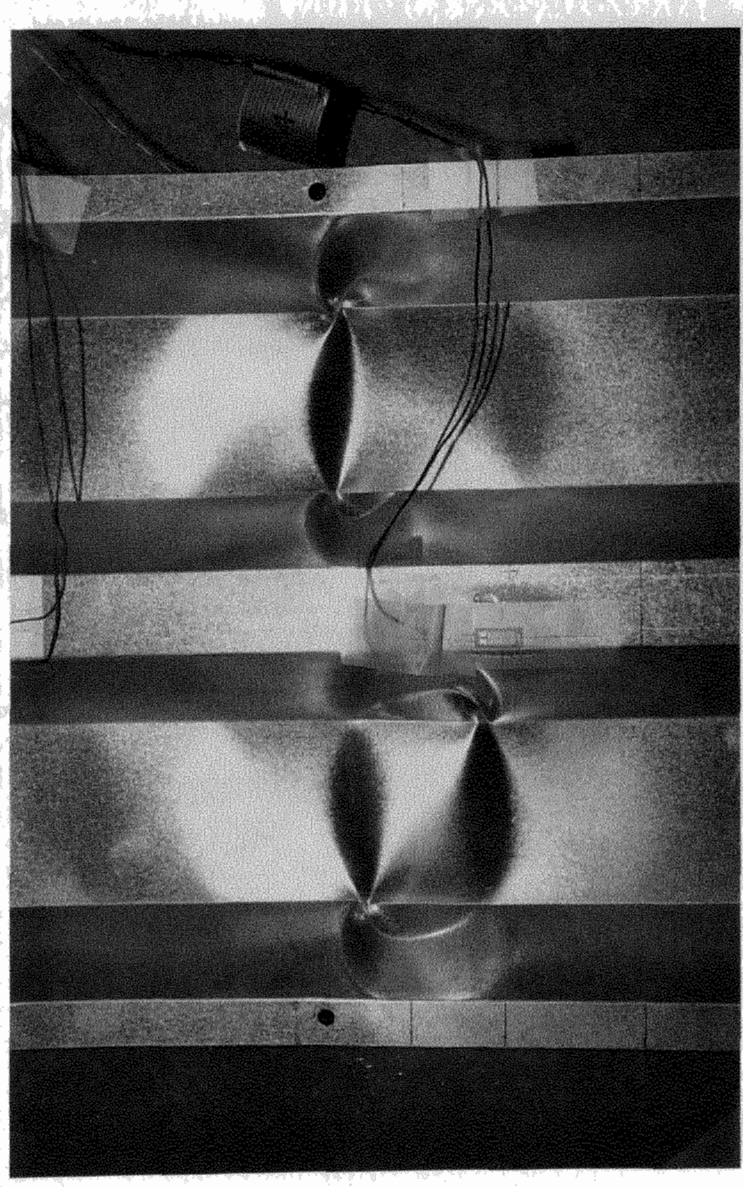

Fig. 4.6.1 Failure Mode of Panels with Screws and Two-Point Loading Condition

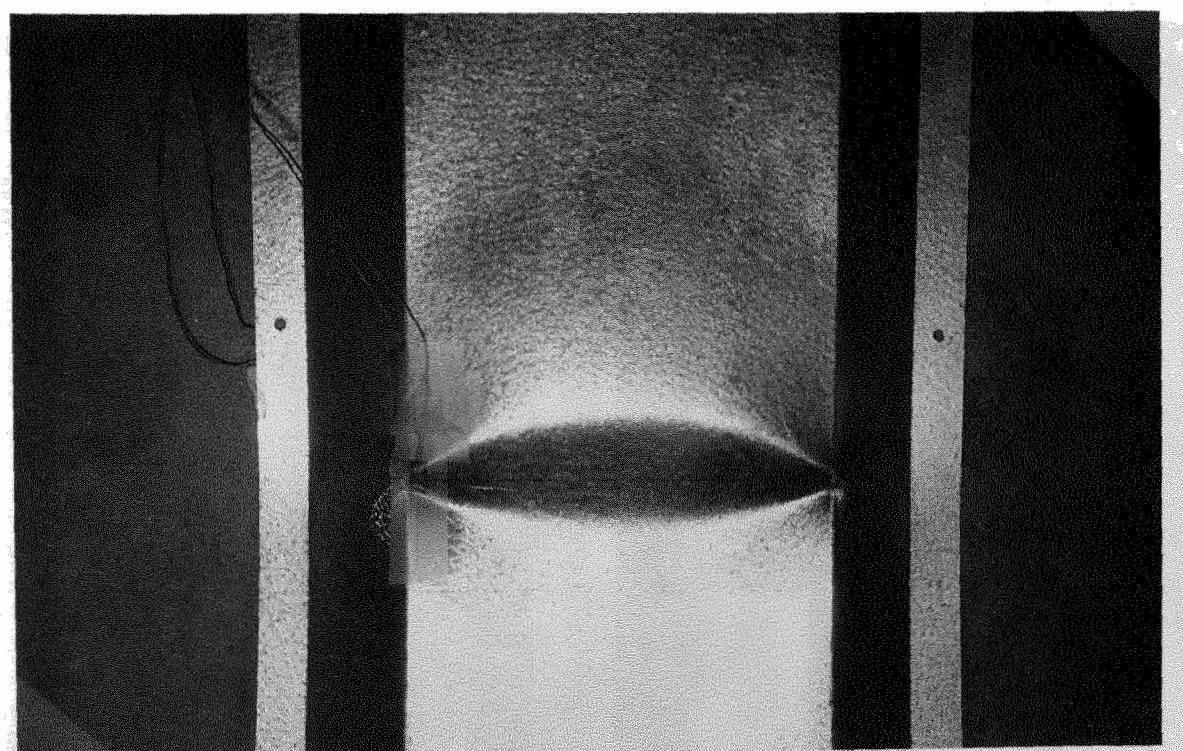

Fig. 4.6.2 Failure Mode of Panels with Screws and Two-Point Loading Condition (Continued)

Fig. 4.6.3 Necking and Fracture Near the Holes in the Panels with Screws

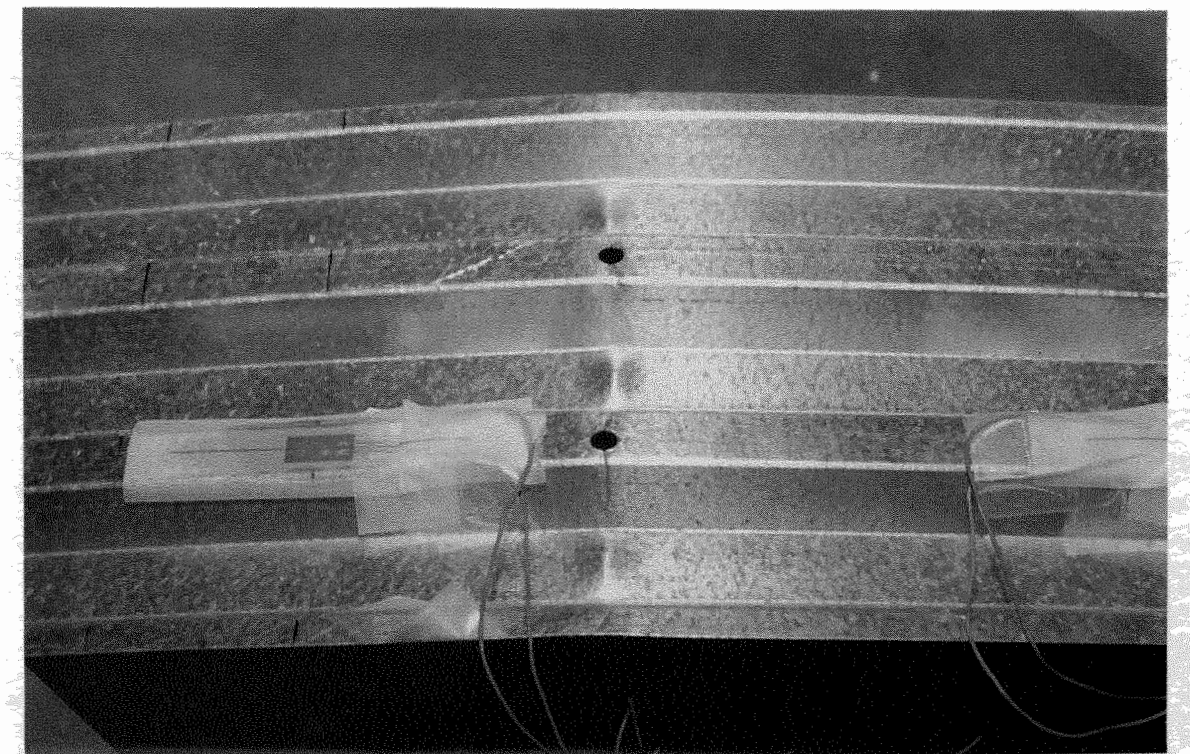

Fig. 4.6.4 Necking and Fracture Near the Holes in the Panels with Screws (Continued)

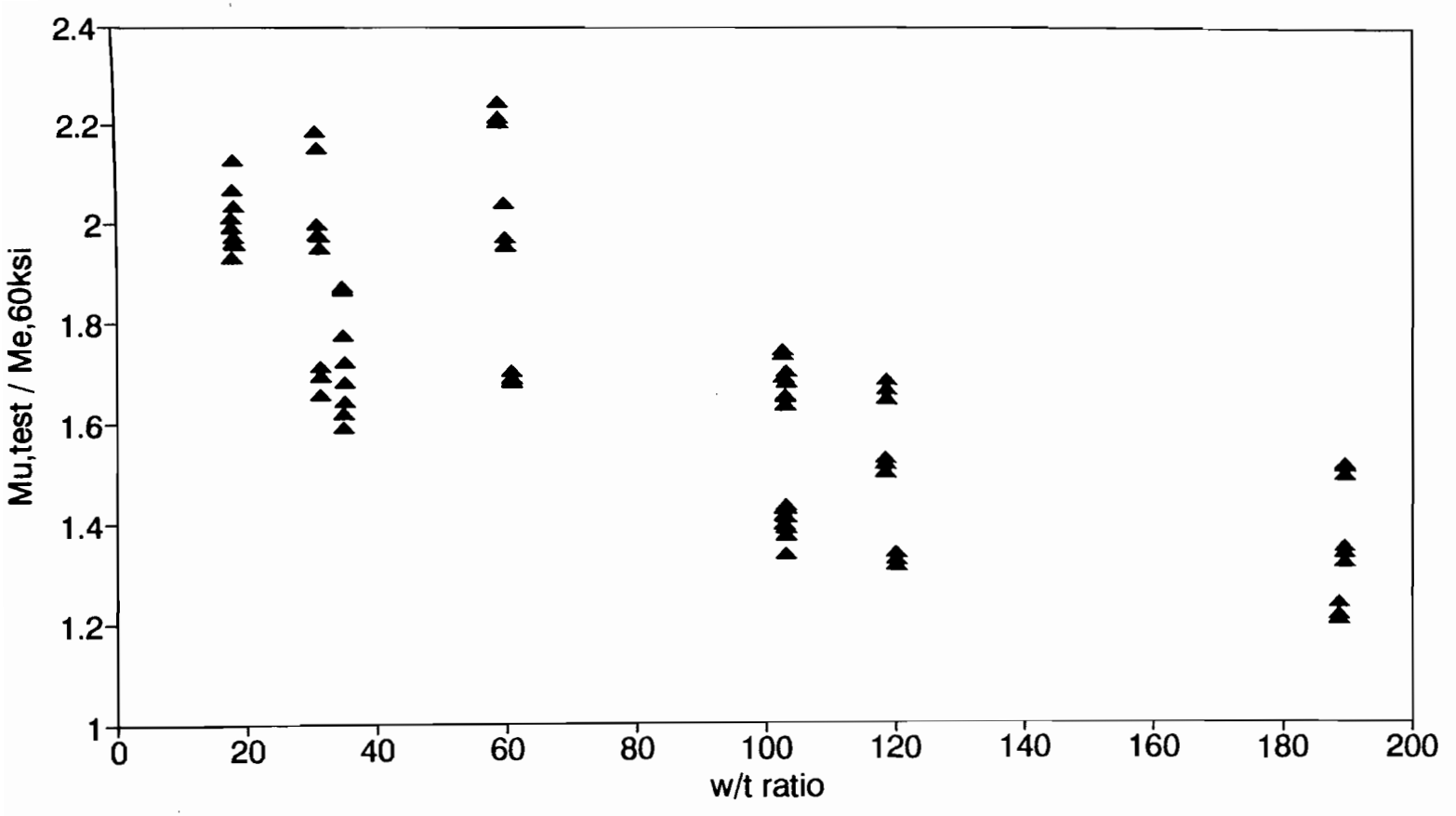

Fig. 5.1.1 Ratio of Tested Ultimate Moment to Calculated Moment Using 60 ksi Stress vs. w/t Ratio of Panels

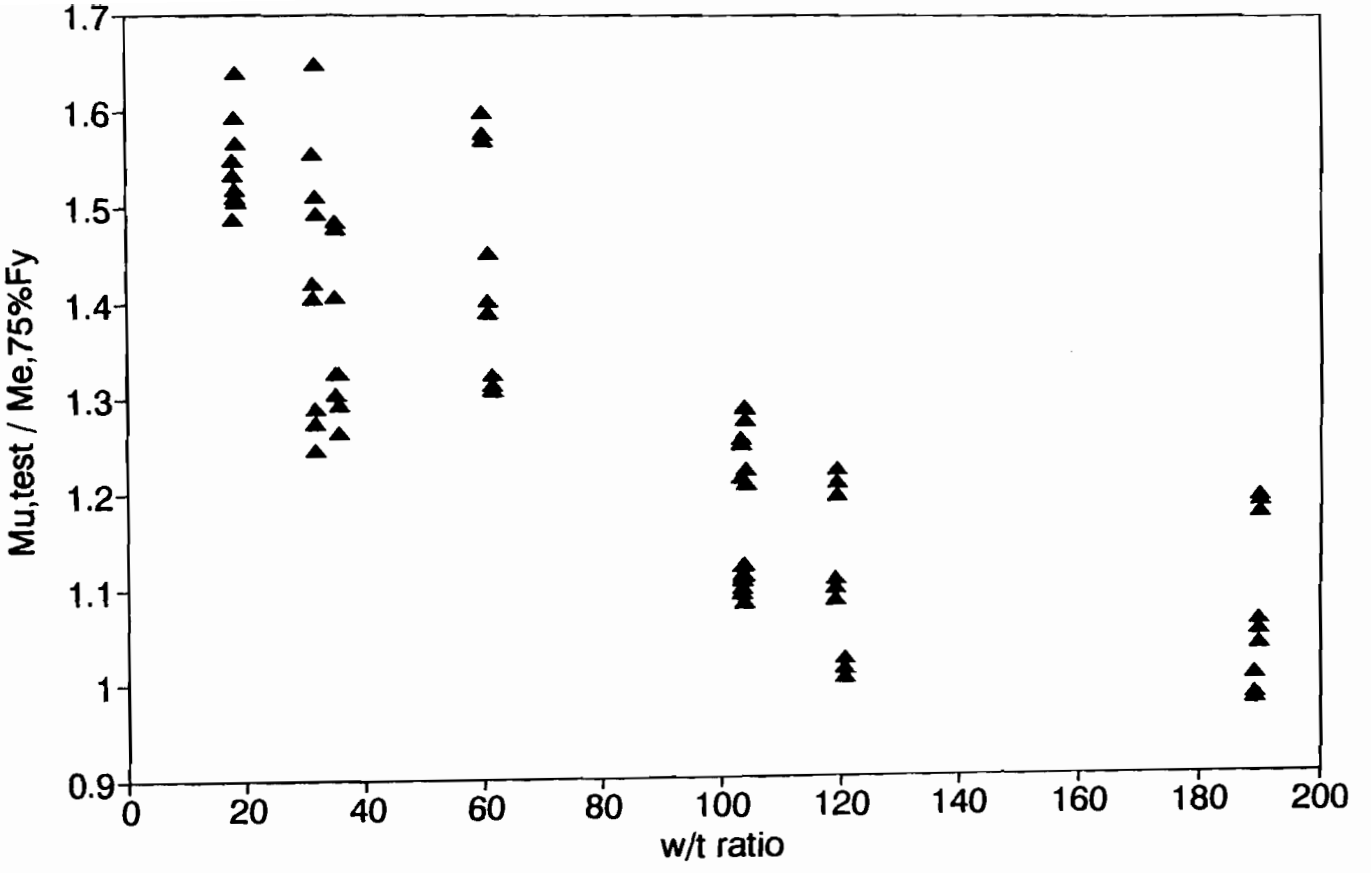

Fig. 5.1.2 Ratio of Tested Ultimate Moment to Calculated Moment Using 75% of Actual Yield Strength vs. w/t Ratio of Panels

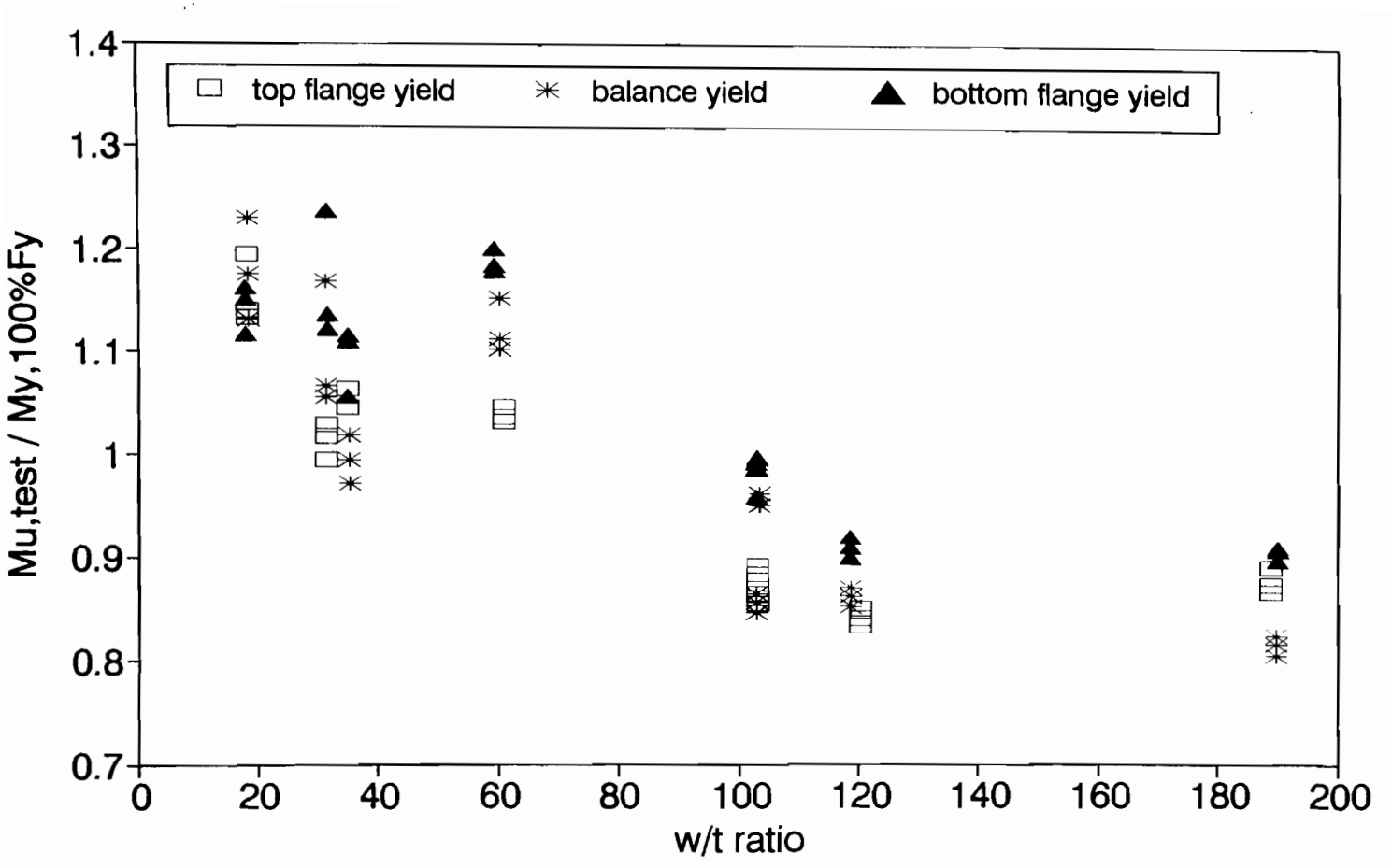

Fig. 5.1.3 Ratio of Tested Ultimate Moment to Calculated Moment Using 100% of Actual Yield Strength vs. w/t Ratio of Panels

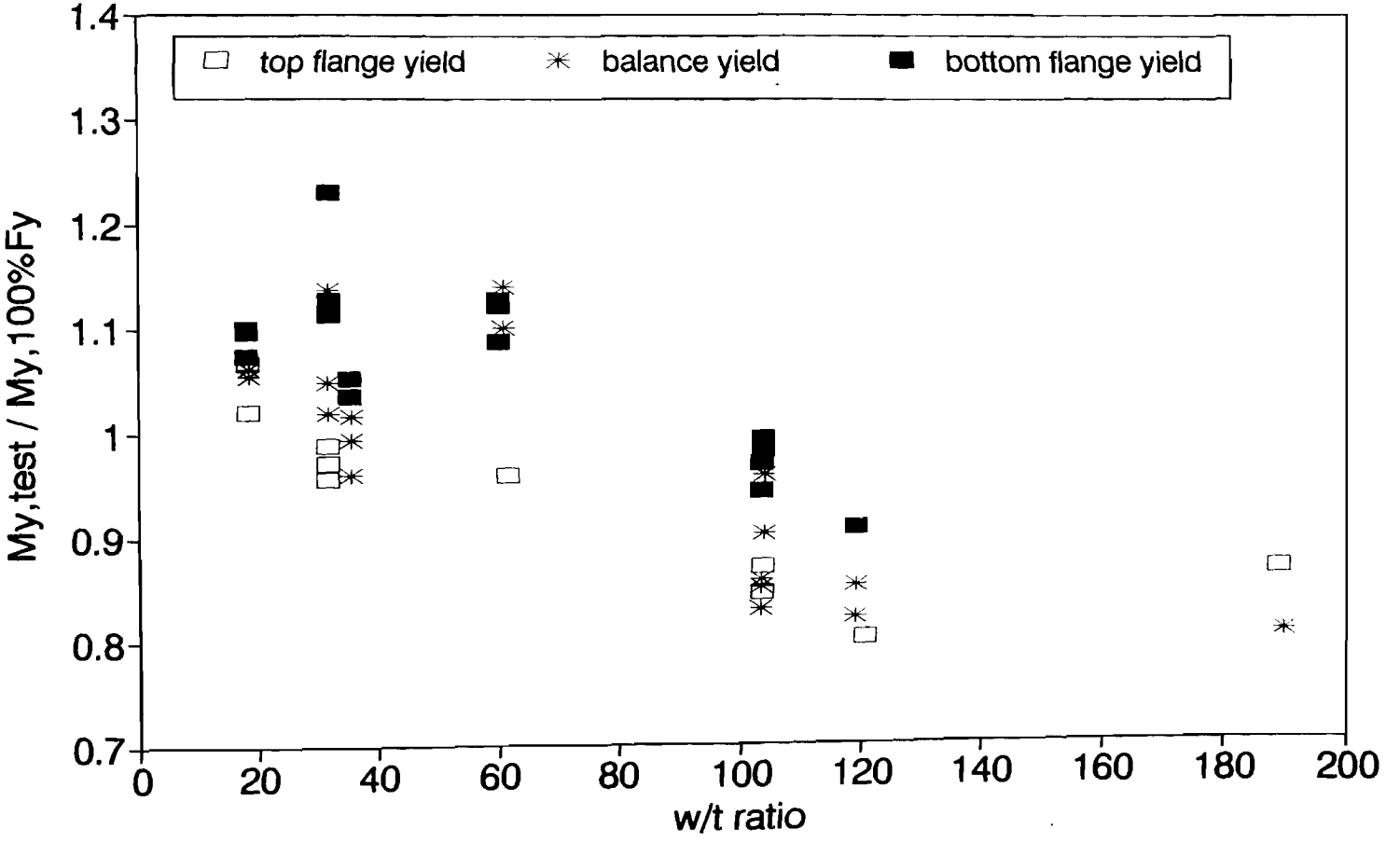

Fig. 5.1.4 Ratio of Tested Yield Moment to Calculated Moment Using 100% of Actual Yield Strength vs. w/t Ratio of Panels

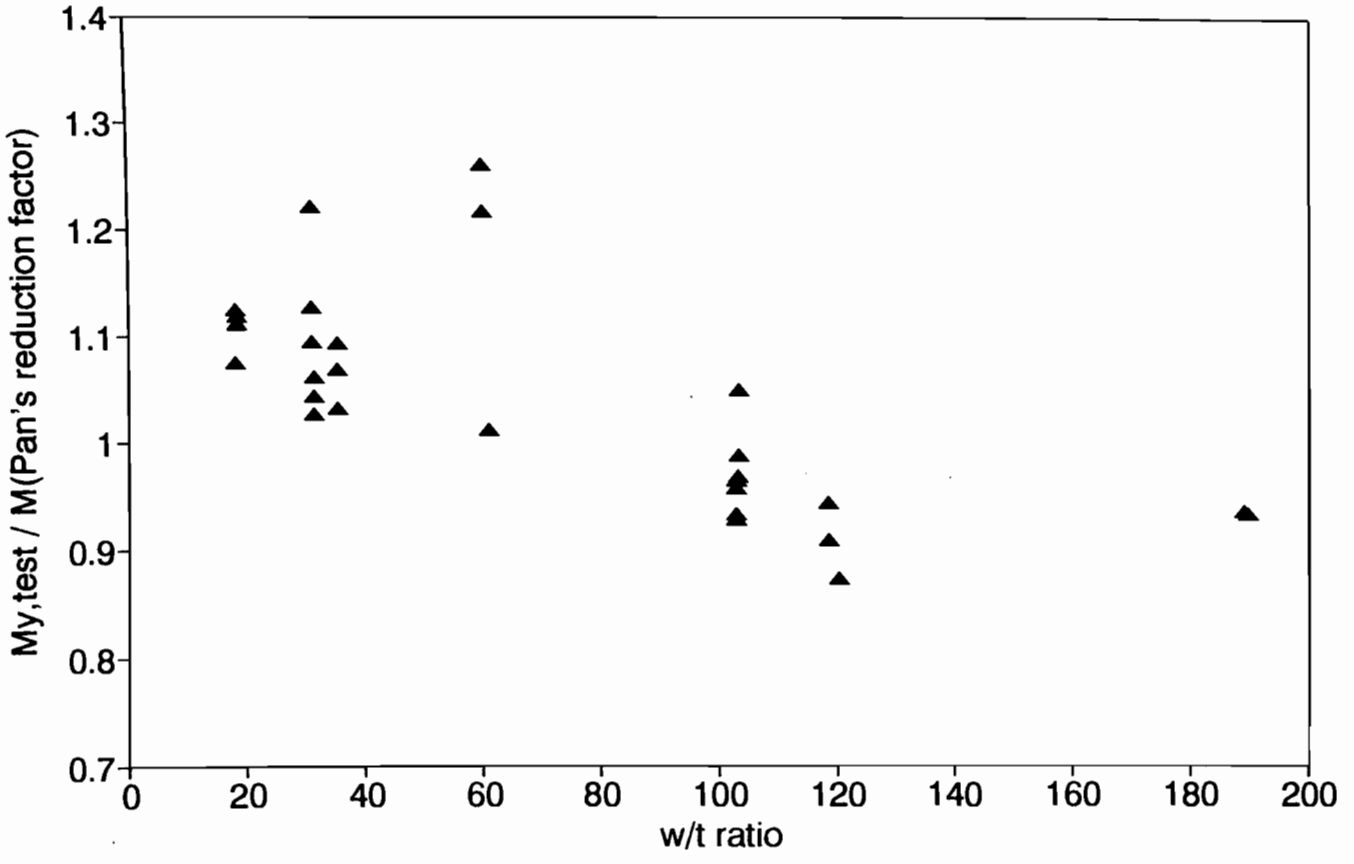

Fig. 5.1.5 Ratio of Tested Yield Moment to Calculated Moment Using Pan's Yield Strength Reduction Factor vs. w/t Ratio of Panels

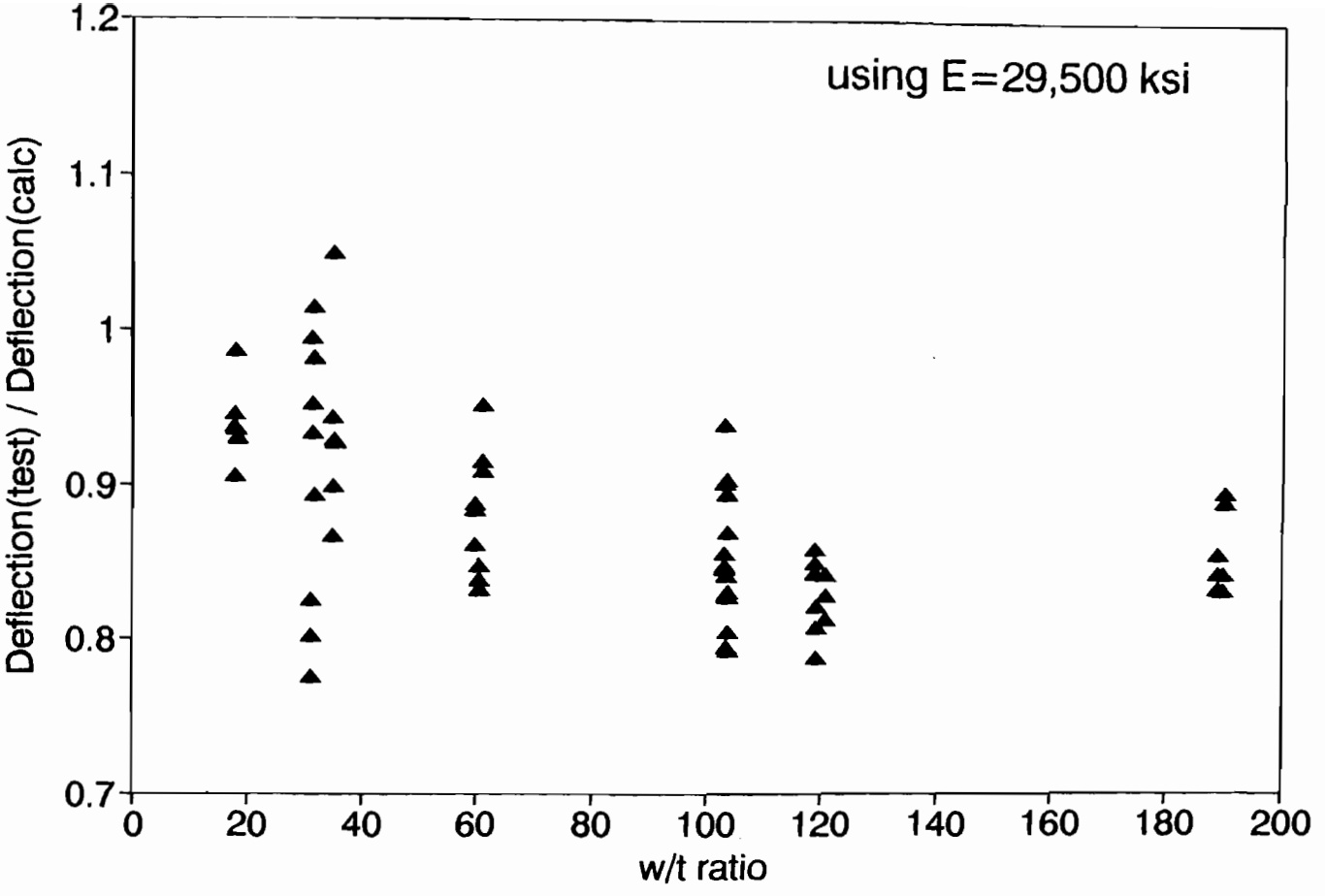

Fig. 5.1.6 Ratio of Tested Deflection to Calculated Deflection at Service Load and Using E=29,500 ksi vs. w/t Ratio of Panels

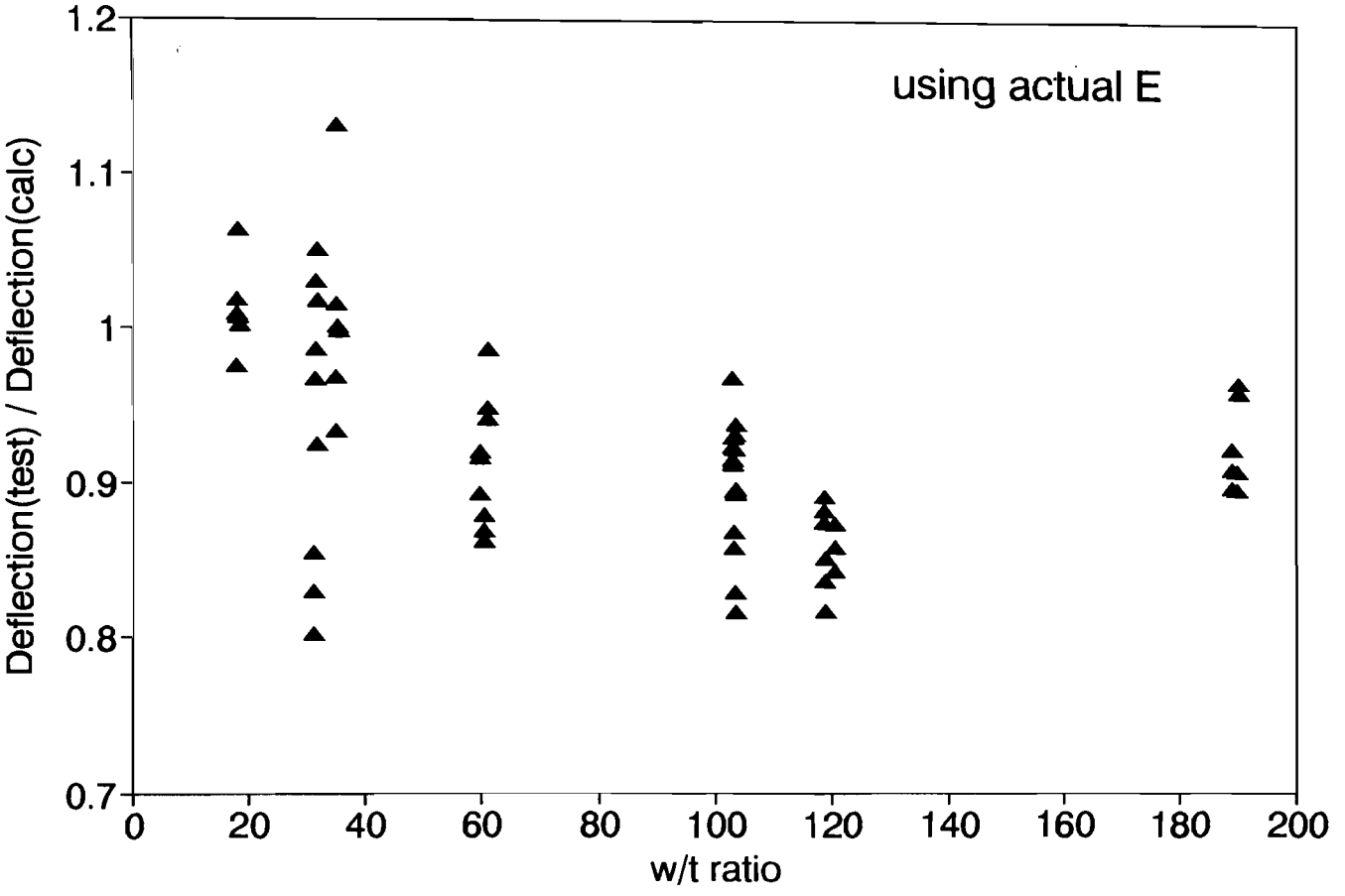

ig. 5.1.7 Ratio of Tested Deflection to Calculated Deflection at Service Load and Using Actual Modulus of Elasticity vs. w/t Ratio of Panels

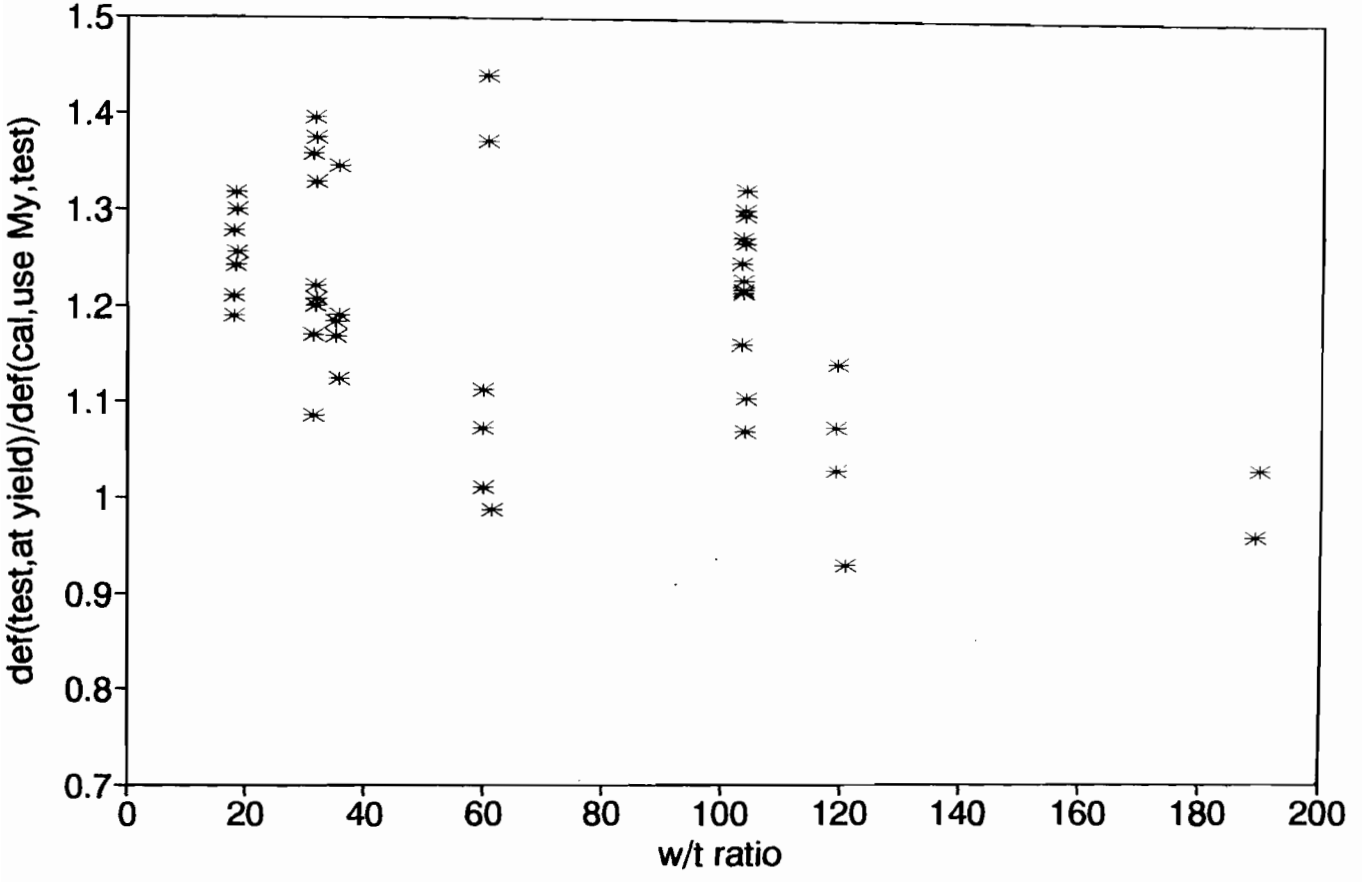

Fig. 5.1.8 Ratio of Tested Deflection at Yielding to Calculated Deflection at Yielding vs. w/t Ratio of Panels

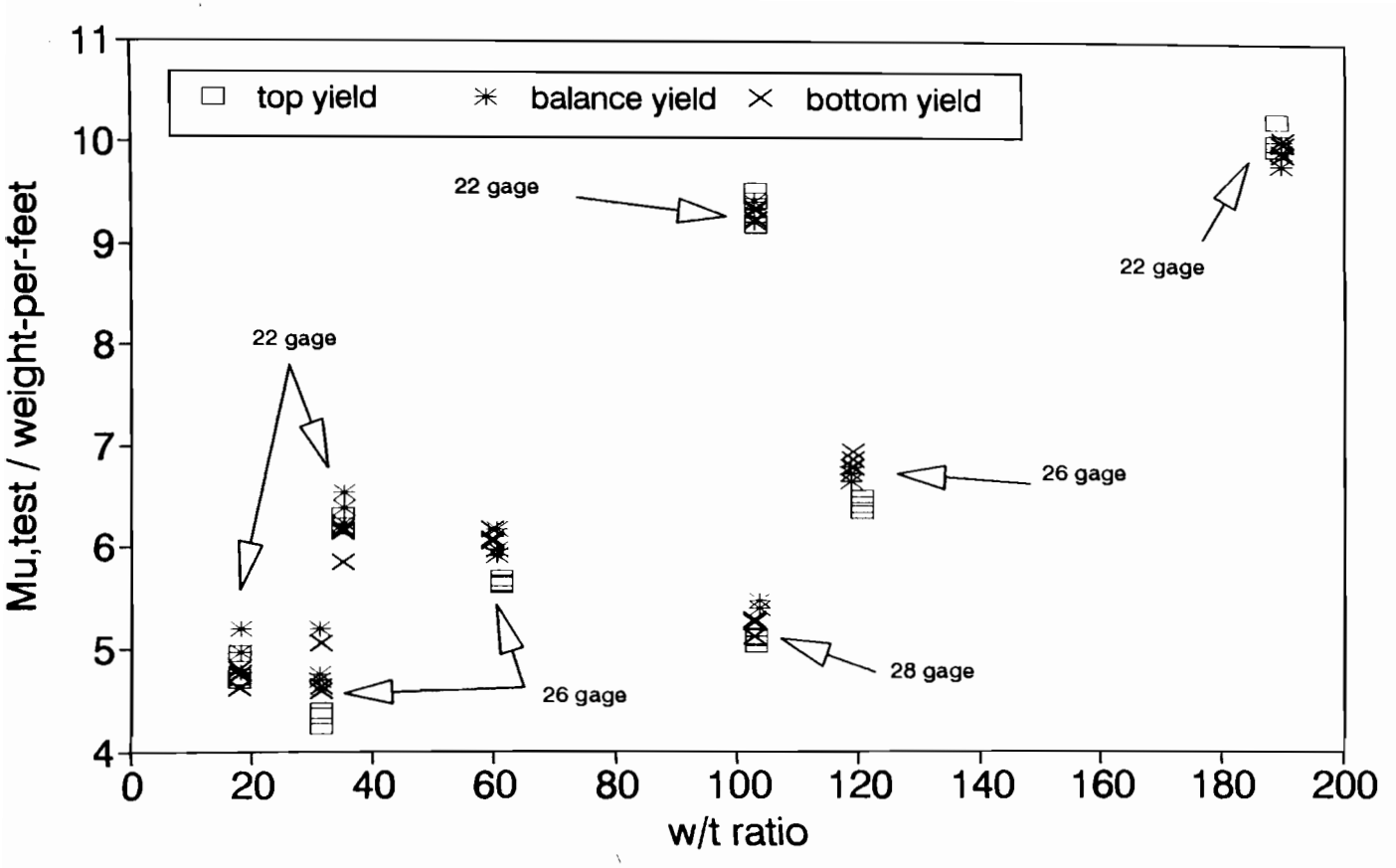

Fig. 5.1.9 Ratio of Tested Ultimate Moment to Weight-Per-Feet of Panel vs. w/t Ratio of Panels

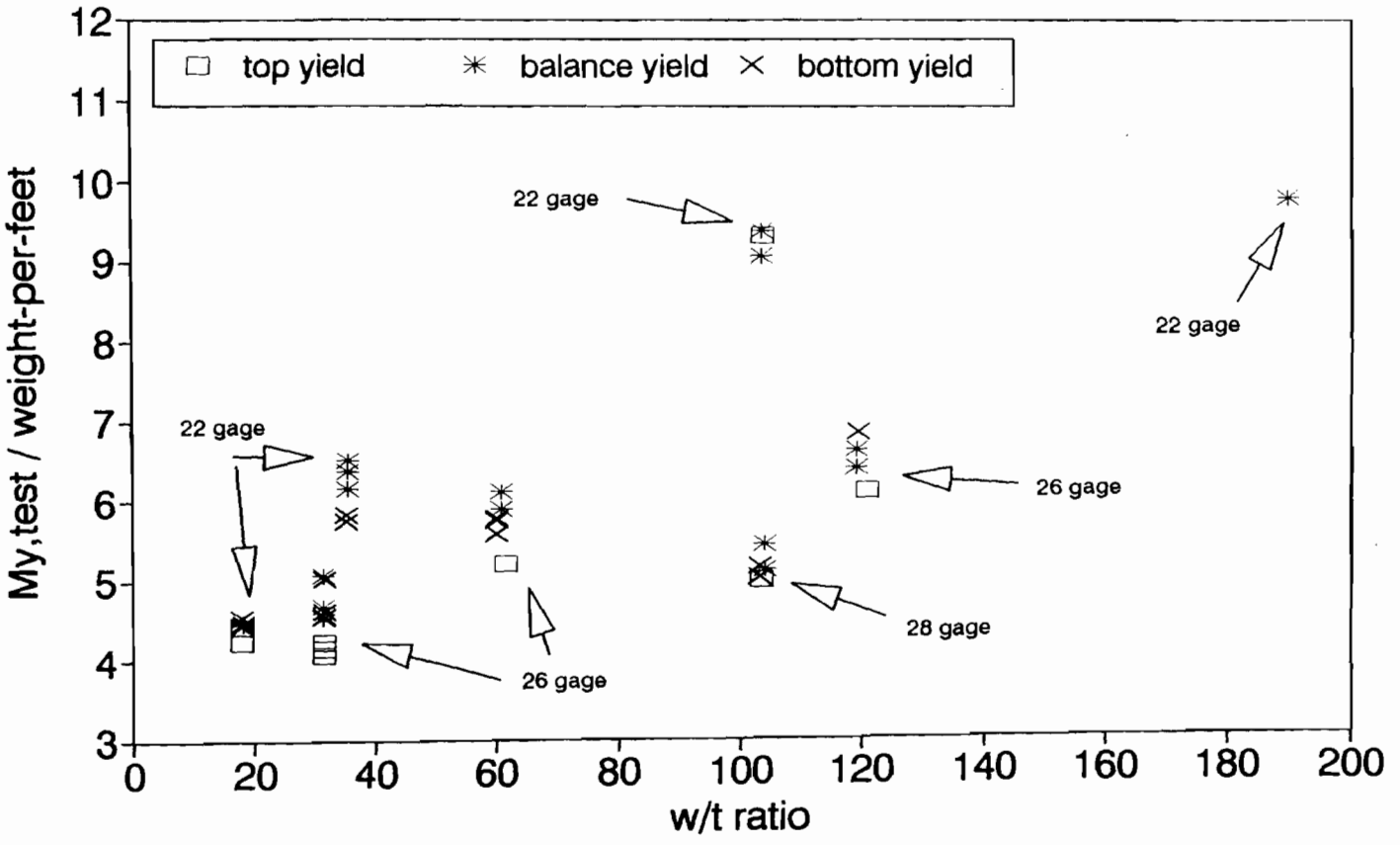

Fig. 5.1.10 Ratio of Tested Yield Moment to Weight-Per-Feet of Panel vs. w/t Ratio of Panels

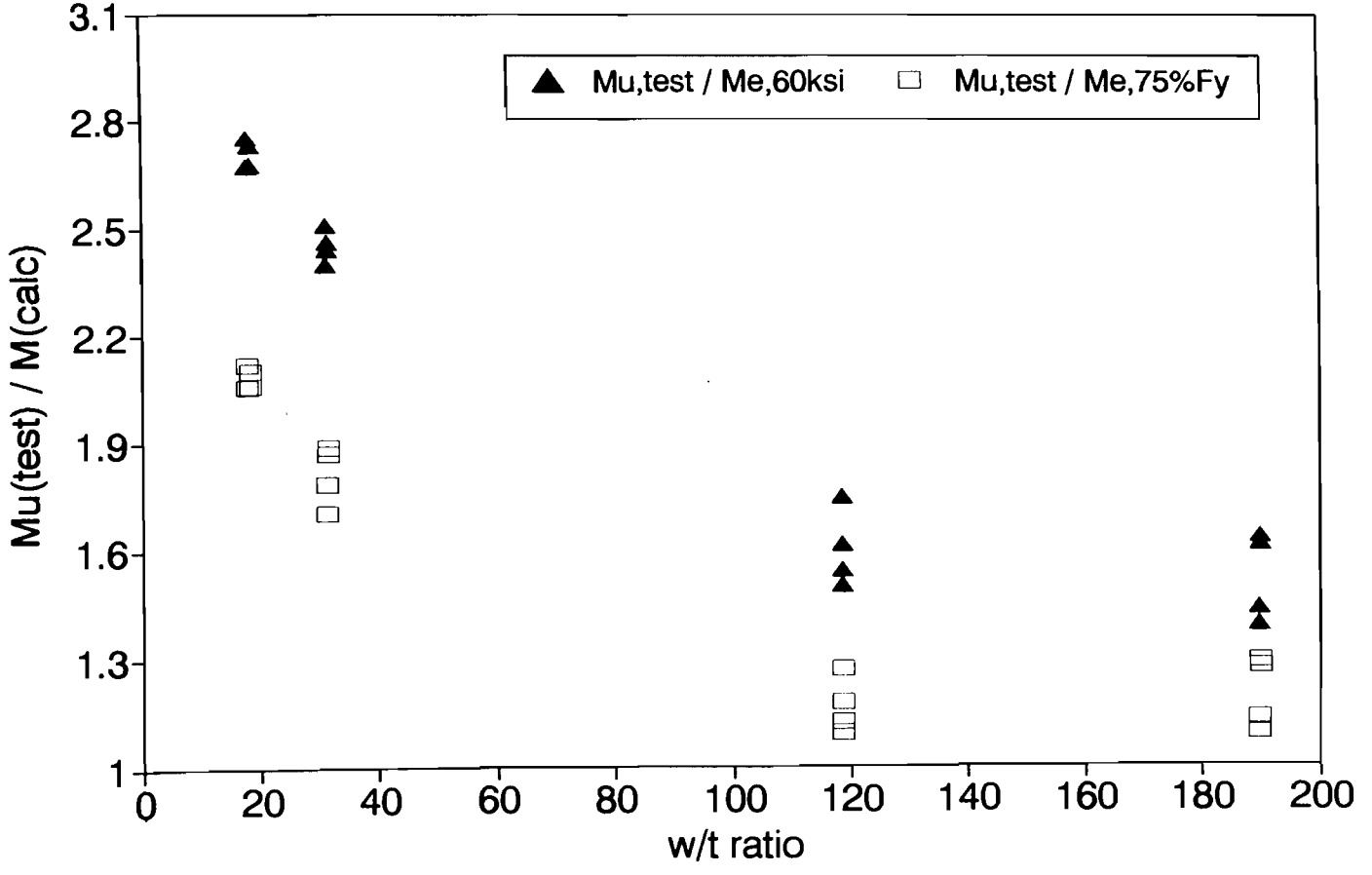

Fig. 5.2.1 Ratio of Tested Ultimate Moment to Calculated Effective Moment vs. w/t Ratio of Panels (One-Point Loading Condition)

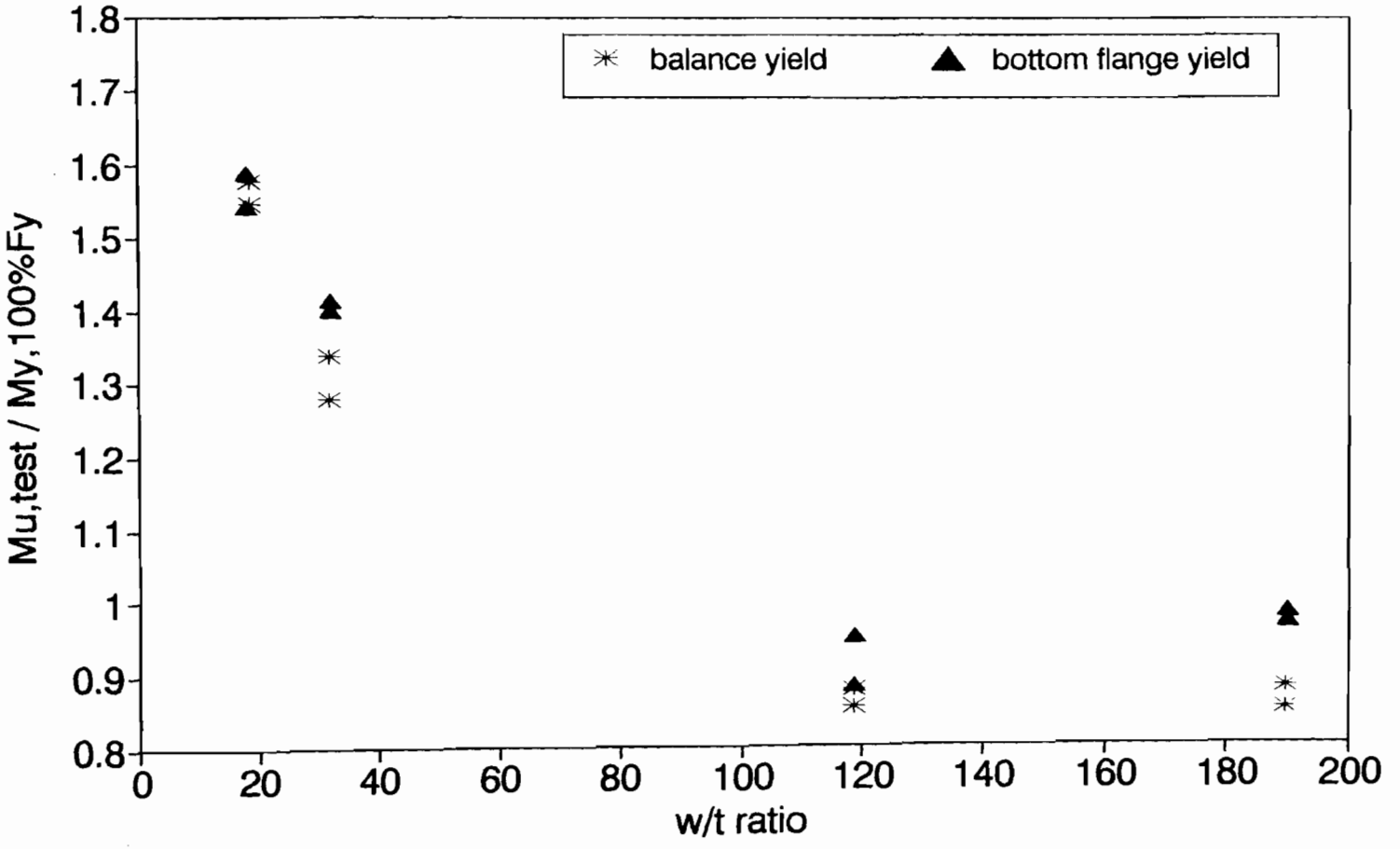

Fig. 5.2.2 Ratio of Tested Ultimate Moment to Calculated Moment Using 100% of Actual Yield Strength vs. w/t Ratio of Panels (One-Point Loading Condition)

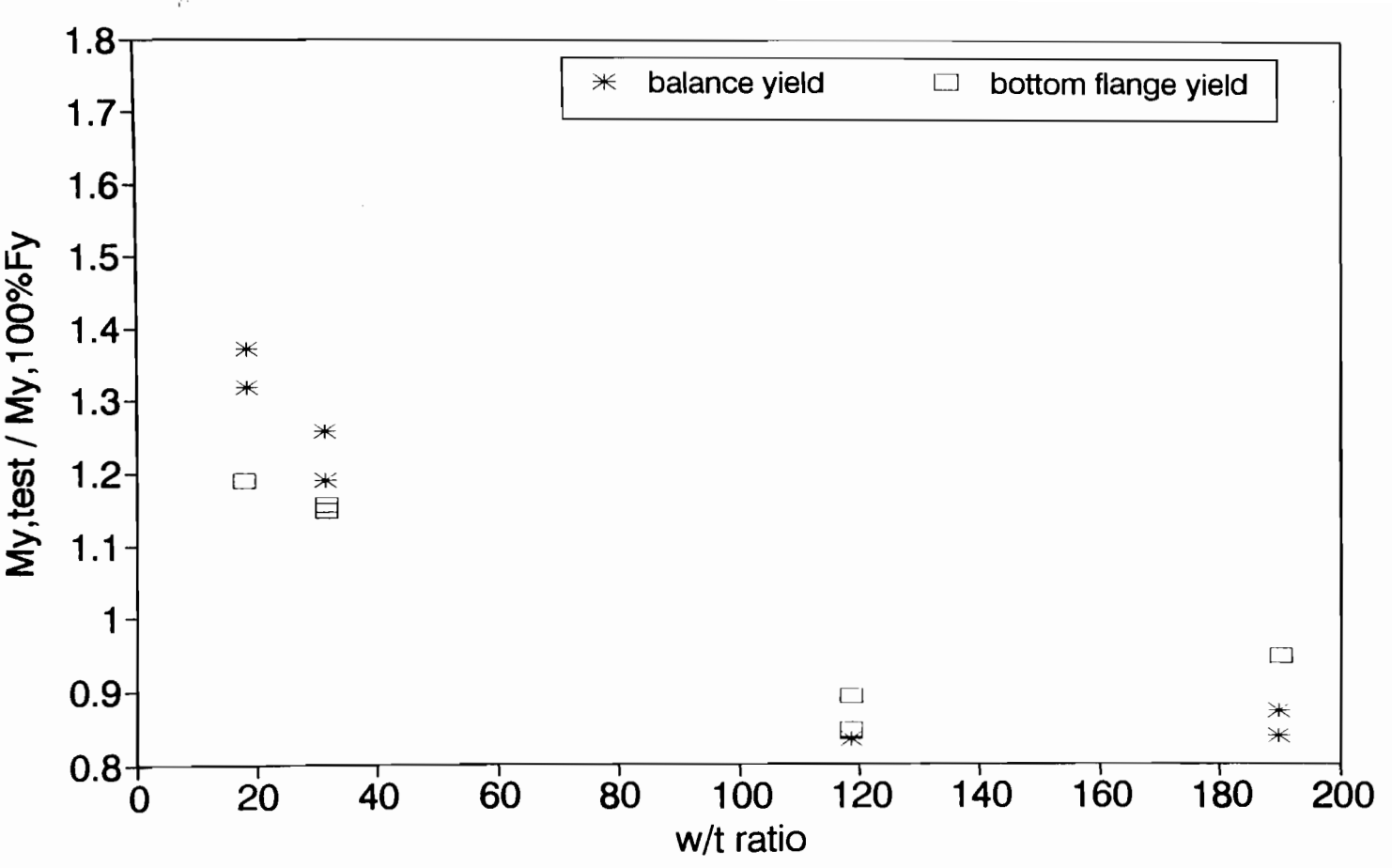

Fig. 5.2.3 Ratio of Tested Yield Moment to Calculated Moment Using 100% of Actual Yield Strength vs. w/t Ratio of Panels (One-Point Loading Condition)

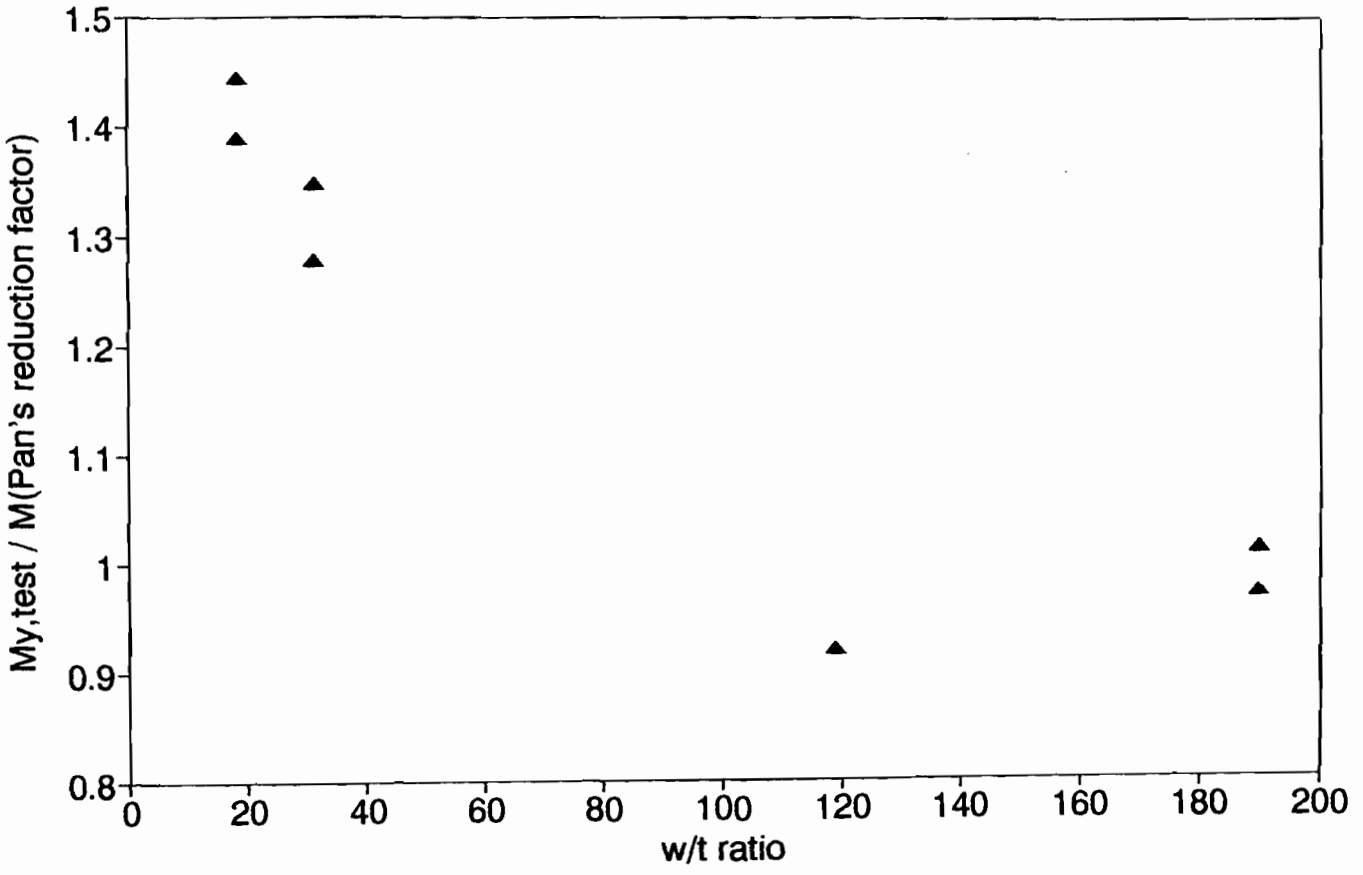

Fig. 5.2.4 Ratio of Tested Yield Moment to Calculated Moment Using Pan's Yield Strength Reduction Factor vs. w/t Ratio of Panels (One-Point Loading Condition)

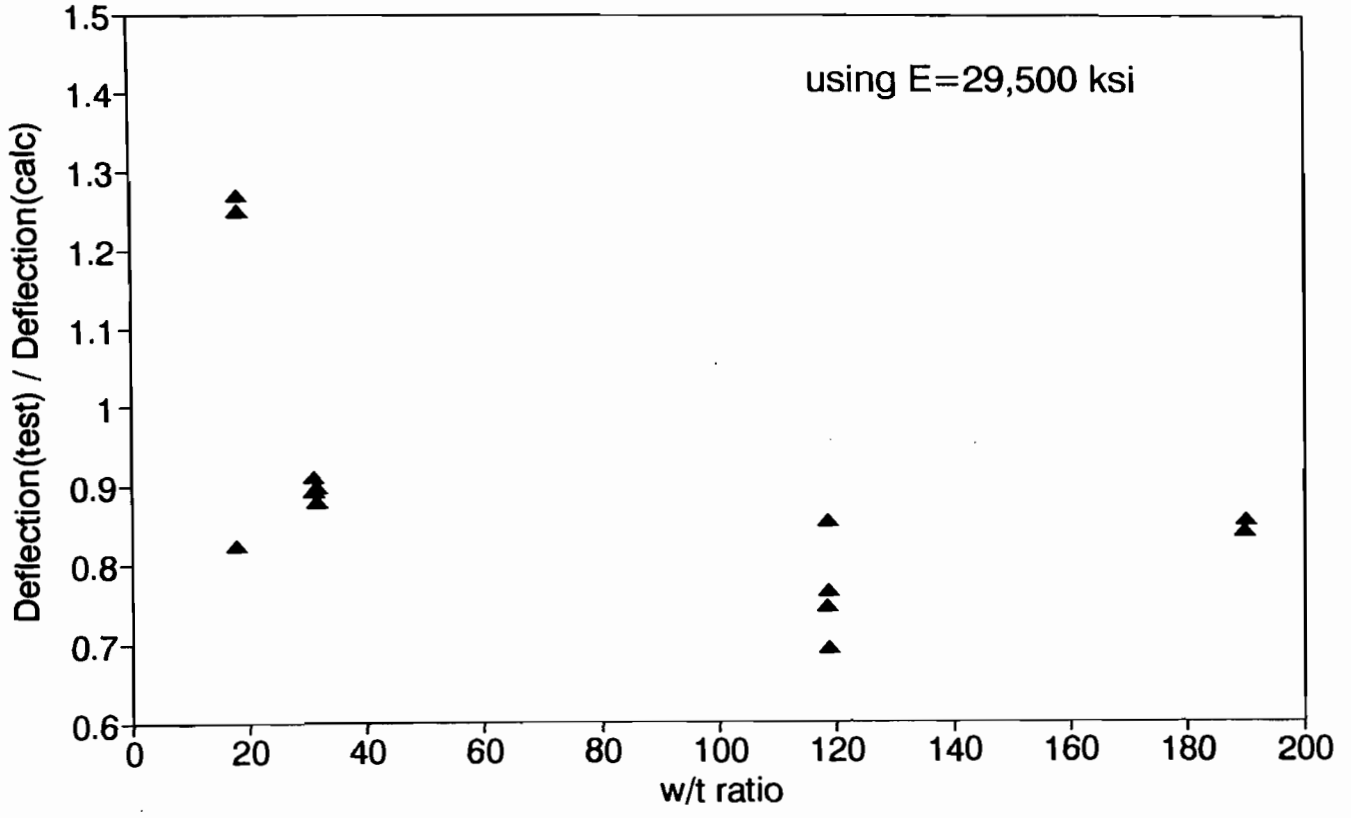

Fig. 5.2.5 Ratio of Tested Deflection to Calculated Deflection at Service Load and Using E=29,500 ksi vs. w/t Ratio of Panels (One-Point Loading Condition)

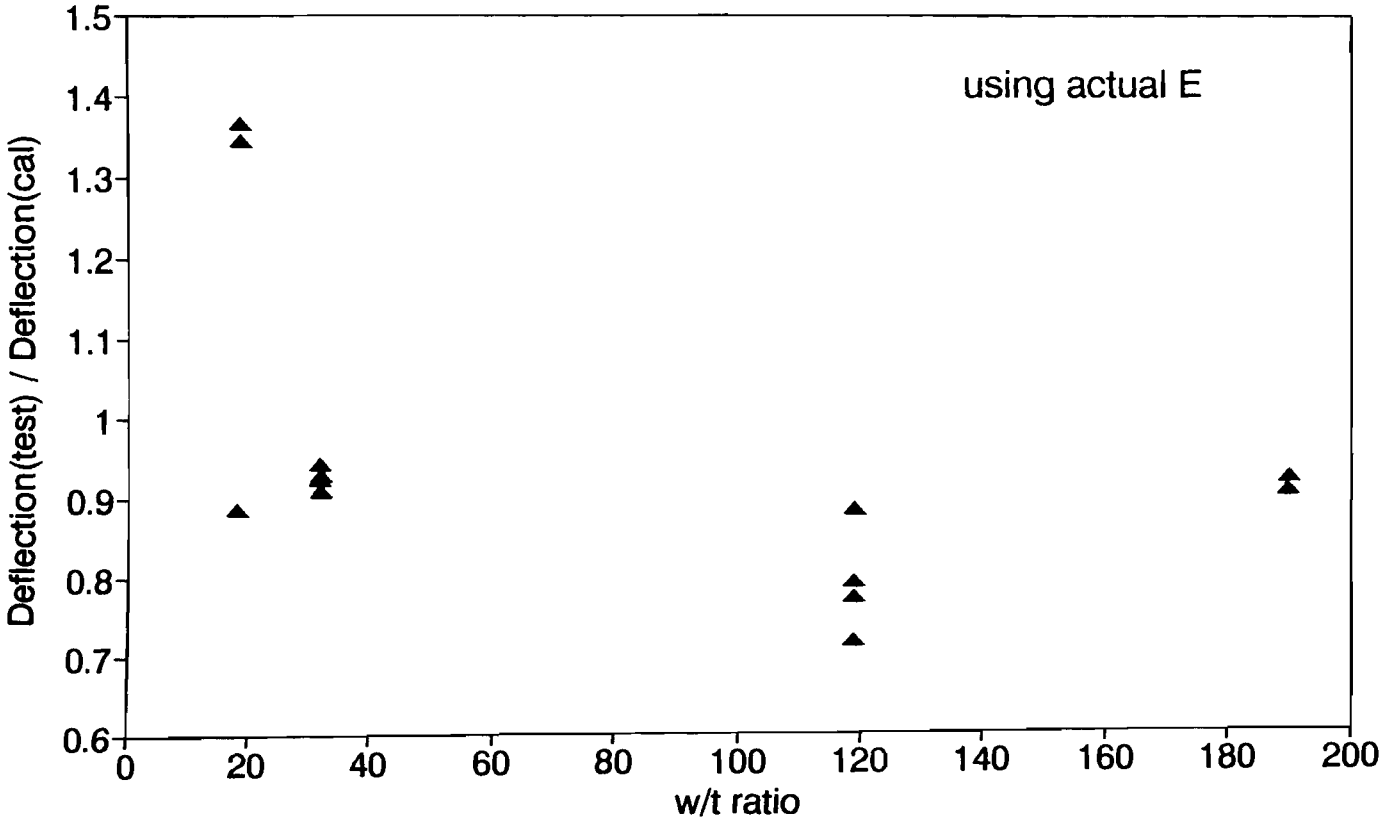

Fig. 5.2.6 Ratio of Tested Deflection to Calculated Deflection at Service Load and Using Actual Modulus of Elasticity vs. w/t Ratio of Panels (One-Point Loading Condition)

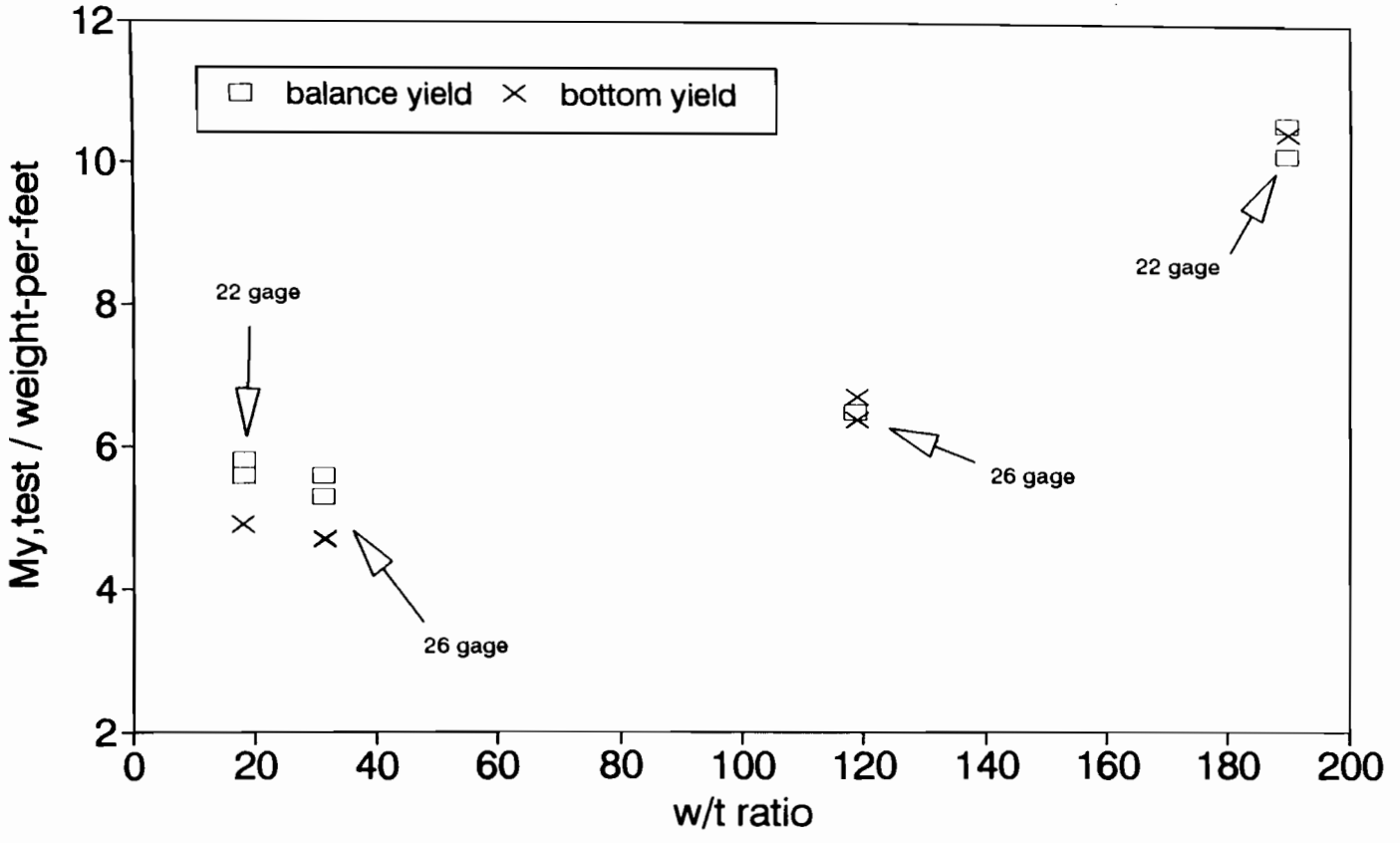

Fig. 5.2.7 Ratio of Tested Yield Moment to Weigh-Per-Feet of Panel vs. w/t Ratio of Panels (One-Point Loading Condition)

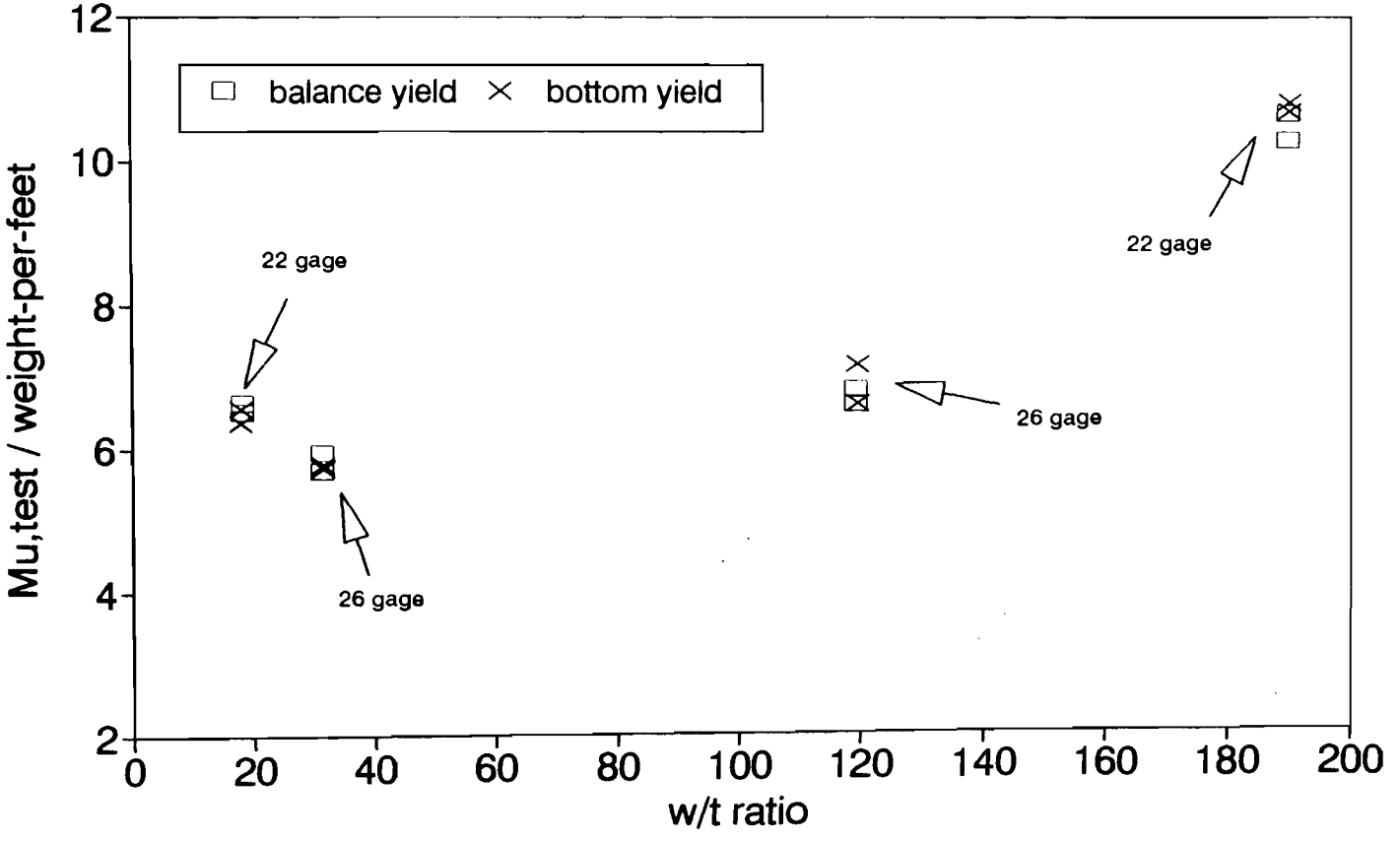

Fig. 5.2.8 Ratio of Tested Ultimate Moment to Weigh-Per-Feet of Panel vs. w/t Ratio of Panels (One-Point Loading Condition)

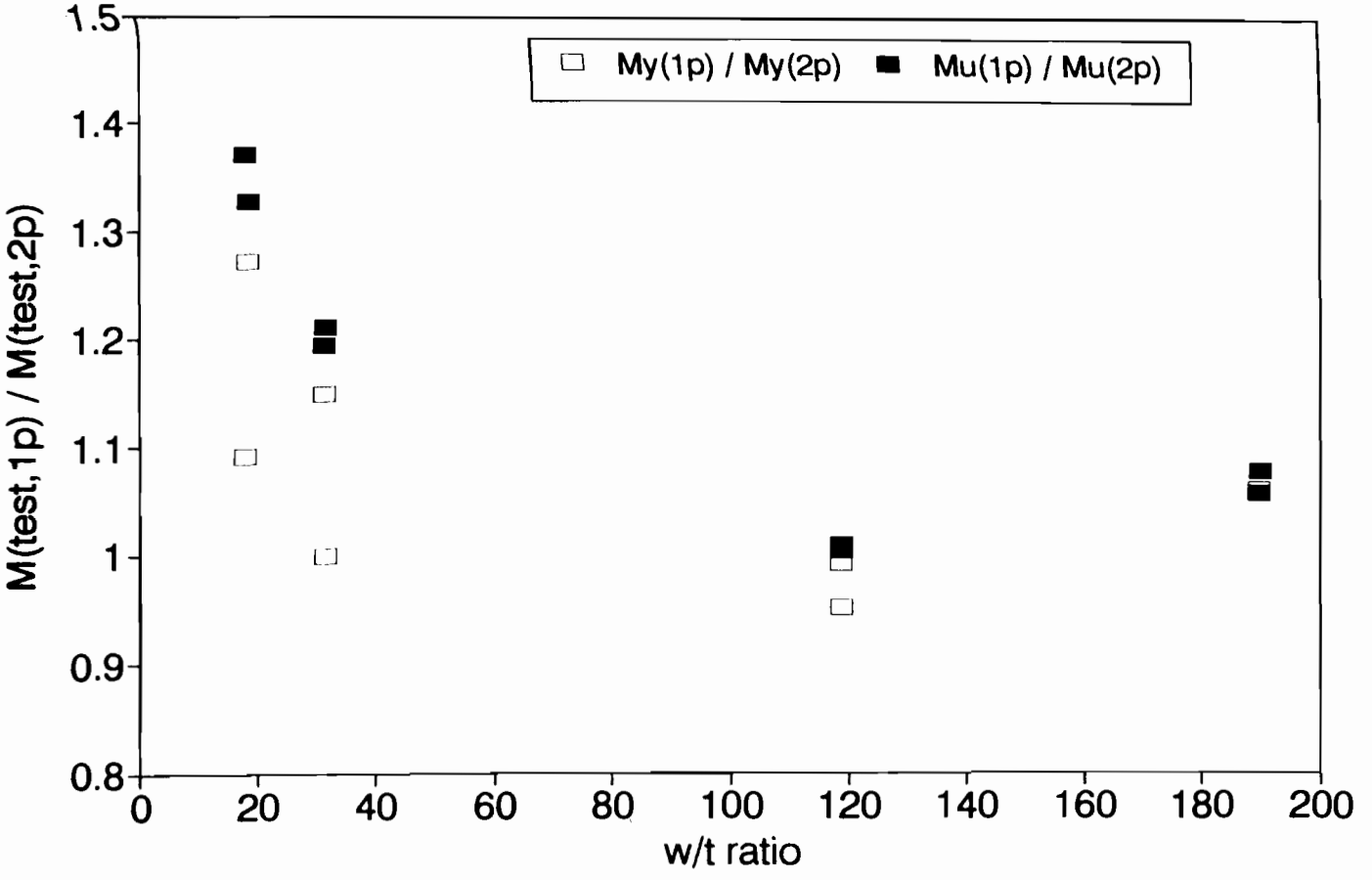

Fig. 5.3.1 Comparison of Tested Moments between One-Point and Two-Point Loading Conditions

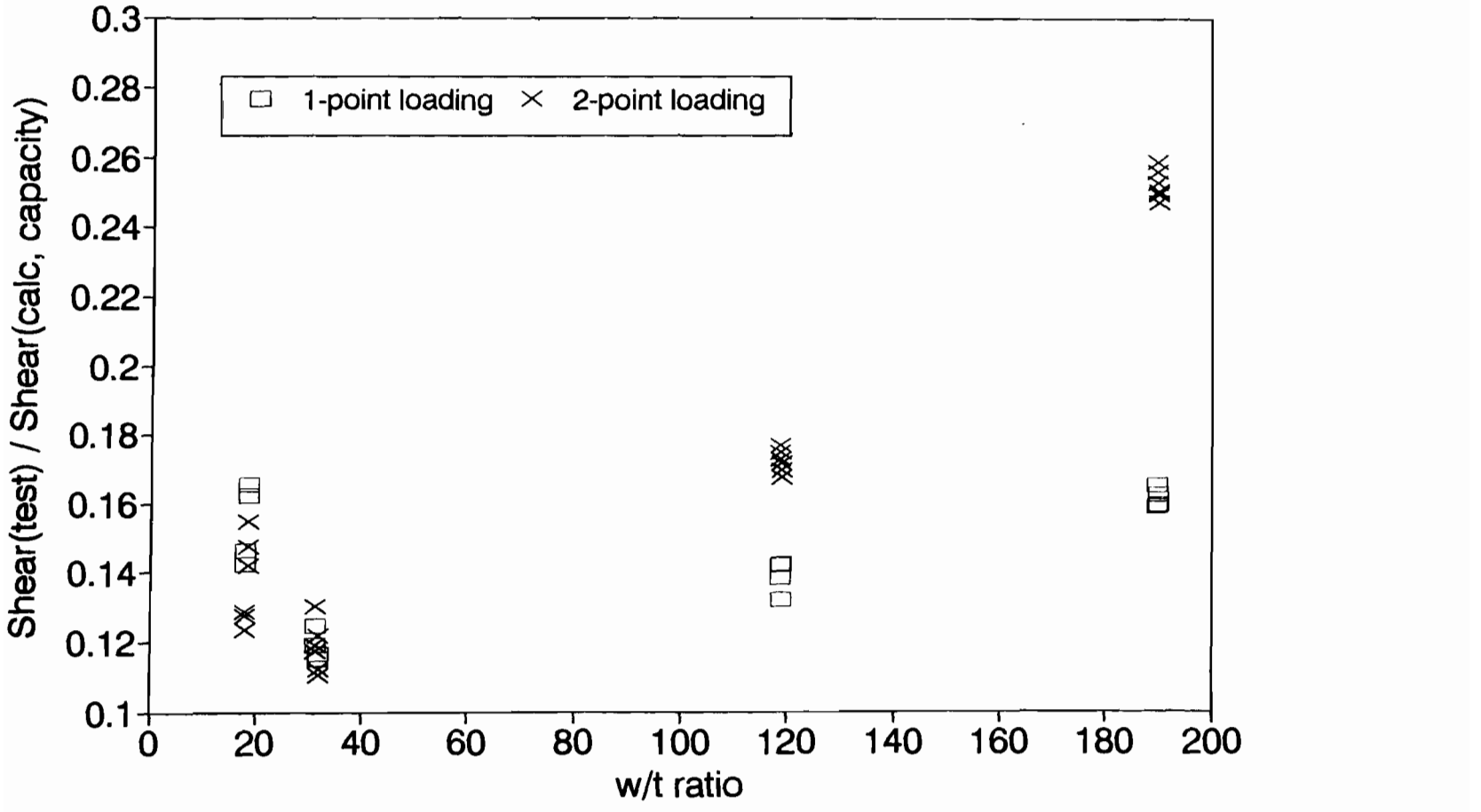

Fig. 5.3.2 Ratio of Tested Shear to Calculated Shear Capacity vs. w/t Ratio of Panels

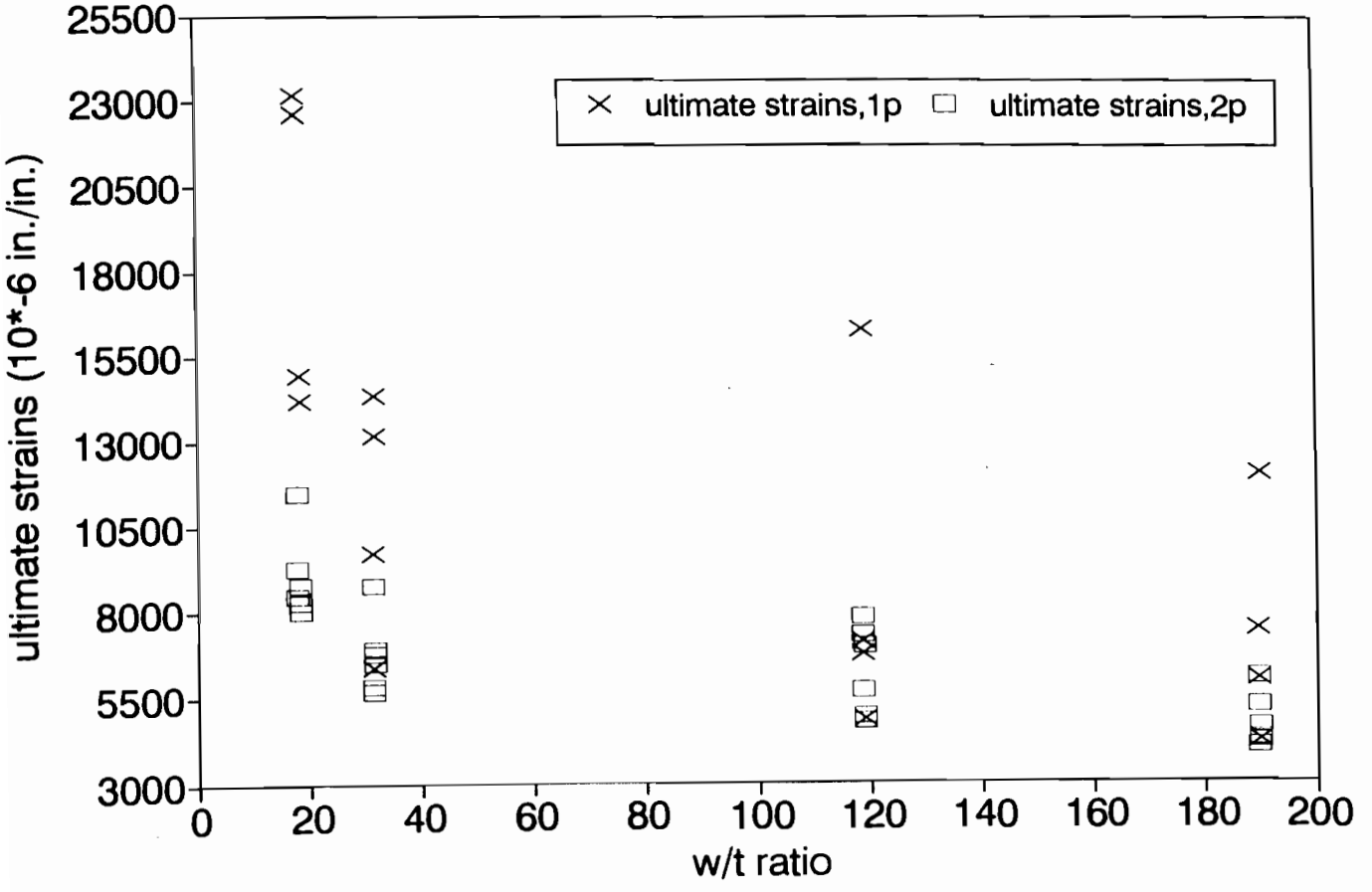

Fig. 5.3.3 Comparison of Tested Ultimate Strains between One-Point and Two-Point Loading Conditions

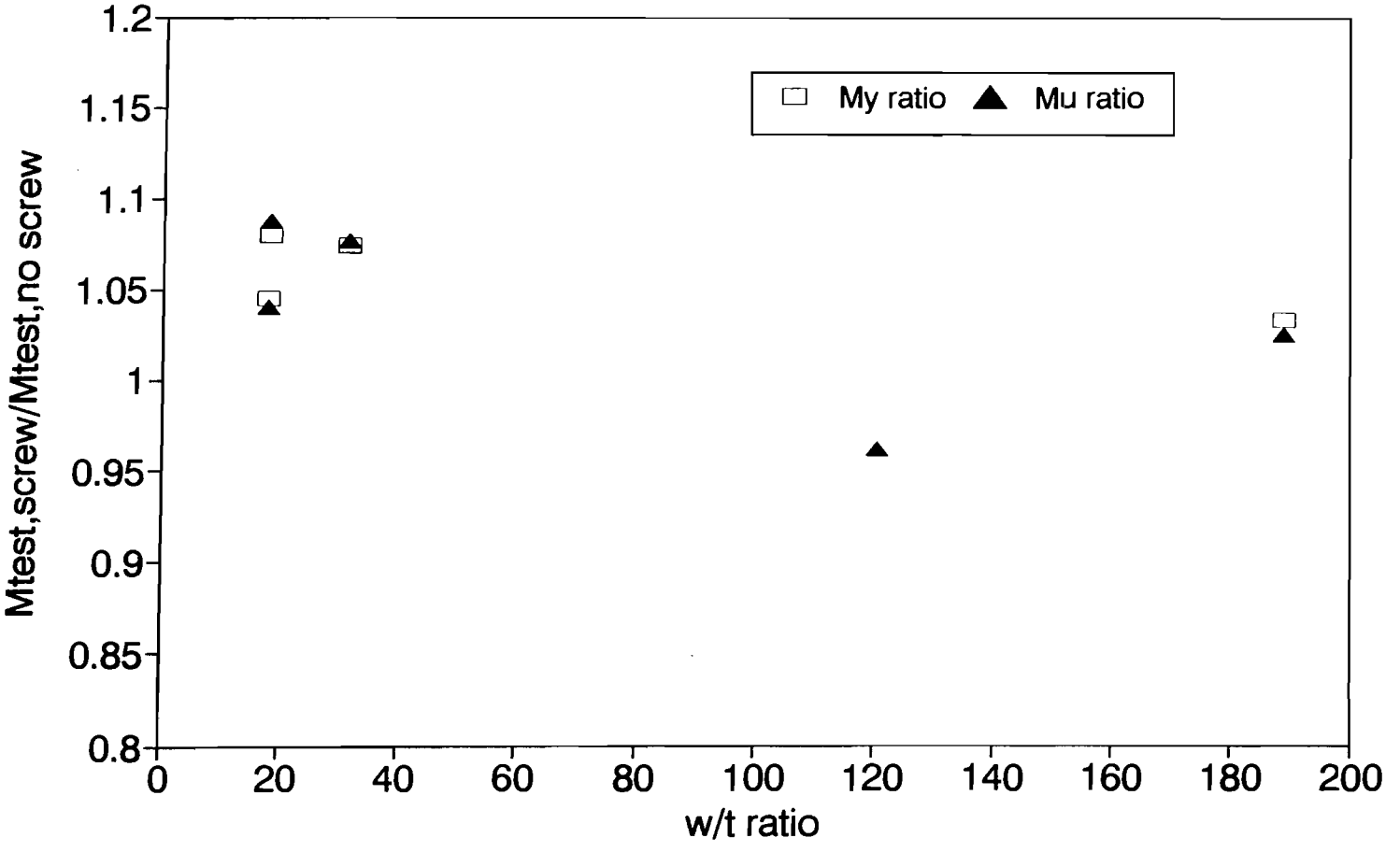

Fig. 5.4.1 Comparison of Tested Moments between Panels with and without Screws

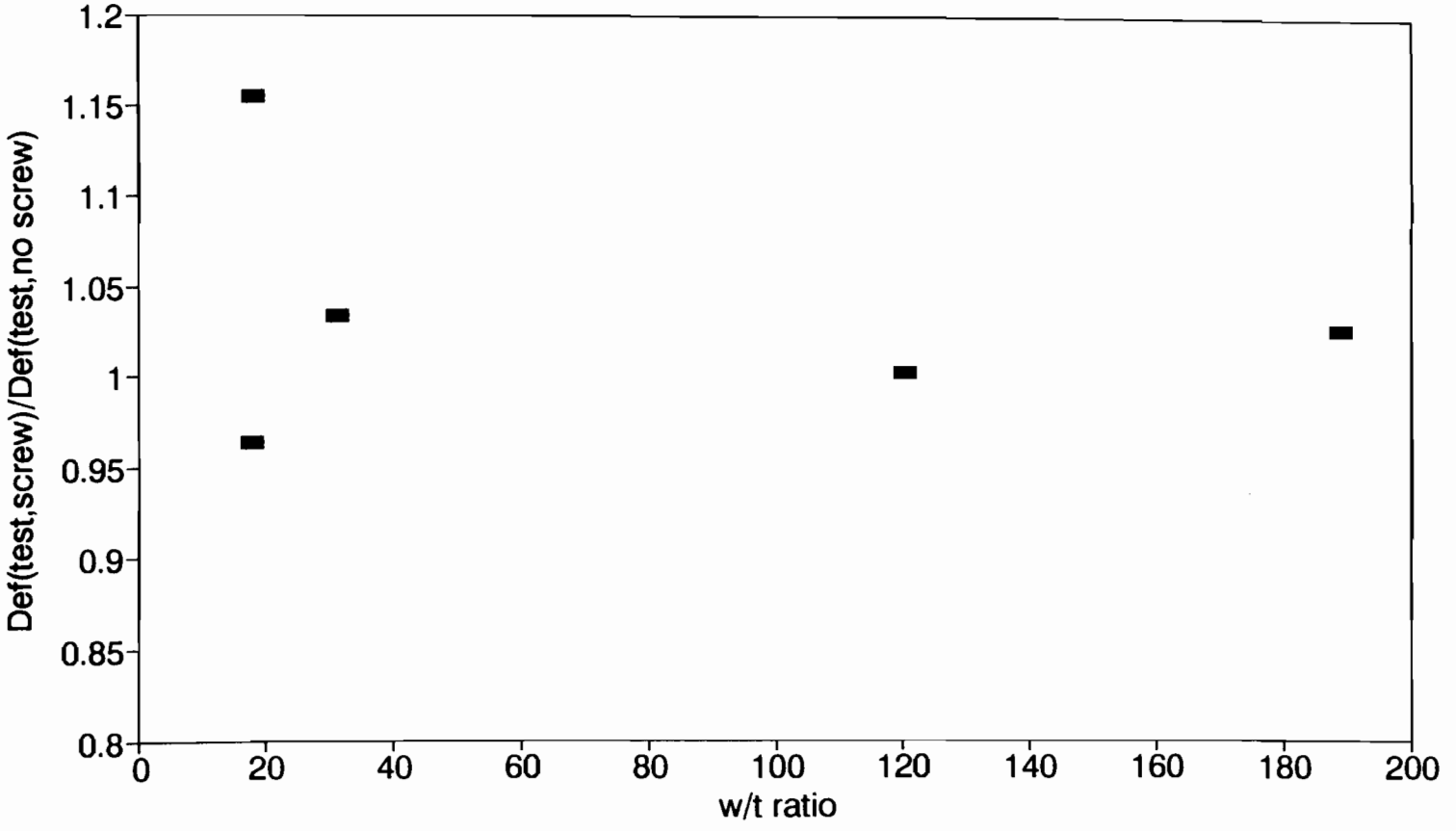

Fig. 5.4.2 Comparison of Tested Deflections between Panels with and without Screws

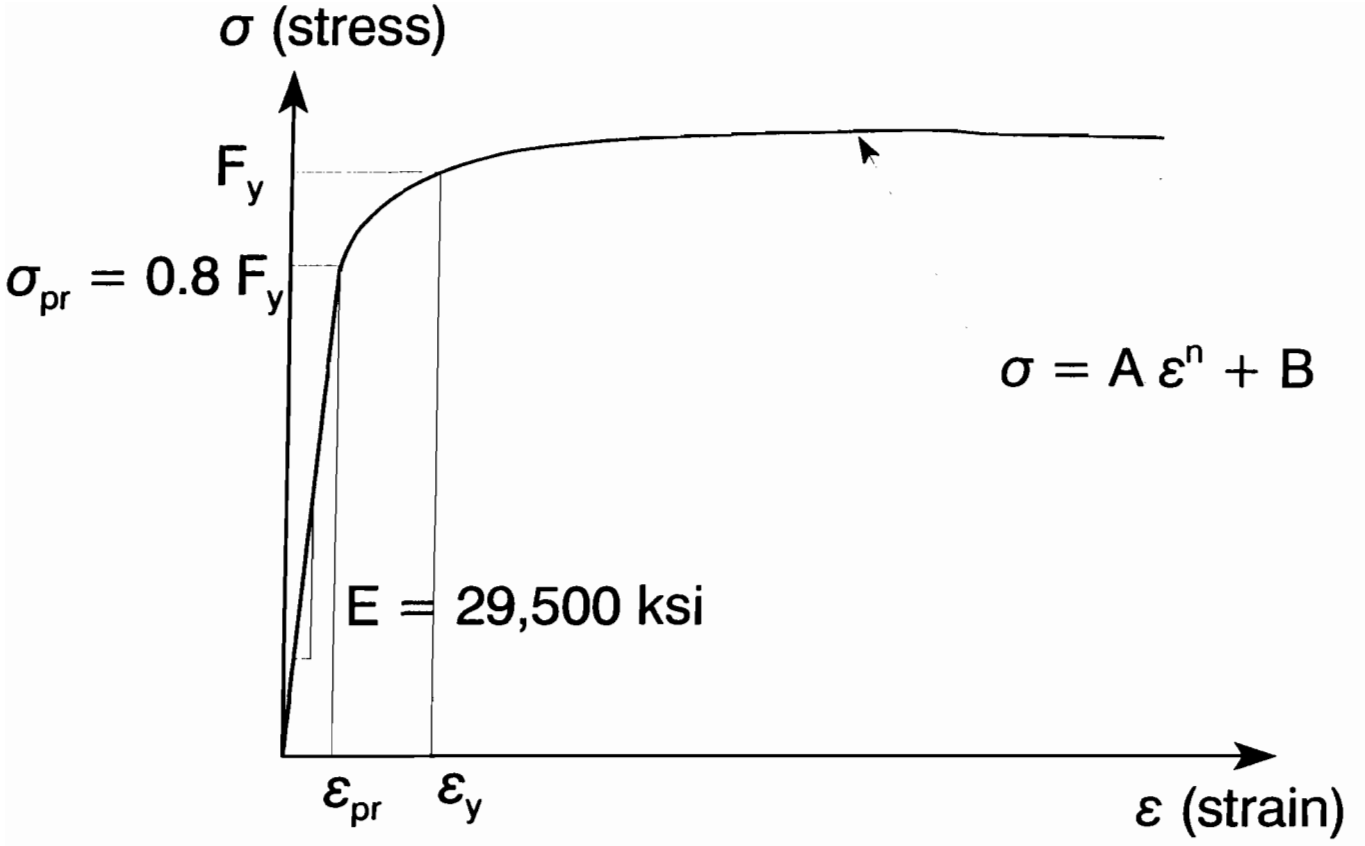

Fig. 6.2.1 Theoretical Model of Stress-Strain Relationship

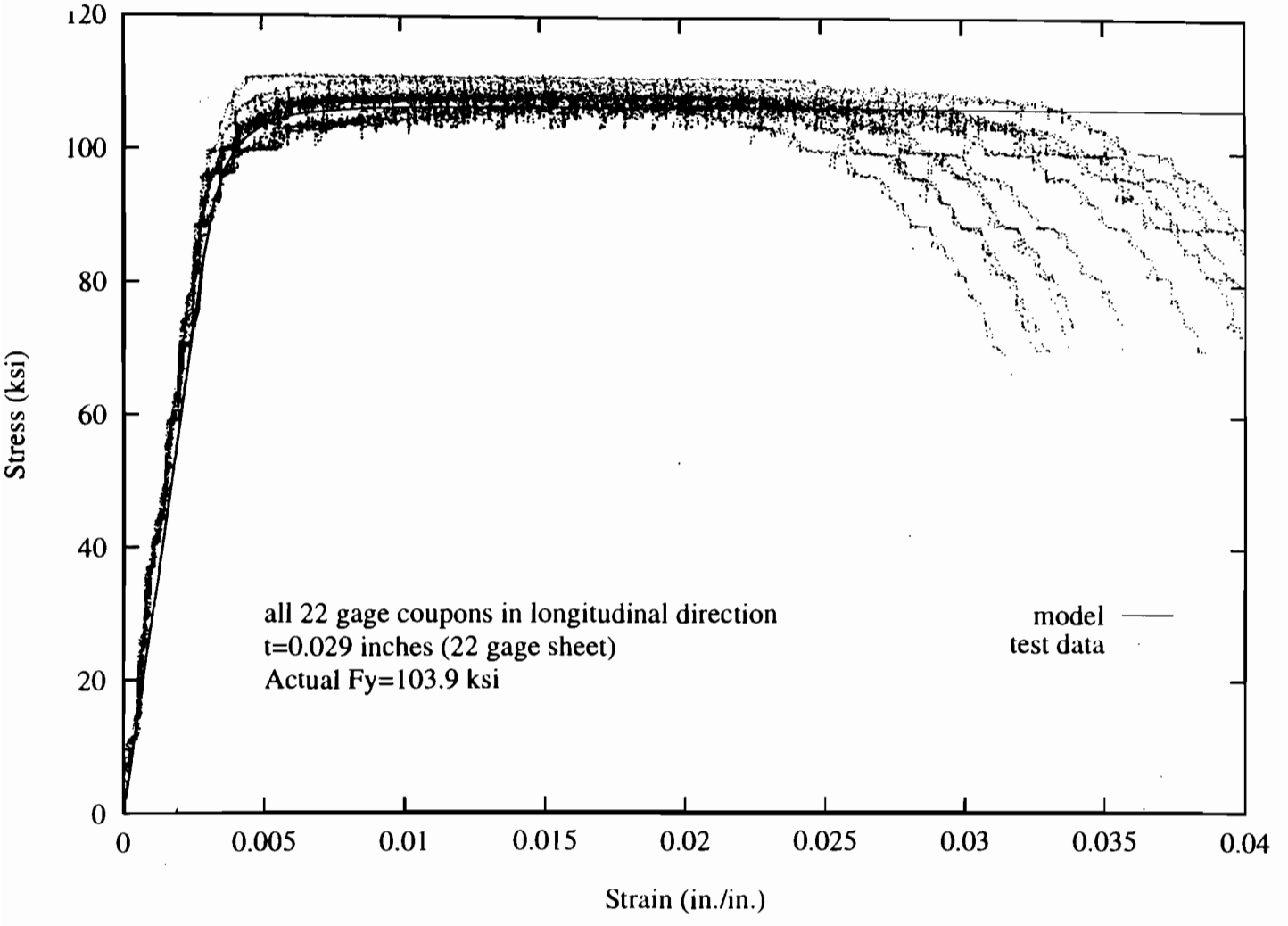

Fig. 6.2.2 Comparison of Tested and Theoretical Stress-Strain Relationships for 22 Gage Sheet Steel

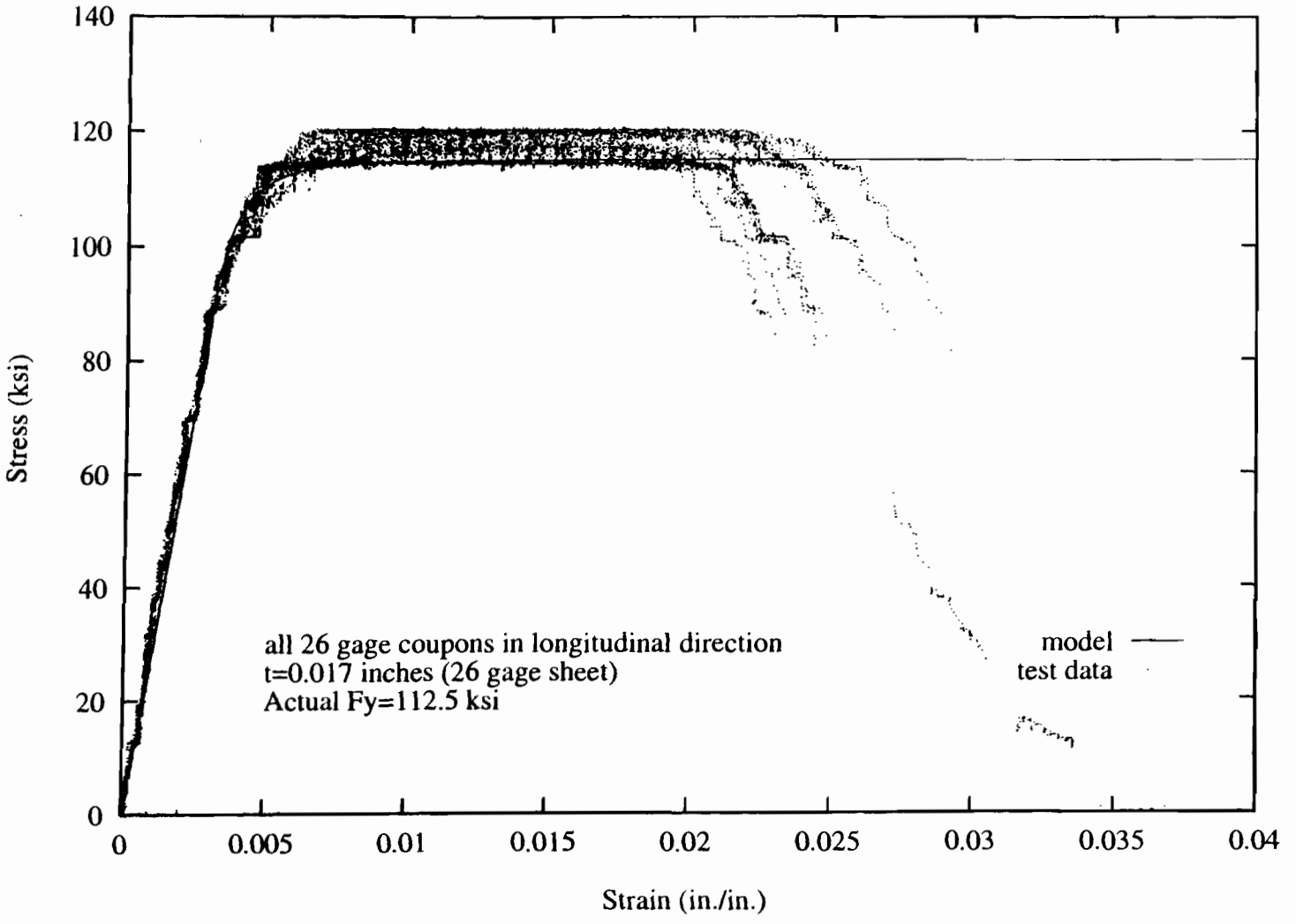

Fig. 6.2.3 Comparison of Tested and Theoretical Stress-Strain Relationships for 26 Gage Sheet Steel

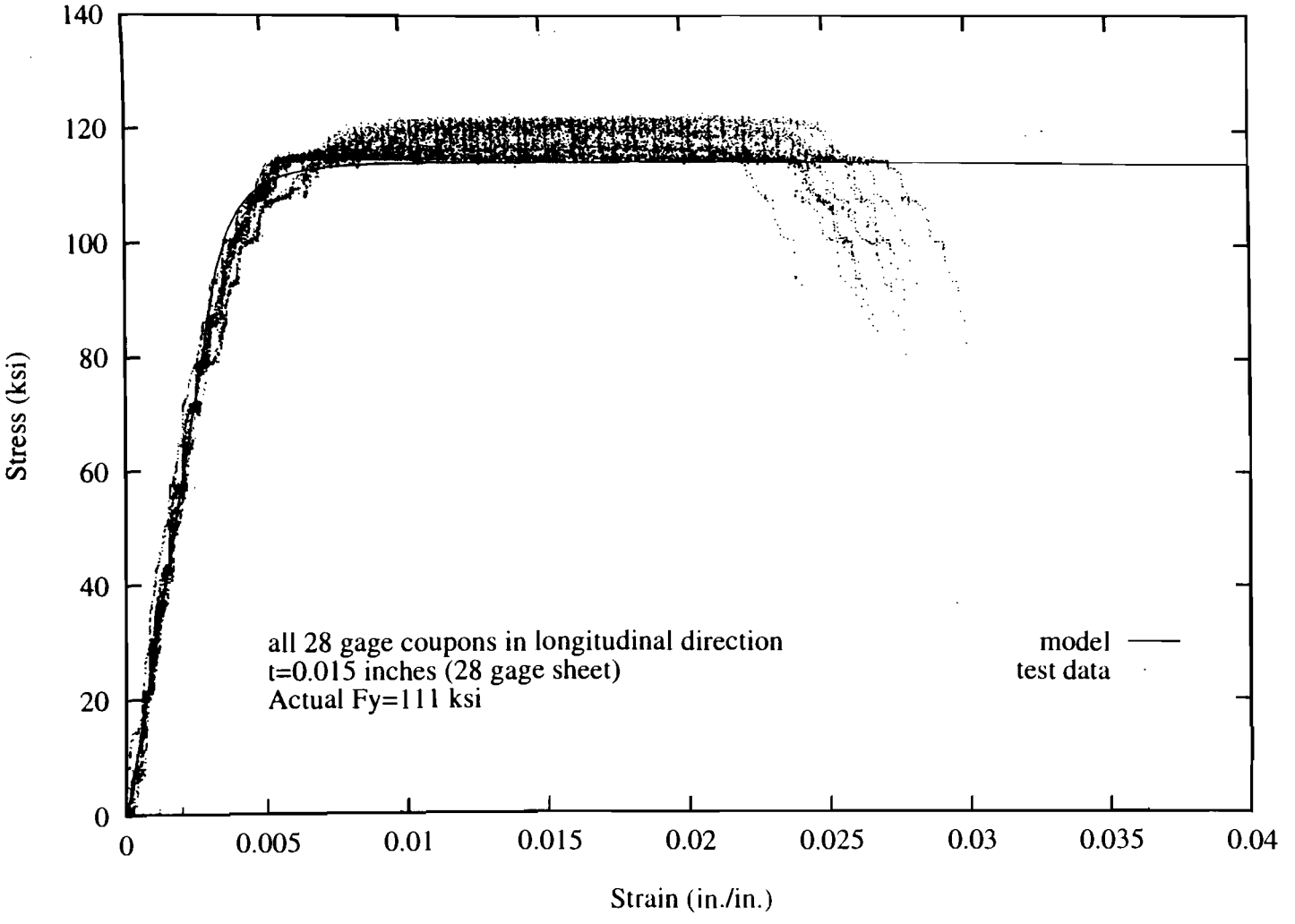

Fig. 6.2.4 Comparison of Tested and Theoretical Stress-Strain Relationships for 28 Gage Sheet Steel

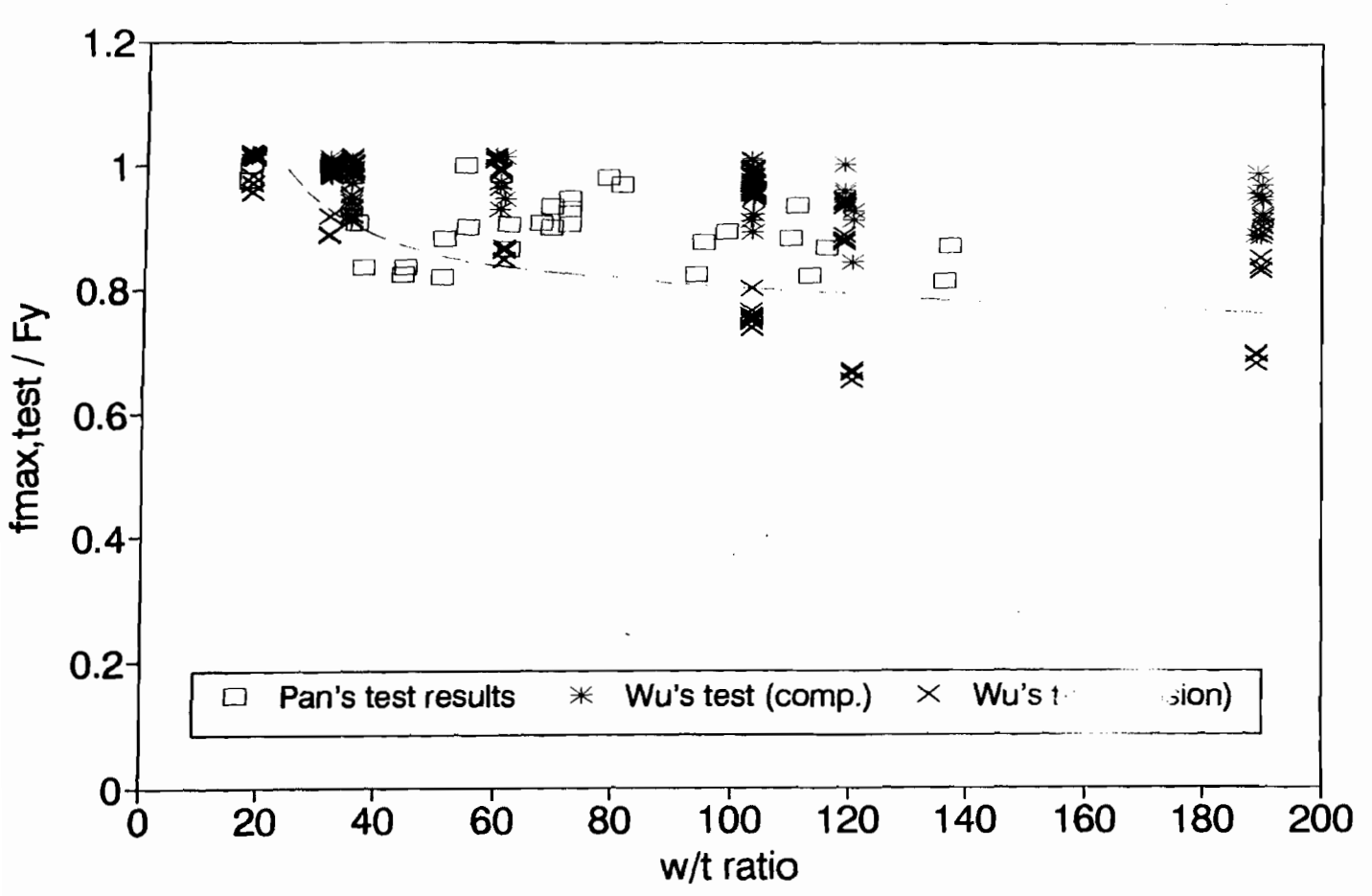

Fig. 6.2.5 Ratio of Tested Ultimate Stress to Actual Yield Strength of Steel vs. w/t Ratio of Panels

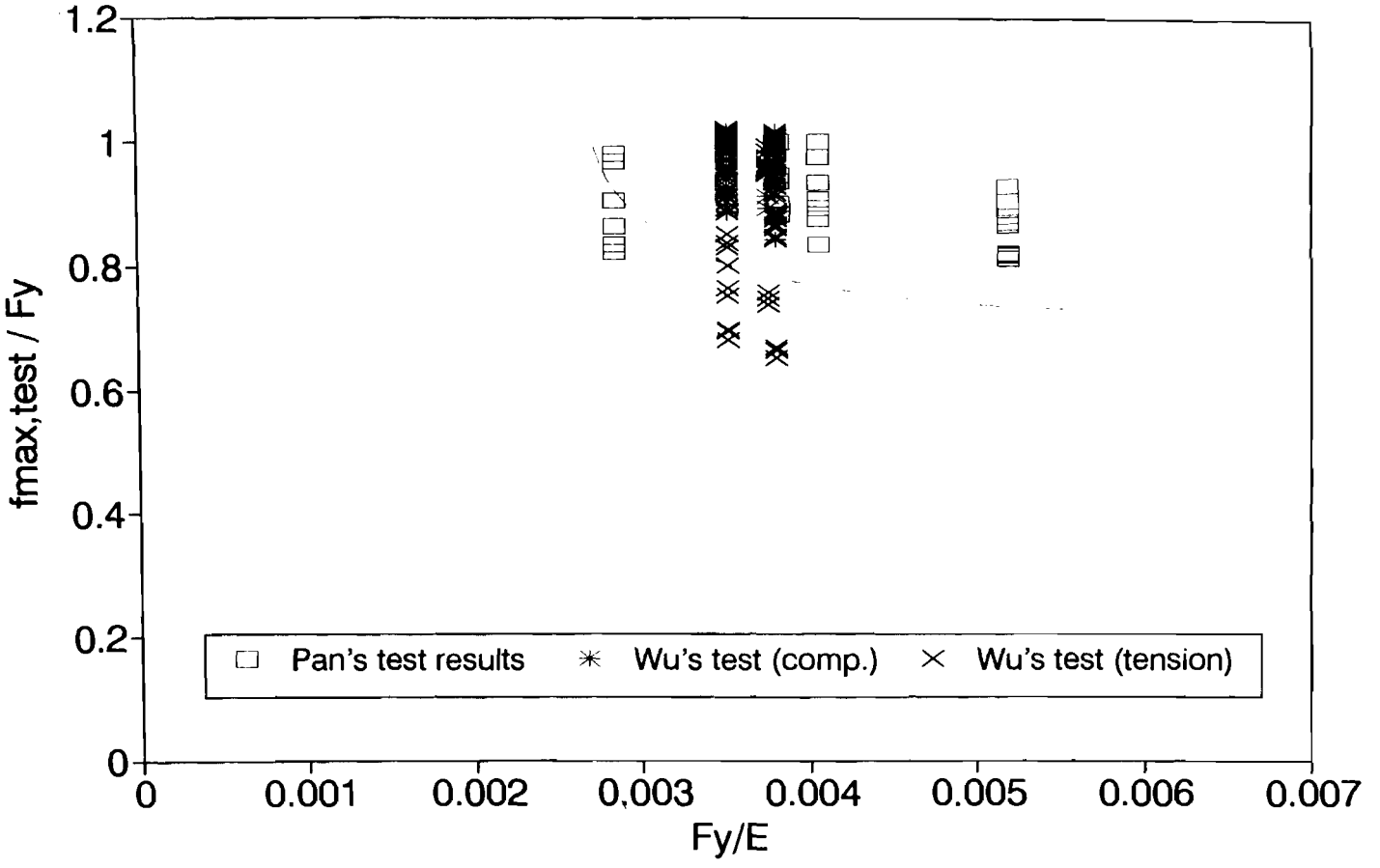

Fig. 6.2.6 Ratio of Tested Ultimate Stress to Actual Yield Strength of Steel vs. F_y/E Ratio of Panels

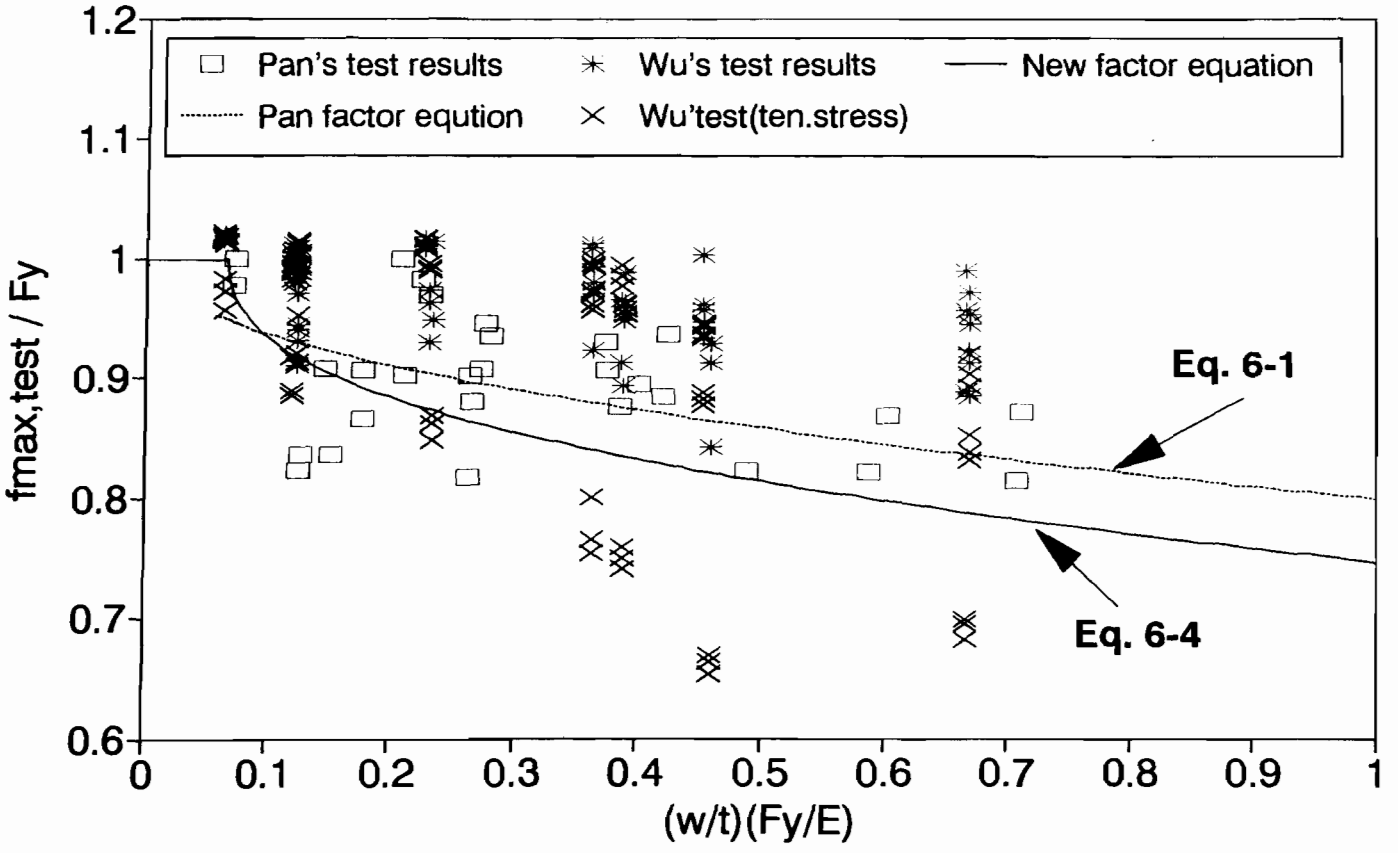

Fig. 6.2.7 Ratio of Tested Ultimate Stress to Actual Yield Strength of Steel vs. $(w/t)(F_y/E)$ Factor

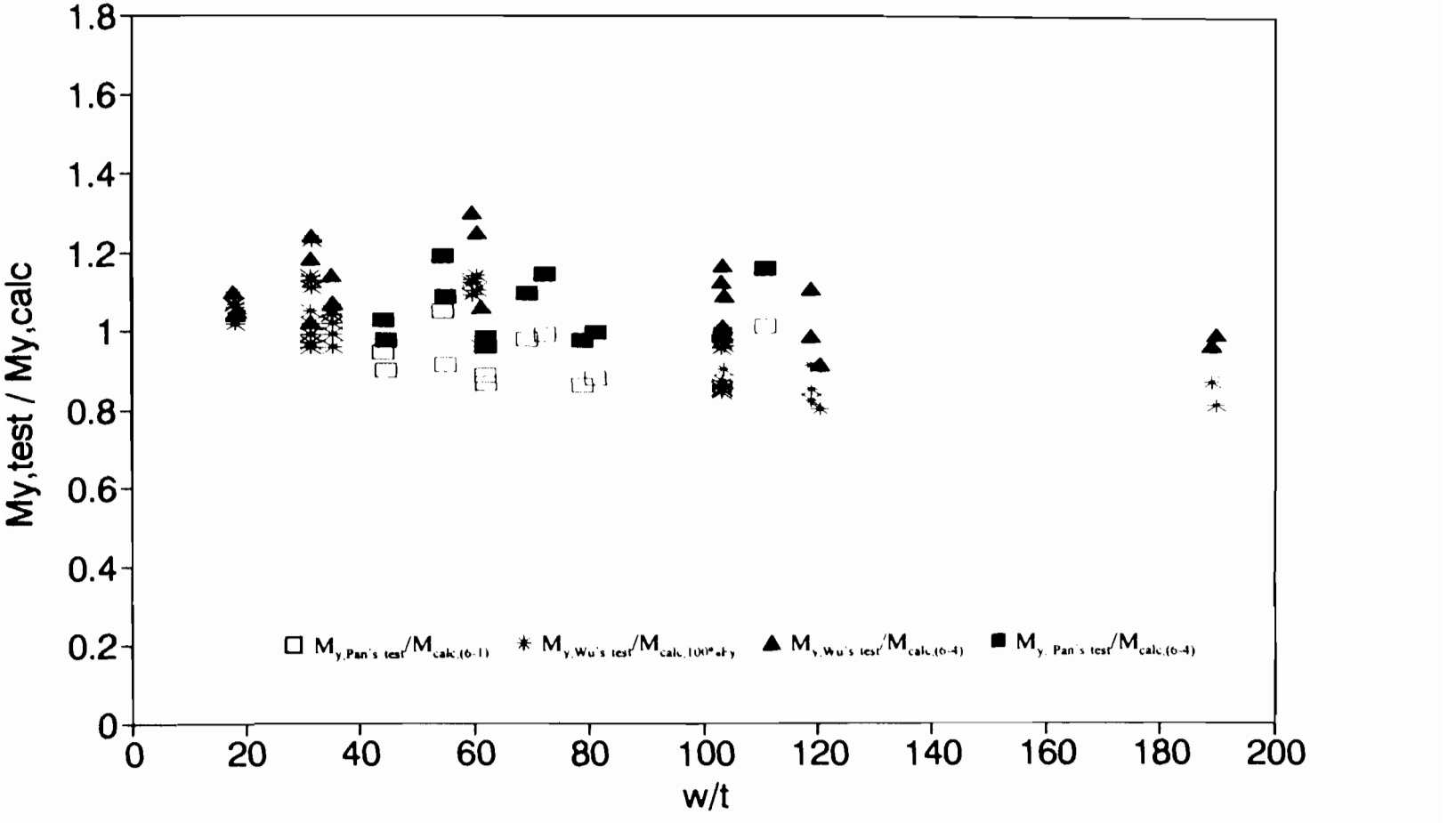

Fig. 6.3.1 Comparison of Tested Yield Moment and Calculated Moment Using the Modified Yield Strength Reduction Factor

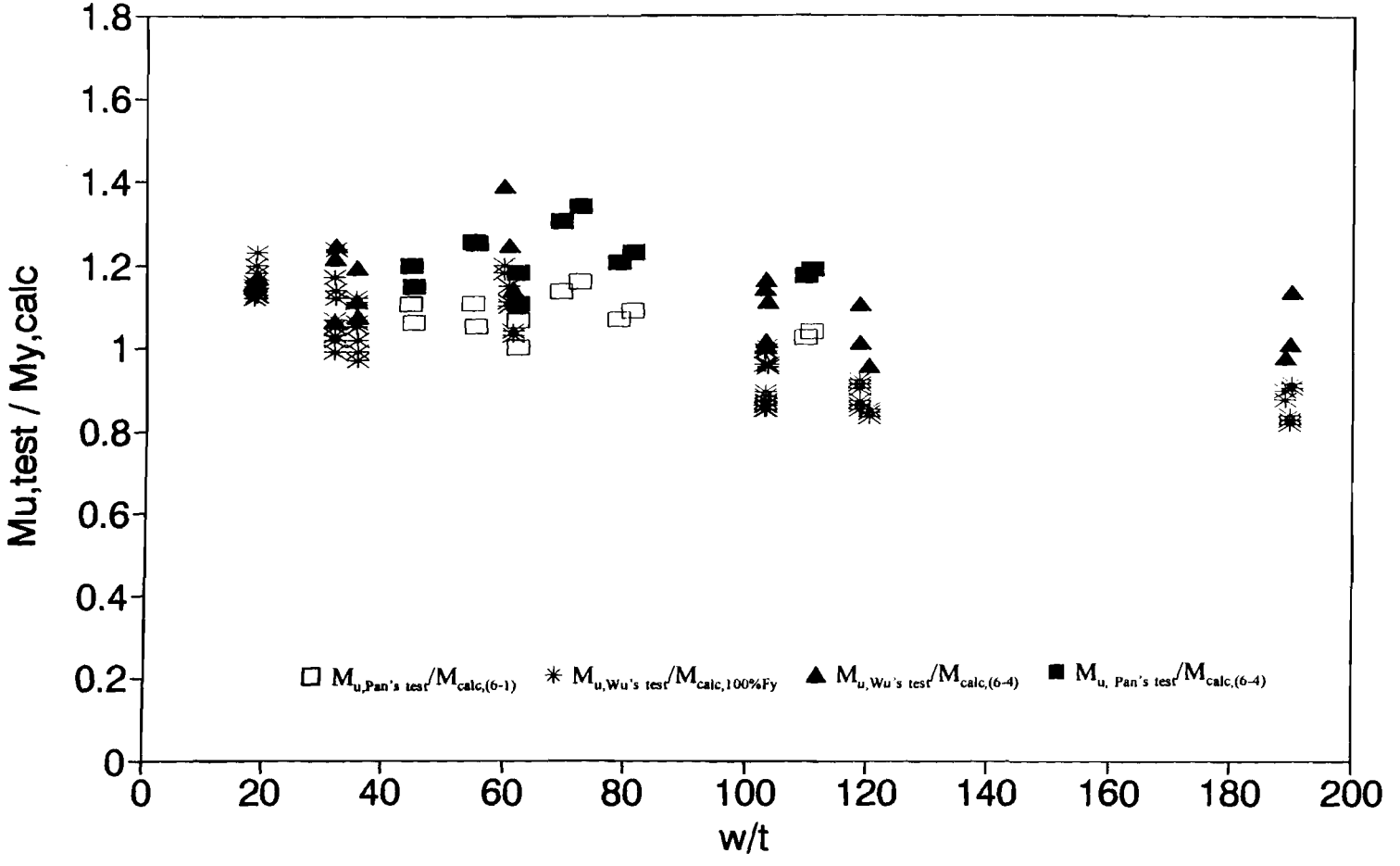

Fig. 6.3.2 Comparison of Tested Ultimate Moment and Calculated Moment Using the Modified Yield Strength Reduction Factor